MINISTRY OF NATIONAL EDUCATION

# THE ANNALS OF "DUNAREA DE JOS" UNIVERSITY OF GALATI

Fascicle IX

## METALLURGY AND MATERIALS SCIENCE

YEAR XXXV (XXXX)
September 2017, no. 3

ISSN 1453-083X

2017
GALATI UNIVERSITY PRESS

THE ANNALS OF "DUNAREA DE JOS" UNIVERSITY OF GALATI
FASCICLE IX. METALLURGY AND MATERIALS SCIENCE
N°. 3 - 2017, ISSN 1453-083X

# Table of Contents

THE ANNALS OF "DUNAREA DE JOS" UNIVERSITY OF GALATI
FASCICLE IX. METALLURGY AND MATERIALS SCIENCE
Nº. 3 - 2017, ISSN 1453-083X

# ENERGY CONSUMPTION ASSESSMENT IN THE WATER TREATMENT PROCESS, BACĂU CITY CASE STUDY

**Florina FABIAN*, Valentin NEDEFF, Narcis BÂRSAN, Emilian MOSNEGUȚU**
"Vasile Alecsandri" University of Bacau, Romania, 600115, Bacau, Romania
e-mail: florina.fabian@yahoo.com

## ABSTRACT

*In the national and international context, two general concerns revolve around water treatment processes. First of all, we talk about energy efficiency and environmental compatibility in the water treatment plants that should be continuously improved for rational energy use and renewable energy sources implementing [1]. Thus, the environmental objectives as reducing $CO_2$ emissions and improve energy efficiency are major concerns today. The purpose of this paper is to conduct a study on a water treatment plant and to develop solutions that will lead to the efficiency improvements of water treatment process in energy consumption terms.*

*By applying the Polyfactorial equation methodology, we can find out the environmental impact of the water treatment process. The total energy demand of water treatment plant Barati (WTP Barati) which treats the water of the city of Bacau was evaluated at 239.94 MW h/y and the highest energy consumption is registered by the technical building, which represent 40 % from total energy consumption. Another important aspect in case of Bacau water treatment plant is the raw water turbidity, which influences energy quantity used for treatment process.*

*The results analysis has highlighted two main conclusions of water treatment plant. The weakest point of the WTP Barati is the water distribution system. These are outdated and affect the treated water quality until it reaches the consumer. The biggest strong point is the raw water quality, which during the winter period reaches a very high level of quality, requiring only a simple chlorination in the treatment system.*

KEYWORDS: water treatment, energy consumption, carbon footprint, energy efficiency

## 1. Introduction

Considering everything that is happening worldwide, water has become the main element in all activities and life support on this planet. When we say the main element of all the activities we refer to population, food, industry, irrigation, cleaning. In their turn non-recoverable waste from these sectors of activity is often thrown into the water [2].

Finally, water potabilization means removing most of organic, inorganic and biological components. The water source of a city can be groundwater or surface water (rivers, lakes etc.).

The water source for drinking water in the town Bacau is Poiana Uzului Lake, the main purpose being water supply and electricity production. The dam is 84 m high, 507 m long and the lake has a length of 3.75 km, an area of 334 hectares and a volume of 98 million cubic meters. Maximum depth of the lake is 64.7 m. The lake is located at a distance of 60 Km SE form Bacau and is situated in Nemira Mountains (Figure 1); also, this lake is not affected by industrial pollution [3].

In general, each human being and everything that is happening on this earth have an impact on the environment, and also the most relevant impact on the environment in water treatment process is related to energy consumption, and if we want to speak about energy efficiency in water treatment process we need to consider the following factors: rational use of energy (mixing time, type of mixer), implementing renewable energy sources, the use of high efficiency machines, the use of advanced water treatment technologies (nanofiltration, reverse osmosis, granular activated carbon) [4]. This study aims at finding out the environmental impact of water treatment process regarding the energy consumption.

***Fig. 1.*** *Poiana Uzului Lake*

## 2. Evaluation method

Environmental impact of the water treatment process regarding the energy consumption can be analyzed through several methods, for example: Carbon Footprint methodology, Externalities of Energy, Polyfactorial equation methodology. In the present case study, we will use the Polyfactorial equation methodology, where we consider different factors [5]: the quantity of energy used for water treatment, working regime, type of flocculant, process and water treatment equipment, sedimentation time and, finally, we make different scenarios. For example, the following scenario: we have water treatment plant (WTP Bacau) and equipment from Bacau where we vary the quantity of energy and chemicals (Figure 2), working regime, type of flocculant and sedimentation time.

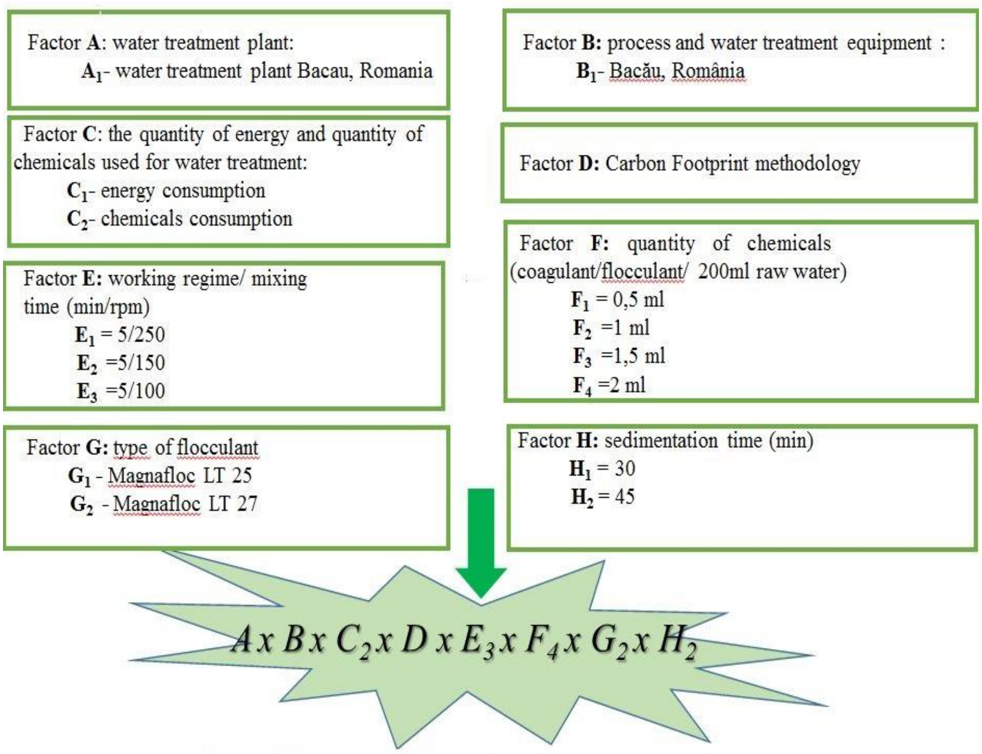


***Fig. 2.*** *Polyfactorial equation methodology*

Water Treatment Plant from Bacau is composed of the following units' components [3]:

- raw water intake and distribution chamber;
- rooms of flowmeters in the form of tanks made of reinforced concrete;
- fast mixing tanks, flocculation tanks and clarifiers lamellar;
- fast sand filters gravitational;
- chlorine contact tank;
- wash water tank;
- sedimentation tank dirty water from washing the filters;
- building support processes and control services
- chamber of sludge collection;
- chlorination building consisting of chlorine storage room, preparation chlorine concentration room, neutralization chamber;
- office building.

This unit components are grouped as shown in Table 1 [3]:

***Table 1.*** *Structure of Water Treatment Plant Bacau*

| Point | Description | Structure |
|---|---|---|
| **MCC 101** | Inlet Works and Clarifier | Pressure Switch for Recycling Pumps |
| | | Pressure Switch for Supernatant Pumps |
| | | Sludge Tank Ultrasonic Level Meter |
| | | Used B. Water Tank Ultrasonic Level Meter |
| | | Inlet Flowmeter |
| | | 12 Pcs Sludge Pneumatic Valve |
| | | Turbidity Meter |
| | | 3 Pcs Clarified Sample Water Solenoid Valves |
| | | PLC |
| **MCC 102** | Filtration | Pressure Switch for Backwash Pump (3 pieces) and Cl Driving Pump (2 pieces) |
| | | Pressure Switch for Booster Set |
| | | Air Compressor (2 pieces) |
| | | Overhead Crane |
| | | Fan Coil (Heating) (2 pieces) |
| | | Level Switch for Drainage Sump (2 pieces) |
| | | Wash Water Discharge Valve |
| | | Wash Water Discharge Flow Meter |
| | | Turbidity Meter (2 pieces) |
| | | Backwash Water Ultrasonic Level Meter |
| | | 8 Pcs Filtered Sample Water Outlet Valves |
| | | PLC Panel |
| | | Lighting Panel LP-FB |
| **MCC 103** | Chlorination | Overhead Crane |
| | | Air Ventilation Fan Storage Room (2 pieces) |
| | | Air Ventilation Fan 1 Chlorinator Room |
| | | PLC Panel |
| | | Lighting Panel LP-CB |
| **MCC 104** | Chemicals | Alum Solution Discharge Flowmeter (4 pieces) |
| | | Al Dilution Water Solenoid Valve (4 pieces) |
| | | Level Switch Alum Tank (2 pieces) |

| | | |
|---|---|---|
| | | Pressure Switch for Lime Circulating Pump (2 pieces)<br>Lime Dosing Solenoid Valve (6 pieces)<br>Level Switch Lime Tank (2 pieces)<br>Pressure Switch for PAC Circulating Pump (2 pieces)<br>Solenoid Valve 1 (Pack Dosing) (3 pieces)<br>Level Switch PAC Tank (2 pieces)<br>Polymer Preparation & Dosing Unit<br>Polymer Solution Discharge Flowmeter (4 pieces)<br>Polymer Dilution Water Solenoid Valve (4 pieces)<br>Sampling Pump No (3 pieces)<br>Inlet Flowmeter Reservoir (3 pieces)<br>Outlet Flowmeter Reservoir (3 pieces)<br>Overhead Crane<br>Reservoir Ultrasonic Level Meter (3 pieces)<br>Lime Ventilator<br>Pac Ventilator<br>Lime Dosing Line Solenoid Valve (4 pieces)<br>Pac Dosing Line Solenoid Valve (4 pieces)<br>PLC panels<br>Lighting Panel LP-CH |
| **105** | Technical Building | Boiler<br>Circulation Pump (2 pieces)<br>Laboratory Equipment<br>pH & Conductivity Meter Water Analyzer Group 1<br>Conductivity Meter Analyzer Group 1<br>Residual Chlorine Meter Analyzer Group 1<br>pH & Conductivity Meter Water Analyzer Group 2<br>Conductivity Meter Analyzer Group 2<br>Residual Chlorine Meter Analyzer Group 2<br>Raw Water Sample Water Solenoid Valve<br>Chlorine Contact Tank Sample Water Solenoid Valve<br>Reservoir 1 Sample Water Solenoid Valve<br>Reservoir 2A Sample Water Solenoid Valve<br>Reservoir 2B Sample Water Solenoid Valve<br>PLC panels<br>Internal Lighting LP-TB<br>External Lighting Panel LP-OL |

*MCC - Motor Control Centers

## 3. Results and discussion

The scheme of water treatment plant of Bacau is structured according to the nature and characteristics of the raw water, as well as the qualitative conditions demanded by consumers' needs, following the most economical and safer operating solutions [6]. The water treatment plant Barati from our case study recorded, over the monitored period of the 12 months of 2015, an electrical energy consumption (Table 2) of about 239.94 MWh/year [7].

As can be seen (Figure 3) in the case of water treatment process in Bacau, the highest annual energy consumption is recorded in the filtration phase, representing more than 20 % of the total energy consumption.

The amount of energy consumed for groundwater extraction is unique to each water system, ranging from the low energy requirements of a gravity feed system to the high energy requirements of an inverse osmosis system pumped by sea [8].

***Table 2.*** *Structure of Water Treatment Plant Bacau* [7]

| Point | Description | MWh/year |
|---|---|---|
| MCC 101 | Inlet Works and Clarifier | 10.77 |
| MCC 102 | Filtration | 50.13 |
| MCC 103 | Chlorination | 33.39 |
| MCC 104 | Chemicals | 48.48 |
| 105 | Technical Building | 97.17 |
| **TOTAL POWER MW h/year** | | **239.94** |

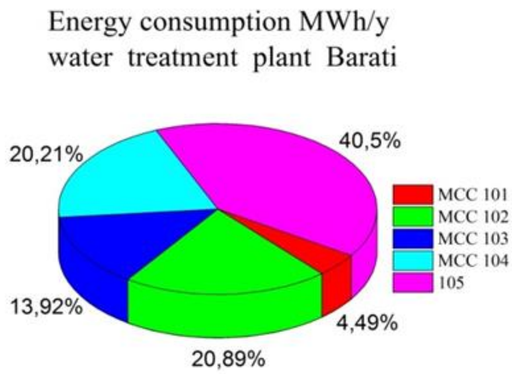


***Fig. 3.*** *Energy consumption for WTP Barati – 2015*

The connection of the equipment to the power supply from the water treatment plant Baraţi is made to the local network and the consumption depends on the turbidity of the raw water as can be seen in Table 3.

As far as energy efficiency and environmental compatibility are concerned, water treatment plants are continuously improved for rational use of energy and the implementation of renewable energy sources. Thus, environmental objectives such as reducing $CO_2$ emissions and optimizing energy efficiency are the main preoccupations. Using advanced efficiency machines, advanced water treatment technologies, it is possible to achieve additional synergies to reduce energy consumption [8].

***Table 3.*** *Energy consumption and water turbidity*

| **Electricity consumption** Process equipment | Average effective flow, $m^3/d$ ($60\ 000\ m^3/d$) | Guaranteed unit electricity consumption, $kWh/m^3$ |
|---|---|---|
| Raw water NTU 1 - 10 | 30,000 | 0.02726 |
| Raw water NTU 10 - 20 | 21,000 | 0.02726 |
| Raw water NTU 20 - 70 | 9,000 | 0.02726 |

## 4. Conclusions

The case study in this research work is focused on the Baraţi water treatment plant located on the Barati hill of the commune Măgura, located at a distance of approx. 6 km from Bacau where the quality of raw water at the entrance in water treatment plant, the quality of the treated water at the exit of storage tank and the amount of energy consumed for water treatment were analyzed and monitored for 12 months (2015).

Analyses of water sources are carried out (surface waters / groundwater) if they are affected by industrial pollution or not, in order to distribute water to the population. Depending on the physico-chemical characteristics of the water, it will go through the water treatment process, which includes a series of stages determined by the level of water pollution.

The evolution of freshwater consumption confirms human evolution, so if at the beginning of the last century the average consumption reached only 240 cubic meters over the whole lifetime of an individual, in the last years it has tripled, according to modern living standards.

Certainly, the main cause, which determined the ascending curve of current water needs and consumption, is technical progress, so that industry and agriculture swallow most of the world's water consumption [9]. The crisis of fresh water resources and especially their efficient management has become among the most important issues of the contemporary world.

## References

**[1]. Bickel P., Friedrich R.**, *Externalities of Energy, Methodology, Update*, European Commission, Stuttgart, Germany, 2005. available at: http://ec.europa.eu/research/energy/pdf/kina_en.pdf (accessed: 07.10.2016).

**[2]. Barrios R., Siebel M., Helm A., Bosklopper K., Gijzen H.**, *Environmental and financial life cycle impact assessment of drinking water production at Waternet*, Journal of Cleaner Production, Amsterdam, Netherlands, vol. 16, p. 471-476, 2008.

**[3]. ***, *The Environment Agreement for the construction of water treatment plant Bacau*, Environmental Protection Bacau Agency Bacau, 2007.

**[4]. Pankaj B., Brown A.**, *World Resources Institute, World Business Council for Sustainable Development, Greenhouse Gas Protocol*, Product Life Cycle Accounting and Reporting Standard, vol. 1, p. 18-20, 84, 2011.

**[5]. ***, *Proiect de reglementare tehnică, Normativ privind proiectarea, execuţia şi exploatarea sistemelor de alimentare cu apă şi canalizare a localităţilor*. Indicativ NP 133–2011, Available at: http://novainstal.ro/tratarea-apei-potabile/, (accessed 30.11.2016).

**[6]. ***, http://novainstal.ro/tratarea-apei-potabile/(accessed on 06.5.2015).

**[7]. Roessler W. G., Brewer C. R.**, *Permanent turbidity standards*, Appl. Microbiol., 15, p. 1114-1121, 1967.

**[8]. Koomey J., Krause F.**, *Introduction to Environmental Externality Costs*, CRC Handbook on Energy Efficiency, USA, 1997.

**[9]. ***, *WABAG Company, Annual report 2015-2016*, no. 17, available at: http://www.wabagindia.com, (accessed: 30.11.2016).

THE ANNALS OF "DUNAREA DE JOS" UNIVERSITY OF GALATI
FASCICLE IX. METALLURGY AND MATERIALS SCIENCE
Nº. 3 - 2017, ISSN 1453-083X

# STUDIES AND RESEARCH ON PIPE NETWORKS WATER LOSSES

**Ştefania CHIRICA[1], Mihail LUCA[2]**
[1] Technical University "Gheorghe Asachi" of Iasi, Romania
[2] Technical University „Gh. Asachi", Mangeron Dumitru Str. 63, 770800, Iasi, Romania,
Tel./Fax: +040 232 270804
e-mail: mluca2015@yahoo.com, stefania.chirica@gmail.com

## ABSTRACT

*The issue of water losses in pipe networks (transmission mains, conveyance and distribution pipelines) is one of the major problems encountered in water supply systems management. The losses have reached very high values, in some cases up to 60% of the water volumes entering the networks, and therefore they require urgent measures to reduce them. In Romania, the average non-revenue water percentage amounts to 48.3%, ranging from minimum values of 22% and maximum values of about 68%. The significance of addressing this issue properly is reflected in the concern of national and international bodies, such as ARA (Romanian Water Association) and IWA (International Water Association), which analyse the systems' status and establish appropriate directions of action to be followed. The powerful development of industry and intensive agriculture in the last decades, in conjunction with global warming, has had a major impact on water resources. In the international context of quantitative and qualitative water sources reduction, adequate water loss management must become one of the water - sewerage agencies' top priority. Solving this issue requires a long-term approach, which involves rehabilitation and modernization measures, appropriate metering for the supply system's conveying water flows, implementation of hydraulic modeling software and leakage detection equipment. Water losses can be found under commercial and physical aspects. Amongst these, the physical ones have the highest share, as they affect all the water supply system components: transmission mains and distribution networks, storage tanks etc. Water loss management must contribute to the efficient resource usage through prevention and intervention measures, adjusted to the particularities of the situation being addressed.*

KEYWORDS: water scarcity, physical and apparent water losses, non-revenue water, pipe degradation

## 1. Introduction

Water supply systems face the issue of water loss in all the components: catchment, treatment plant, storage tanks, distribution network, etc., materializing in losses of raw and treated water, intended for domestic, commercial and industrial consumption. Distribution networks are often faced with this issue, given the vast pipeline networks, their operational and maintenance process peculiarities and the high costs required by their optimal management. In the international context of global warming phenomenon, one of the priorities regulated at national and international level ought to be to water losses reduction and viable water sources protection. Water scarcity must be fought with massive investments in the water supply systems' infrastructure, rehabilitation, modernization, monitoring and prevention works for the defects, which lead to water loss.

## 2. Material and method

The material analyzed consists of the water supply system: water tanks, adductions, distribution network, connections, etc. The largest water losses are recorded in the pipeline network. In this case, defects resulting from the embedding environment, operational process and maintenance conditions lead to losses that directly affect consumers. The water losses, which go undetected, cause major problems in regard to the stability of the land where the pipelines are located, whilst the visible ones, which manifest themselves in a spectacular way, visible on the surface, create major discomfort and material damages.

The research methodology seeks to analyze the methods used by water – sewerage utility companies to limit losses and repair the deficiencies which manifest themselves in the water supply systems. The variety of the methods used results from the extremely varied situations that may occur on the ground. The nature of the deficiencies which lead to the appearance of water losses requires the adoption of measures adjusted to the specifics of the problem, so that the efficiency of the damages localization and repair is maximal. The methodology used to reduce water losses should be chosen based on a number of factors such as:

- the location of the defect (distribution pipes, connections, water tanks, valves, etc.);
- the size of the deficiency;
- the volume of water loss caused;
- the characteristics of the embedding environment in the analyzed area;
- consumers' distribution, etc.

## 3. Results and discussion

Water loss reduction can be summed up to a series of activities, which use methods to decrease the percentage of non-revenue water and protect the available water sources. The implementation of a water loss reduction methodology should use elements adjusted to the specificity of the water supply system studied. The components in question are inspected and analyzed using both human and material resources, together with top of the range equipment and technologies in the field of water loss detection and reduction.

The main methods used to control water losses are analyzed below.

1. Pressure management is used to monitor and analyze pressure values in the network's main nodes, to correlate the pressure in the supply and consumption nodes, or to configurate the network into district monitored areas and reduce pressure by installing line valves. A constant drop in the pressure value implies the existence of water losses and an increase of the pressure value indicates faults in the valves and pipes or changes in the recorded consumption.

2. District metering allows the water flow to be recorded at the entrance and exit points of an area isolated by valves and supplied through a single node. The water loss is determined by isolating the area analyzed and by cutting off the consumers' water supply. The subsequent isolation of pipe sections in the studied area allows the accurate identification of the losses.

3. The partial metering is used for measuring the water flows conveyed through the water supply system at the catchment point, storage tanks, pumping stations, treatment plants, consumers, etc. The metered water volume must be found in the billed volumes and the ones used for the system's own consumption, otherwise, the difference between these values is quantified into water loss components.

4. Nighttime flow measurements consist of keeping track of the water level variation inside storage tanks, the use of district metering or of the water balance in the studied area. The recorded nocturnal consumption, which exceeds a minimum threshold determined according to the number of inhabitants, is considered to be one of the water losses' components.

5. Pipe network inspection involves:

- the use of water loss detection equipment (loggers, correlators, electronic ears, etc.) to identify hidden defects in the pipeline;
- visual inspections of the water supply system components to reveal noticeable flaws and damages.

The equipment and technology used is mainly based on locating the source of the noise produced by water when it exits through a defect on the pipe with pressure.

6. The water balance drawn up both for the entire water supply system coverage area and for each sub-system, illustrates the distribution of water volumes supplied into the system and shows the critical points of the water scheme, which contribute to the amplification of the water loss phenomena.

7. The rehabilitation and modernization of the water supply system involves:

- the replacement and rehabilitation of damaged pipe sections, valves and network constructions;
- the usage of state of the art high performance materials;
- the upgrading of measurement and control equipment etc.

The radical nature of this method leads to a significant decrease of water losses, however, due to the very high investment costs it implies, it is recommended only in those cases where the other methods of control and loss reduction would not be successful.

8. The SCADA (supervisory control and data acquisition) software implemented for the entire water supply system takes the data recorded from the water system components and sends them to the dispatcher where the information is analyzed, thus ensuring effective control of physical water losses.

9. Making the GIS (Geographic Information System) model by integrating and processing field collected data, which then, exported, provides

information on the existing infrastructure and the history of the maintenance and operational works carried out. The information provided is used for:

- the configuration of the network into district monitored areas;
- the implementation of the pressure management;
- the planning of the inspection, rehabilitation and modernization activities.

10. The implementation of the hydraulic model for the water supply systems should be operated by collecting field data, processing them and calibrating the initial model. The calibrated model provides information on network flows and pressures, allows simulation and identification of optimal district areas, sets the minimum night flow, illustrates the effect of pressure management and marks sensitive areas identified in the water supply system.

Water losses are categorized into apparent losses and actual losses. The category of apparent water loss is made up of the component resulting from measurement errors and from unauthorized (fraudulent) consumption. Addressing this loss category focuses primarily on:

- elements which analyze the performance of the measurement equipment;
- network inspection campaigns;
- the identification of illegal links.

The contribution of apparent water losses to the total losses in a water supply system is very small compared to the real losses. The category of real (physical) water losses consists of the volumes of water lost from storage tanks, distribution network, adductions and connections up to the point of consumption. Physical water losses fall into three broad categories:

- visible and reported;
- hidden and unreported;
- background leaks.

The last two categories, the hidden and the background losses, are the ones which sum up the highest volumes and occupy the largest share of the total water losses recorded in a water supply system. Loss reduction measures are largely focused on addressing and remedying deficiencies, which cause physical water loss.

Reducing water losses with nocturnal flow measurements is a method that allows the operator to locate and identify the size of the defect through which water leaks from the pipeline network or storage tanks. The method is based on the principle that, between 00:00-04:00, the recorded consumption is considered to be a component of water loss. However, for the method and measurements to be accurate, a minimum nocturnal flow value, corresponding to household consumption is considered. The values obtained above this threshold are quantified as water losses. The specialty literature shows some basic values of the minimum nocturnal consumption (Table 1), but these values have to be adjusted to the specificity of each area. Operators should establish the minimum night consumption for each sector analyzed, taking into account the industrial or commercial type of activities carried out in the studied area, as well as the domestic one, through the use of meters. The statistical data show that the value of the minimum night flow is influenced by the total number of connections, the length of the pipelines in the analyzed area, the age and their execution materials (Jaber M.A. Alkasseh *et al.*, 2013).

***Table 1.*** *Estimated values for night consumption (Cheung P.B. et al., 2010)*

| Number of inhabitants in the analyzed area | Minimum night flow (l/min) |
|---|---|
| < 10,000 | 0.01 |
| 10,000 – 50,000 | 0.01 – 0.02 |
| 50,000 – 150,000 | 0.02 – 0.025 |
| 150,000 – 500,000 | 0.025 – 0.05 |
| > 500,000 | 0.05 – 0.1 |

In order to obtain real-time data that reflect the field situation with the use of nocturnal measurements, it is required increased attention from the operator as this study method is based on work procedures and carefully selected equipment for that purpose. Among the most important factors to consider are listed (Werner M. *et al.*, 2011):

- choosing the appropriate flowmeters to record the system's minimum flow rates with high precision;
- adequate district area configuration, so that flows entering and leaving the study region can be effectively monitored;
- adequate installation of the recording equipment, sensors and data transmission devices used;
- regular inspections of the equipment and its field calibration when the situation in the study area requires it.

Regional Operator S.C. APAVITAL S.A. monitors the water volumes entering and leaving the system through more than 60 district areas and transition flow meters. In the case of pumping stations, pipelines serving different areas as well as those with a different pressure regime are monitored. The values obtained are recorded in monthly summarizing tables, together with the observations made by the operator. The accuracy of the recorded data is influenced by the phenomena that may occur during a monitoring interval. The analysis of the results obtained must also take into account the observations of the operator. These refer to:

- methods of calculating the resulted flows;
- flaws in the measuring equipment and repair works;
- consumers' information;
- data transmission errors;
- values which do not fall within the normal consumption limits, etc.

The Red Cross district metering area is located in the western part of Iaşi metropolitan area, being situated in the Păcurari storage tanks area (Fig. 1). The small size of the monitored surface (Fig. 2) allows for an analysis of recorded water consumption and flows through the water supply system, highlighting the problems encountered in this study area.

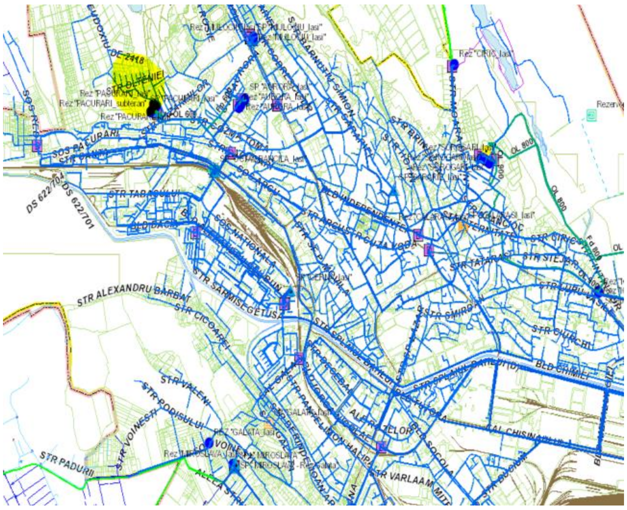

***Fig. 1.*** *Framing of the study area in the water supply system assembly of Iaşi county*


***Fig. 2.*** *Red Cross district metering area*

Measurements conducted in the Red Cross district area during 2009, 2012 and 2014 show the variation in the minimum and maximum hourly flow rates in the system for this particular study area. Interpretation of the obtained data has been done through:

- the reference values found in the specialty literature;
- the hydraulic characteristics of the water supply system (flows, pressures, specific consumption and consumption categories);
- the constructive characteristics of water utility networks (materials, diameters, operational span).

Measurements conducted in the Red Cross district area in 2009 (Fig. 3) show maximum flow rates exceeding 15 $m^3/h$. At the same time, the minimum flows range around 7.6 $m^3/h$. The lowest recorded values are during 22.01.2009 - 23.01.2009, between 23:00 and 05:00 time slot. On 23.01.2009, the 02:00-03:00 time slot shows maximum hourly flow rates of 9 $m^3/h$ and a minimum hourly flow rate of about 7.5 $m^3/h$. The values recorded in this case far exceed the values estimated in the specialty literature. The data show that the pipeline network is damaged and records major water losses. Such values show the urgent nature of the rehabilitation and replacement measures needed by the pipeline network. In their absence, the damages will be more and more frequent, the defects will multiply, and the lost water volumes will continue to increase.

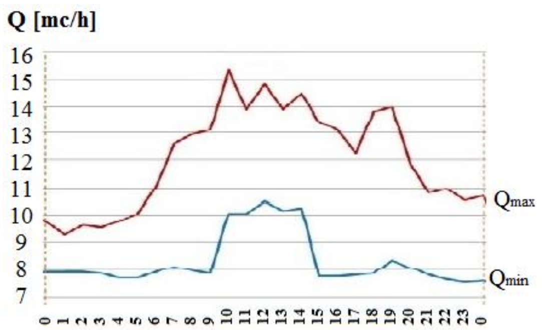


***Fig. 3.*** *Flow rate measurements conducted in in the Red Cross district on 22.01.2009 (color code: red – $Q_{max}$, blue – $Q_{min}$)*

Measurements conducted in the Red Cross district area during 2012 (Fig. 4) show an increase in the minimum recorded flows rates compared to the values from 2009. Within a three-year period, the minimum hourly rate has increased and is now situated around 12 $m^3/h$, slightly surpassing 13 $m^3/h$ during peak time. The hourly time slot with the lowest recorded consumption is 03:00-04:00 when the minimum hourly flow rate is 12 $m^3/h$, and the maximum is around 13.4 $m^3/h$. Also, increases in the maximum hourly flow rate were observed, coming close to 19 $m^3/h$, higher than 15 $m^3/h$ in 2009.

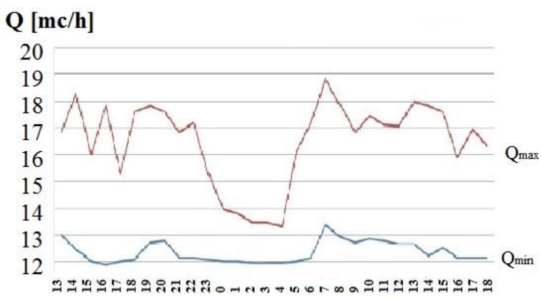


***Fig. 4.*** *Flow rate measurements conducted in in the Red Cross district area during 13.03.2012 – 14.03.2012 (color code: red – $Q_{max}$, blue – $Q_{min}$)*

Compared to 2009, there is an increase of 4.5 $m^3/h$ of the minimum hourly flow rate. The 57% increase in nocturnal water consumption shows the magnitude of the water loss phenomenon in the pipeline network. The additional consumption as compared to 2009 suggests that during the three years no measures have been taken to replace, rehabilitate or modernize the pipeline network serving the analyzed area.

The measurement campaign conducted during 10.01.2014 - 13.01.2014 (Fig. 5) shows much lower values than those obtained in 2009 and 2012. On 11.01.2014 it was recorded the maximum hourly flow rate of about 10.3 $m^3/h$. The minimum hourly flow rate was obtained during 00:00-06:00 time slot, and its value is below 1 $m^3/h$. Compared to the data obtained in previous measurement campaigns, the values are much lower. The maximum hourly flow rate of 10.3 $m^3/h$ is lower than the value achieved in 2012 for the minimum hourly flow rate. Such values show the actual magnitude of the losses. Replacement and rehabilitation of pipelines in the Red Cross district area led to significant decreases in water losses.

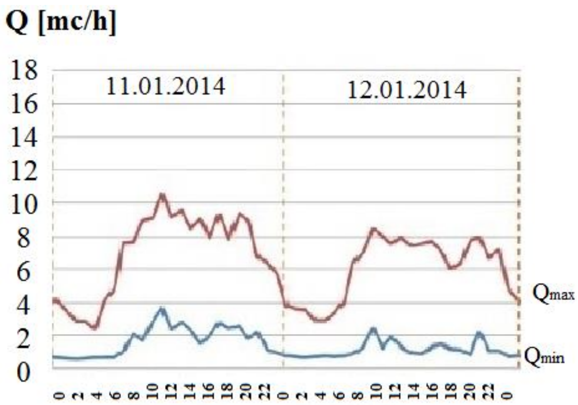


***Fig. 5.*** *Flow rate measurements conducted in in the Red Cross district area during 11.01.2014 – 12.01.2014 (color code: red – $Q_{max}$, blue – $Q_{min}$)*

The data recorded during 2009, 2012 and 2014 were analyzed and taken into account, showing the evolution of the minimum and maximum hourly flows obtained during the studied periods (Table 2).

The analysis of the data from Table 2 shows the evolution of the minimum and maximum hourly flow rates recorded during 2009 - 2014 in the Red Cross district area. The variation in the minimum and maximum hourly flow rate values from the measurements shows the significant increase in water consumption between 2009 - 2012. The value of the minimum hourly flow has increased with about 4.40 $m^3/h$, which represents a percentage increase of about 57.89%. The time slot in which these values were recorded, namely 23:00-05:00, is characterized by minimal levels of water consumption. Furthermore, there is no industrial activity in the Red Cross district area, and commercial businesses in this space do not require water consumption during the night. The only type of consumption in the analyzed sector is domestic, but the values obtained are well above the normal data found in the specialty literature for this time interval. Thus, the data obtained suggests water loss in the network. The analysis of the next time interval, 2012-2014, demonstrates the effectiveness of the reduction measures undertaken by the water-sewerage agency. The decrease in the minimum consumption by 11.20 $m^3$/h represents a reduction of 92.67% of the flows conveyed through the water supply system.

***Table 2.*** *Analysis of the values obtained during 2009 - 2014 in the Red Cross district area*

| Specific values | 2009 | 2012 | 2014 |
|---|---|---|---|
| $Q_{min}$ [$m^3$/h] | 7.60 | 12.00 | 0.80 |
| Time slot | 23:00<br>05:00 | 03:00<br>04:00 | 02:00<br>06:00 |
| Variation [$m^3$/h] | - | + 4.40 | - 11.20 |
| Variation [%] | - | + 57,89 | - 92.67 |
| $Q_{max}$ [$m^3$/h] | 15.30 | 18.80 | 10.30 |
| Time slot | 10:00<br>11:00 | 06:00<br>08:00 | 10:00<br>12:00 |
| Variation [$m^3$/h] | - | + 3.50 | - 8.50 |
| Variation [%] | - | + 22.87 | - 45.21 |

The study of maximum hourly flow rates recorded in the Red Cross district area shows a similar evolution to the one of the minimum hourly flow rates, although the magnitude of the water loss phenomenon is not highlighted to the same extent. The period between 2009 and 2012 is characterized by increases in water consumption by up to 22.87%. The maximum values are recorded in the consumption intervals 10:00-11:00 and 06:00-08:00. As with the minimal hourly flow rate variation, peak values were significantly reduced during the 2012 - 2014 monitoring period. The consumption decrease of 8.50 $m^3$/h represents a decline of 45.21%. Thus, a stricter control of the volumes transported across the network is achieved. The actions and measures implemented by the operator aligns the performance of the water supply system to the European and global standards and guidelines for reducing water scarcities as well as improving water volume extraction and protecting viable water sources.

## 4. Conclusions

1. Water supply systems face the problem of water loss, a phenomenon which can be found at all the components (catchment, treatment plant, pumping stations, adduction, storage tank, distribution network, etc.).

2. Water - sewerage companies use specific methods to reduce water losses recorded in the system, adjusting them to field conditions correlated with data obtained from a thorough analysis of the operated networks.

3. One of the most applied methods for identifying and detecting water losses consists of using the nighttime flow rate, when the values recorded with the measuring equipment are only justified by the presence of water losses in the system analyzed.

4. The nocturnal flow measurements conducted between 2009 and 2014 in the Red Cross district area show the magnitude of the "water loss" phenomenon, evidenced both by an upward and a downward trend for the water flows conveyed through the system.

5. Values recorded between 2009 and 2012 illustrate the speed of degradation of the elements which make up water systems and the magnitude of water losses in the absence of rehabilitation and upgrading measures adjusted to the specific situation of the field.

6. The analysis data from 2014 highlights the efforts of the regional operator S.C. APAVITAL S.A. to reduce water losses through massive investments in the water supply system infrastructure, as pointed out by the very low values of the minimum hourly flows recorded.

## References

**[1]. Cheung P. B., Girol G. V., Abe N., Propato M.,** *Night flow analysis and modeling for leakage estimation in a water distribution system*, Integrating Water Systems (CCWI 2010), At 2010 Taylor & Francis Group, London, ISBN 978-0-415-54851-9, p. 509-513, 2010.

**[2]. Fantozzi M., Lambert A. O.**, *Residential Night Consumption – Assessment, Choice of Scaling Units and Calculation of Variability*, IWA Water Loss Congress, Manila, Philippines, February 2012.

**[3]. Jaber M. A. Alkasseh, Mohd Nordin Adlan, Ismail Abustan, Hamidi Abdul Aziz, Abu Bakar, Mohamad Hanif**, *Applying Minimum Night Flow to Estimate Water Loss Using Statistical Modeling: A Case Study in Kinta Valley*, Malaysia, Water Resources Management, vol. 27, issue 5, p. 1439-1455, March 2013.

**[4]. Lambert A. O., Hirner W.**, *Losses from Water Supply Systems: Standard Terminology and Recommended Performance Measures*, International Water Association, 2000.

**[5]. Luca M., Alexandrescu S. A.**, *Modern techniques for measuring the flow rate through water conveyance pipes*, Bulet. Instit. Politehnic din Iași, Secțiunea Hidrotehnică, Tom LVI (LX), Fasc. 4, p. 31-38, ISSN: 1224-3892, 2010.

**[6]. Thornton J., Lambert A. O.**, *Progress in practical prediction of pressure: leakage, pressure: burst frequency and pressure: consumption relationships*, Proceedings of the IWA Specialised Conference "Leakage 2005", Halifax, Nova Scotia, Canada, 2005.

**[7]. Werner M., Maggs I., Petkovic M.**, *Accurate measurement of minimum night flows for water loss analysis*, 5th Annual WIOA NSW Water Industry Engineers & Operators Conference Exhileracing Events Centre, Newcastle, p. 31-37, 29-31 March, 2011.

THE ANNALS OF "DUNAREA DE JOS" UNIVERSITY OF GALATI
FASCICLE IX. METALLURGY AND MATERIALS SCIENCE
Nº. 3 - 2017, ISSN 1453-083X

# THE INFLUENCE OF WASTE WATER COMPOSITION ON THE PUMPING SYSTEM CORROSION

**Manuela-Cristina PERJU[1,*], Cristian SAVIN[1], Costică BEJINARIU[1], Carmen NEJNERU[1], Dragoş-Cristian ACHIŢEI[1]**
[1] Technical University "Gheorghe Asachi" of Iasi-Romania, Department of Technologies and Equipments for Materials Processing, Blvd. Mangeron, no. 51, 700050, Iasi, Romania
e-mail: cryss_ela@yahoo.com

## ABSTRACT

*Wastewater piping systems in urban agglomerations or industrial areas have problems with the wear and tear of equipment and water transport pipelines used. The problems are related to hydromechanics wear and corrosion due to the presence of solid particles transported with water and due to the residual chemical compounds resulting from industrial technological processes, as well as the presence of biological waste from domestic consumers. In the paper are presented the corrosive characteristics of the waste waters and a review of the effects of wear and corrosion in the case of submersible pumps is made.*

KEYWORDS: wastewater, corrosion, wear

## 1. Introduction

Industrial or domestic wastewater pumps are used to transport fluid containing chemical compounds and industrial and organic wastes from the user to the treatment plants. They are also used for drainage of surface water (floods) and sewers (for transport between treatment plants) [1].

Pumps are recommended for transport: liquid phases containing solvents and chemical solvents, as well as powders, sand, colloidal substances and suspensions; fluids containing air or gas bubbles at the surface of the water or dissolved in the interior; crude sludge; rain water; wastewater with faces [2].

Drainage pumps may be provided with a shredder, which is intended to grind the slurry, in order to facilitate the solid matter transportation of the wastewater. Wastewater pumps (domestic and industrial) are generally high power centrifugal pumps working under heavy conditions because the water contains powerful organic and nonorganic corrosive agents as well as suspensions and abrasive particles of various sizes and shapes [3-5].

## 2. Wastewater composition

The wastewater composition varies, containing sewage waste including pathogenic bacteria, organic and nonorganic particles, emulsions, dissolved gases, etc., with a pH ranging from 6 to 9 (mainly acid pH).

The most corrosive is sulfuric acid that is found in high concentration in waste water [2, 6]. During operation, a mechanical wastewater pump must bear various mechanical and chemical stresses, such as:

- mechanical shock of different intensities, variable contact angles of the particles. The abrasion degree of the particles varies according to their shape and size [7];
- thermal and mechanical action, as the pump works outdoors in winter must withstand temperatures down to -35 °C (at temperatures below 0 °C there is the risk of water freezing within the plenum and transport pipes, micro-cracks occurring due to the increase with 9% of the volume of frozen water) and summer to 50 °C; that work in the submerged state must withstand the speed and strength of the water with abrasive particles;
- cavitation due to turbulent waste water is a danger to the integrity of the pump sub-assembly;
- acid pH of water which increases the content of active ions and chemical reactivity of the liquid;
- the corrosion of sulfuric acid and sulfur dioxide dissolved in water, resulting from the decomposition of the organic origin substances;
- enhanced corrosion due to the presence of dissolved oxygen in the transported liquid, which modifies the acidity of the water [8];
- accelerated flux corrosion represents the removal of the protective oxide layer from the pump

metal (especially in low-alloy steels and gray cast iron).

The speed of this process is determined by the oxygen content, the leakage rate and the chlorine content [9, 10];

- operating irregularities due to the variable viscosity of the wastewater and the presence of suspended particles of different sizes [11, 12];

- the action of aerobic and anaerobic bacteria on the pump metal;

- the chemical attack of hydrogen sulfide ($H_2S$), which is produced by sulfur-reducing bacteria in wastewater that flows into sewage.

a) b)

***Fig. 1.*** *a) Holes in a gray cast iron housing due to the presence of sand in the transfer fluid; b) Intercrystalline corrosion in the cast iron casing favorized by the presence of solid suspensions*

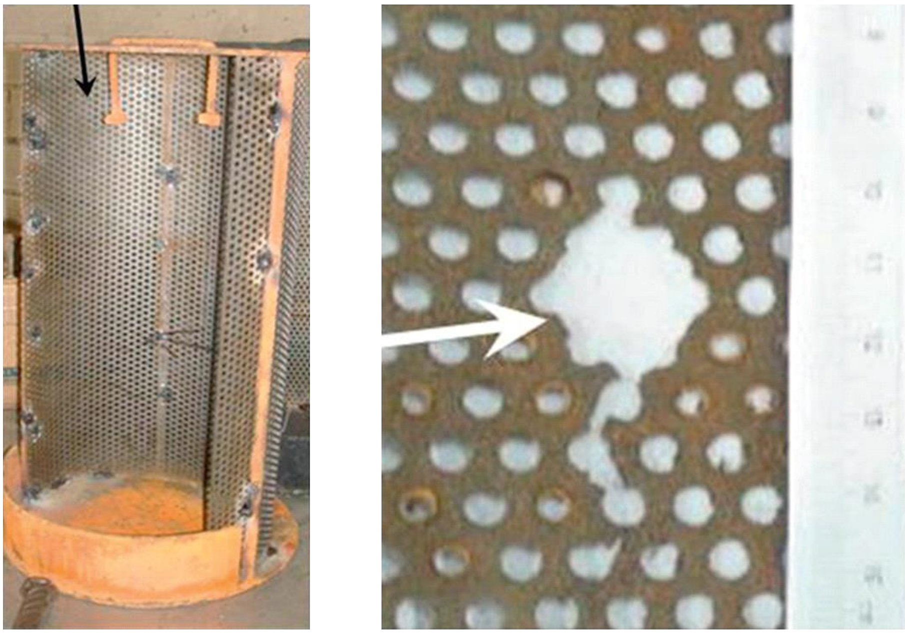

a) b)

***Fig. 2.*** *Severe degradation of austenitic stainless steel due to the combined action of mechanical abrasion and acid corrosion of the liquid transported medium; a) a filter; b) detail*

***Fig. 3.*** *Submerged wastewater pump*

In addition to factors such as pH, temperature and organic wastewater, the flow velocity and the impact of specific compounds in the liquid must be incorporated into the sulfide reactions and bacterial growth.

The wastewater pumps materials must be compatible with the pumped liquid solution so that the wear and corrosion of the materials forming the inner chambers and the transport elements are within tolerable limits.

Because the pump is the heart of the filtration system, it must have the ability to supply and maintain the desired flow and pressure, as the dirt accumulates on the filter material [13, 14].

## 3. Influence of wastewater composition on corrosion of pumping systems

Wastewater represents a chemical aggressive environment due to the presence of corrosive and abrasive elements, such as:

- dissolved oxygen;
- household waste, such as chloride, fluoride, sodium, organic dejection substances;
- acids formed from the decomposition of biological substances;
- sulfur compounds ($SO_2$, $H_2S$, $H_2SO_4$, etc.);
- aerobic and anaerobic bacteria that create biogenic acids (produced by a biological process);
- fungi and suspensions of biological residues, gravel, sand and other solids of organic and nonorganic nature.

Authors studied the characteristics of wastewater corrosion [15-18].

Figure 4 shows the classic representation of partially filled pipeline containing waste water with a variety of organic and sulfur compounds. Typically, the channel is half filled and the pipe speed is maintained at about 0.6 m/s.

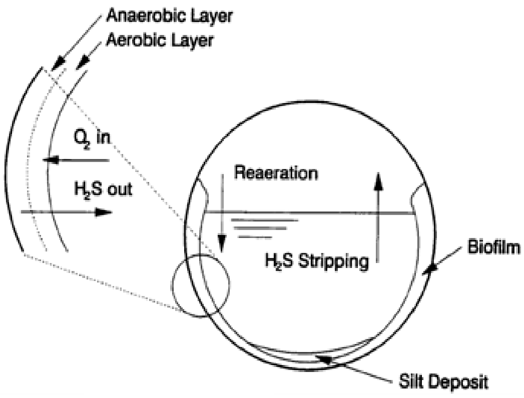


***Fig. 4.*** *Typical sewage section* [19]

Glass and heavy organic particles are deposited on the bottom, while the bacterial deposits develop on the channel walls to form a biofilm or slurry layer. This layer of film and biofilm provides an excellent growth medium for bacteria, protected by the shear forces of the flowing waste water.

This channel contains several micro-media: the space above the liquid is usually filled with abundant oxygen air; the liquid may be either aerobic or anaerobic, depending on the oxygen demand and the reaction speed; the layers of silica and biofilm may also be aerobic or anaerobic.

Wastewater may contain iron oxides or iron chlorides, their presence giving a red color, earth-color to the water, and the presence of manganese or oxides giving a black color to wastewater. Oxides can also be found in the form of granules and are in the form of fine powders subsequently dissolved in water or as mud or sludge [20].

The transport pipelines are clogged with powdered substances and solid microparticles forming wall-adherent protuberances.

The percentage of chlorides and sulphides in water increases the amount of deposits on the walls of the pipes and the corrosion of the transport system.

At the fluid displacement speed and laminar flow, there is the possibility of chemical corrosion reactions (oxidations, etc.) carried out by ionization and low speed diffusion [21].

In the case of turbulence flows, the laminar layer on the pipe walls is thin and then the corrosion speed is higher. Turbulence swirls are enhanced by the presence of depositions on the walls. So, the more deposits on the walls, the more intense corrosion.

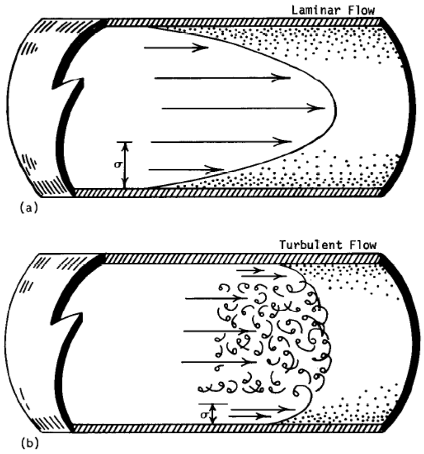


***Fig. 5.*** *Comparison of oxygen diffusion in laminar flow (a) and turbulent (b)* [15]

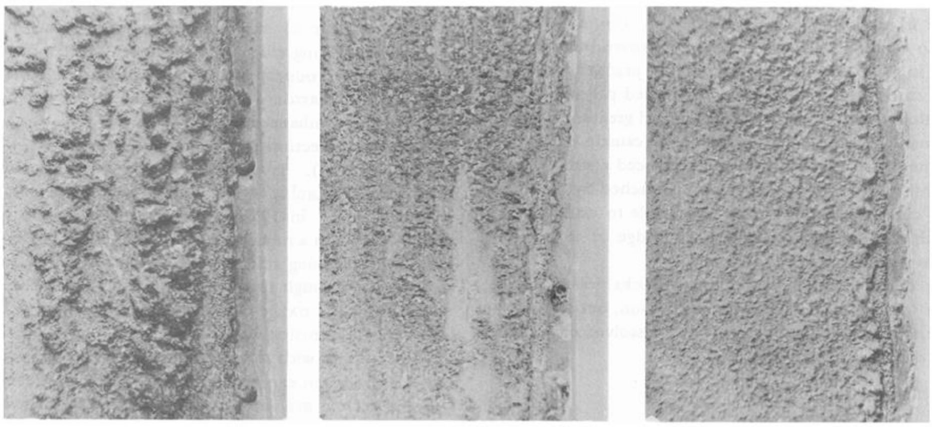

0.06 m/s 0.33 m/s 0.67 m/s

***Fig. 6.*** *The effect of deposition velocity on turbulent flow* [15]

Therefore, in wastewater, turbulences that forms at high flow rates and velocities, allow oxygen to reach the inner surface of the pipeline more quickly, and corrosion rates are higher.

Types and concentrations of contaminants in waste water from domestic sources are well known - fats, oils, grease, soaps, organic matter, dirt, human waste, food waste, etc. - normally in total concentrations below 1000 ppm (0.1%).

The most common chemical contaminants in domestic water are chlorides, nitrogen compounds and a wide variety of organic compounds. Sulfate and phosphate ions are present.

The household wastewater pH is typically between 6 and 7, lightly on the neutral side where there is greater use of soaps and household cleaning materials, most of which are slightly alkaline to enhance the detergents efficiency.

Sewage and other wastewater contain significant levels of biological and organic materials, including many bacteria that remain active in waste streams.

From the corrosive point of view, the most important types of bacteria are those that metabolize sulfur compounds because this microbiological activity can produce acid chemicals that are corrosive to concrete, steel or iron. Some bacteria also oxidize ferrous ions to ferric ions, which makes the local environment more corrosive to carbon steel.

## 4. Analyzed wastewater pumping system

A single-channel, low-pressure centrifugal pump was analyzed, both macroscopically and SEM analysis to highlight areas with significant wear and corrosion.

It can be seen that the inner part of the pump rotor, which works submerged in the liquid resulting from the domestic activities, is much corroded.

The rotor material was analyzed on the Foundry Master spectrometer and found to be a nodular cast iron alloyed with Ni and W. The chemical composition is shown in Table 1.

a) b)

***Fig. 7.*** *Single-channel low pressure centrifugal pump; a) a rotor; b) rotor corroded and worn area*

***Table 1.*** *The chemical composition of the pump rotor*

| Element | Fe | C | Si | Mn | P | S | Mo | Ni | W | Cr | Balance |
|---|---|---|---|---|---|---|---|---|---|---|---|
| Percent | 78.1 | 4.5 | 2.55 | 0.15 | 0.8 | 0.15 | 0.2 | 9.34 | 2.29 | 0.08 | 1.84 |

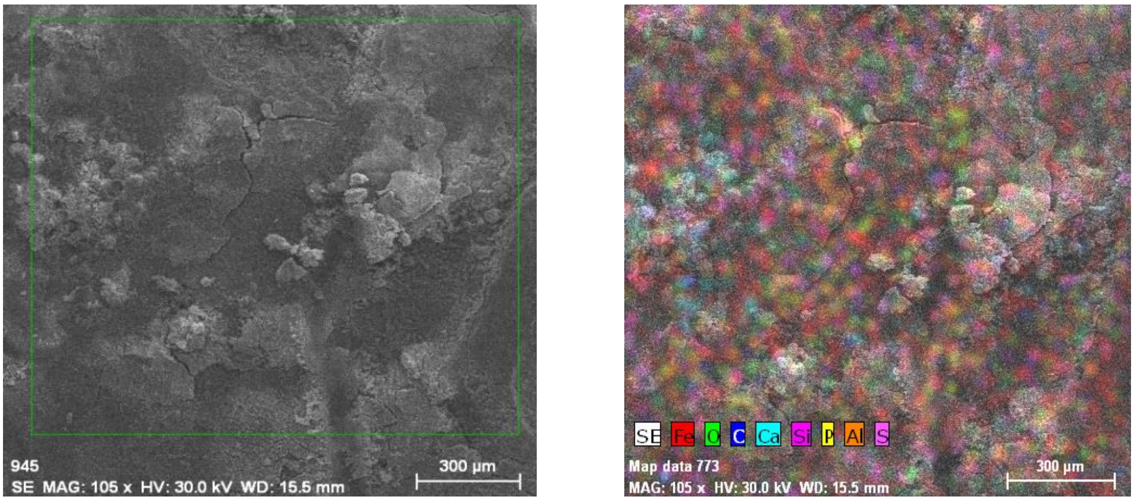


a) b)

***Fig. 8.*** *SEM microstructure of the pump rotor*

SEM analysis shows the presence of mixed oxide particles of waste substances from the wastewater. An EDX analysis was also carried out showing a distribution of the substances on the corrosion film area.

## 5. Conclusions

The analysis of the corrosive factors in the working environment of the waste water pumps requires finding efficient and relatively cheap solutions for improving wear and corrosion resistance of the transport galleries inside the pumps.

Materials used in the construction of pumps (brass, medium and high alloyed steels with Cr and Ni, alloyed cast iron) have good corrosion resistance characteristics, but are limited to wear resistance.

The pump analyzed is made of chromium and tungsten alloyed cast iron and shows in the work channel material rupture and tearing due to the solid particles moving with high speed into the pump cavities.

## References

**[1]. Pracht G., Perschnick N.**, *A material challenge – Pumps in sulphuric acid application*, Procedia Engineering, 138, p. 421-426, 2016.

**[2]. Karassik I. J.**, *Pump handbook*, (3rd ed.) McGraw-Hill, 2001.

**[3]. Escobar J. A.**, **Romero A. F., Lobo-Guerrero J.**, *Failure analysis of submersible pump system collapse caused by assembly bolt crack propagation by stress corrosion cracking*, Engineering Failure Analysis, 60, p. 1-8, 2016.

**[4]. Swapan K. D., Parikshit M., Sandip G. C., Goutam D., Raghuvir S.**, *Effect of microstructures on corrosion and erosion of an alloy steel gear pump*, Engineering Failure Analysis, 40, p. 89-96, 2014.

**[5]. Christoph P.**, *Do coatings protect against corrosion and wear?*, World Pumps, p. 32-38, November 2005.

**[6]. Pantazopoulos G. A.**, *A process-based approach in failure analysis*, J Fail Anal Prev, 14(5), p. 551-553, 2014.

**[7]. Tian H. H., Addie G. R., Visintainer R. J.**, *Erosion-corrosion performance of high-Cr cast iron alloys in flowing liquid–solid slurries*, Wear, 267, p. 2039-2047, 2009.

**[8]. Smith P., Kraenzler T.**, *Reducing effects of corrosion and erosion*, World Pumps, p. 38-41, 2017.

**[9]. Psyllaki P. P., Pantazopoulos G., Pistoli A.**, *Degradation of stainless steel grids in chemically aggressive environment*, Eng Fail Anal, 35, p. 418-26, 2013.

**[10]. Metwally I. A., Gastli A.**, *Correlation between eddy currents and corrosion in electric submersible pump systems*, International Journal of Thermal Sciences, 47, p. 800-810, 2008.

**[11]. Azimian M., Bart H. J.**, *Erosion investigations by means of a centrifugal accelerator erosion tester*, Wear, 328-329, p. 249-256, 2015.

**[12]. Vazdirvanidis A., Pantazopoulos G., Rikos A.**, *Corrosion investigation of stainless steel water pump components*, Engineering Failure Analysis, xxx, p. 1-8, 2016.

**[13]. Vanaei H. R., Eslami A., Egbewande A.**, *A review on pipeline corrosion, in-line inspection (ILI), and corrosion growth rate models*, International Journal of Pressure Vessels and Piping, 149, p. 43-54, 2017.

**[14]. Hernandez-Sandoval J., Gonzalez-Lopez R., Hernandez-Rodriguez M. A. L., Guzmán A. M.**, *Localized corrosion in an electrical submergible pump (ESP)*, Engineering Failure Analysis, 53, p. 124-131, 2015.

**[15]. Larson T. E.**, *Corrosion by Domestic Waters*, Illinois State Water Survey, Urbana, Bulletin, 59, p. 1-28, 1975.

**[16]. Luukkonen T., Heyninck T., Ramo J., Las U.**, *Comparison of organic paracids in wastewater treatment: Desinfection, oxidation and corrosion*, Water Research, vol. 85, p. 275-285, 2015.

**[17]. Jin J., Wu G., Zhang Z., Guan Y.**, *Effect of extracellular polymeric substances on corrosion of cast iron in the reclaimed wastewater*, Bioresource Technoloy, vol. 165, p. 162-165, 2014.

**[18]. Mahbuboor R. Choudhury, Ming-Kai Hsieh, Radisav D. Vidic, David A. Dzombak**, *Corrosion management in power plant cooling system using tertiary-treated municipal wastewater as makeup water*, Corrosion Science, vol. 61, p. 231-241, 2012.

**[19]. Neethling J. B., Mah R. A., Stenstrom M. K.**, *Causes and control of concrete pipe corrosion*, University of California, 1989.

**[20]. Hari P. N.**, *Sediment Erosionin HydroTurbines*, (Ph.D thesis), Faculty of Engineering Science and Technology, Norwegian University of Science and Technology (NTNU), Trondheim, Norway, 2010.

**[21]. Adnan A. N., Man-Hoe K.**, *Erosion wear on centrifugal pump casing due to slurry flow*, 364-365, p. 103-111, 2016.

THE ANNALS OF "DUNAREA DE JOS" UNIVERSITY OF GALATI
FASCICLE IX. METALLURGY AND MATERIALS SCIENCE
Nº. 3 - 2017, ISSN 1453-083X

# STUDIES REGARDING THE PROPERTIES MODIFICATION OF AISI 310S STEEL

**Dragoș-Cristian ACHIȚEI, Ramona CIMPOEȘU, Manuela-Cristina PERJU, Nicanor CIMPOEȘU, Andrei-Cătălin ȚUGUI**
"Gheorghe Asachi" Technical University of Iași, Romania
e-mail: dragos_adc@yahoo.com

## ABSTRACT

*The paper presents an analysis of classical heat treatments, which can be applied to AISI310S steel samples. The influence of these heat treatments was highlighted by micro-hardness measurements – Vickers method, and also the structural analysis made on electronic microscope, at different magnitudes. The AISI 310S steel is part of chrome-nickel stainless steels and presents good resistance properties. These properties are due to principal alloying elements (nickel, chrome) and recommend its being used in corrosive medium and high temperatures.*

KEYWORDS: steel, properties, stainless, refractory

## 1. Introduction

The alloying of the steel with various chemical elements can induce a good corrosion resistance in aggressive environments, in water, in atmosphere or at high temperatures oxidation.

Alloying elements help the appearance of a superficial layer, compact and adherent of resistant oxides at the chemical action of the work environment.

The stainless or refractory steels are alloyed with chrome or chrome-nickel in order to enhance their resistance at chemical action of the environment. In combination with elements which present a high tendency to form carbides, like titanium, niobium, molybdenum and tungsten, the chrome-nickel high alloyed steels form the base of austenitic and austenitic-ferrite refractory steels.

The refractory and anticorrosive steels are high alloyed with chrome, with additions of:

- Aluminum and silicon – which increase the oxidation resistance at high temperatures;
- Molybdenum, vanadium and tungsten – which increase the resistance properties;
- Nickel – which increase the tenacity and plastic deformation processing.

The stainless steels present a good chemical stability associated with good mechanical properties, especially long-time resistance.

Oxidation resistance at high temperatures of refractory steels is assured by the forming of a stable layer, compact, protector of oxides: $SiO_2$, $Cr_2O_3$ and $Al_2O_3$. The stainless steels alloyed with nickel can be used in cryogenic environments.

The structure of laminated or forged austenitic steels consists in an austenitic mass with numerous special carbides included. The special carbides, included in base mass, stopped the slippage and harden the plastic deformation at the work temperatures in exploitation. The δ ferrite, which appears in austenite – ferrite steels, is often unstable and is discomposed even at higher annealing temperatures, and also at maintaining work temperatures in exploitation.

To point out the existent structural constituents, a multiple attack is necessary. Through royal water attack are first revealed the outlines of different crystallites. The next electrolytic attack with chromic anhydride 10% in water solution has colored the fine carbides in black, meanwhile the σ phase was removed through dissolution.

## 2. Experiments

### *2.1. Determination of alloying elements*

The chemical composition is determined through quantitative spectral analysis, using a Foundry Masters optical spectrometer, type 01J0013, calibrated for iron analysis base.

***Table 1.*** *Chemical composition of analyzed samples (wt.%)*

| **Fe** | **C** | **Si** | **Mn** | **P** | **S** | **Cr** | **Mo** |
|---|---|---|---|---|---|---|---|
| 52.3 | 0.122 | 1.08 | 1.46 | 0.0272 | 0.005 | 24.1 | 0.12 |
| **Ni** | **Al** | **Co** | **Cu** | **Nb** | **Ti** | **V** | **W** |
| 20.1 | 0.0055 | 0.2 | 0.0837 | 0.0252 | 0.085 | 0.0714 | 0.02 |

## *2.2. Industrial applicability*

The analyzed steel is part of stainless steels, type 12NiCr120 – refractory and anticorrosive steels category.

The names it has are 1.4845 after EN10095; 310S after AISI; 12NiCr250 after STAS.

Stainless Steel 310, combining excellent high temperature properties with good weldability and ductility, is designed for high temperature service.

SS 310 resists oxidation in continuous service at temperatures up to 1150 °C provided reducing sulfur gases are not present. SS 310 is also used for intermittent service at temperatures up to 1040 °C.

Stainless Steel 310S is used when the application environment involves moist corrodents in a temperature range lower than that which is normally considered “high temperature” service.

The lower carbon content of SS 310S does reduce its high temperature strength compared to 310.

Typical applications: heat exchangers, furnace parts, combustion chambers, welding filler metals, gas turbine parts, jet engine rings, incinerators, recuperates, rolls for roller hearth furnaces.

## *2.3. Structural modifications induced through heat treatments*

Recommendations regarding the heat treatments regime applied to the refractory steels:

The martensitic and ferritic refractory steels will be submitted to some annealing heat treatments, regarding the increase of machine processing.

The annealing temperatures are between 750-850 °C, with maintaining times established according to chemical composition and thickness of the materials. It can be observed that after the recommended annealing, the steel has a plastic component.

The austenitic refractory steels will be subjected to solution quenching, to increase especially the corrosion resistance.

The samples were heat treated, according to the work specific parameters (see Table 2).

The heating and maintaining of heat treated samples were made in an electric furnace, with resistors and fixed hearth, type UTTIS CE12.

The samples have small dimensions and are obtained through cutting on METACUT 250 machine, using an abrasive disk and cooling with water.

***Table 2.*** *Mechanical properties and heat treatments*

| $R_{p0.2}$ [N/mm$^2$] | $R_m$ [N/mm$^2$] | $A_5$ [%] | HB | Annealing [°C] | Environment | Quenching [°C] | Environment |
|---|---|---|---|---|---|---|---|
| 225 | 490 | 20 | 140-190 | 850-900 | Furnace | 1050-1100 | Water |

***Table 3.*** *Adopted parameters of applied heat treatments*

| | Initial temperature [°C] | Final temperature [°C] | Maintaining time [min] | Cooling environment | Cooling speed |
|---|---|---|---|---|---|
| Annealing | 20 | 850 | 10 | Furnace | Slow |
| Quenching | 20 | 1100 | 10 | Water | Fast |

## *2.4. Structural analysis*

With the help of scanning electronic microscopy, we can obtain images of topography and characteristic composition of sample surface.

The formation of images is realized with the help of a primary electrons fascicle, very thin, which scan the sample surface.

Through the interaction of the primary electrons with the surface, some of them are refreshed, and another part determines the forming of the secondary electrons.

The image is realized with these electrons, either secondary, or refreshed, which creates a contrast dependent by the incident angle of fascicle and the sample composition.

Regarding the microscopic examination, the samples were cut with a machine with abrasive disk and water cooling, then polished on abrasive papers, polished on felt soaked with aluminum oxide and attacked with chemical reactive.

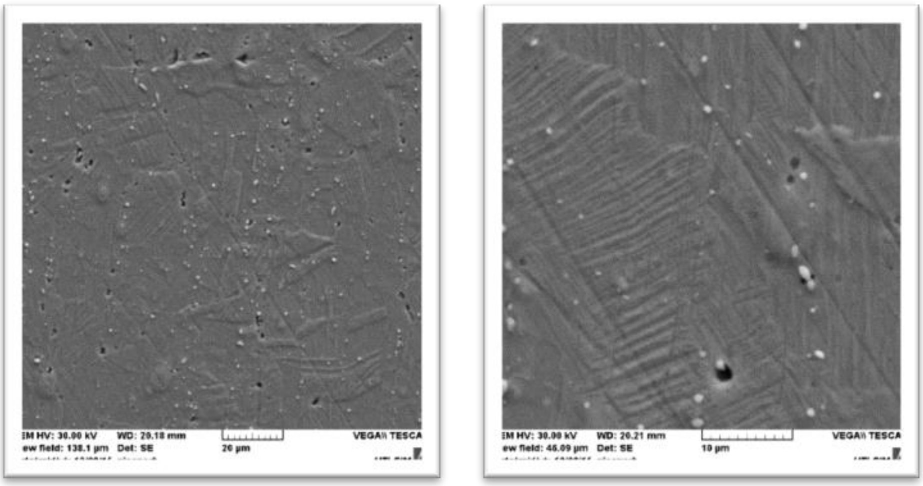

a. AISI 310 steel structures in initial state

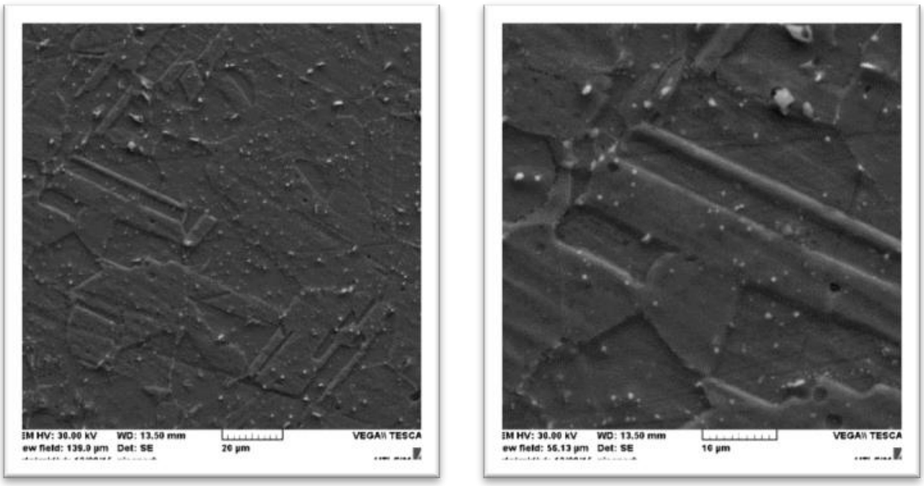

b. AISI 310 steel structure after annealing heat treatment

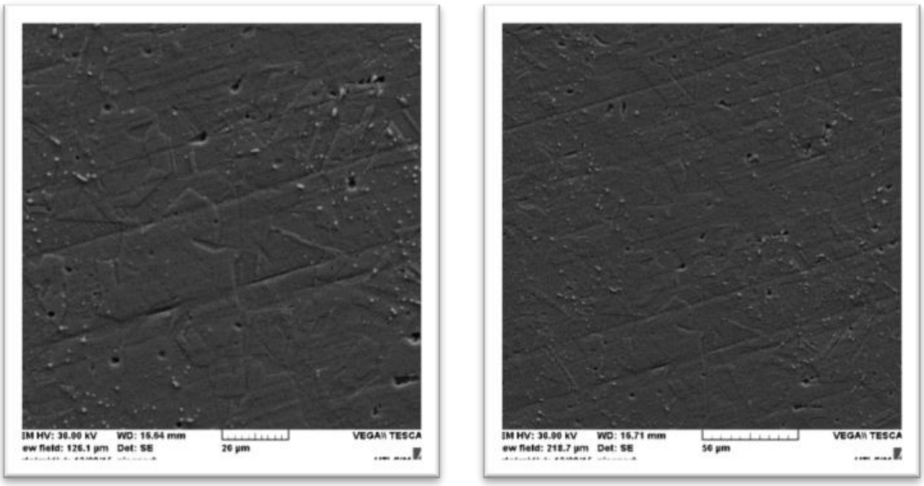

c. AISI 310 steel structure after quenching heat treatment

### *2.5. Hardness measurements*

The hardness determination provides indications regarding the mechanical resistance of the alloy, imposing or not the utility of applying the heat treatments.

Vickers microhardness method consists in pressing a pyramidal penetrator, with low speed and a certain force (in this case – 50 grams), on the sample material, for 15 seconds.

The analyzed samples were prepared through polishing on abrasive paper, to remove the oxide traces or other substances resulted from the polishing process.

***Table 4.*** *Measured values of hardness for the samples, after each heat treatment*

| Nr. | The initial state | | After annealing | | After quenching | |
|---|---|---|---|---|---|---|
| | HV | $HV_{med}$ | HV | $HV_{med}$ | HV | $HV_{med}$ |
| 1. | 472 | **438** | 268 | **269** | 369 | **325** |
| 2. | 425 | | 287 | | 313 | |
| 3. | 416 | | 251 | | 292 | |

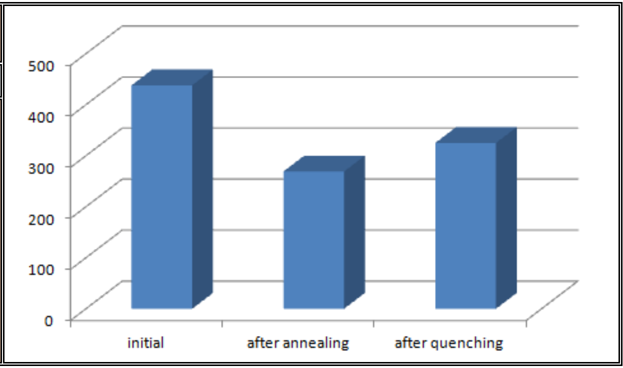


## 3. Conclusions

The quantitative determinations of alloying elements, made through the quantitative spectral analysis, have demonstrated that the analyzed samples fit in the imposed limits by standard for AISI 310 steel.

The diversity of industrial application where AISI 310 alloy is used imposes the study of some heat treatments of improving the machine processing and also establishing final properties necessary in exploitation.

That is why the recommended parameters were established according to specialty references and experiments were made at medium values of intervals.

The microstructure of AISI 310 was analyzed with the help of a Vega Tescan electronic microscope, with different magnitudes.

From the SEM images analysis specific structures of alloy in initial exploitation state can be highlighted, and also after the 2 applied heat treatments.

The evaluation efficiency of applied heat treatments was made with the help of hardness measurements, through Vickers microhardness method, using a loading force of 50 grams.

The obtained values fit in specific limits of the material and applied heat processing.

## References

**[1]. Hosseini H. Shah, Shamanian M., Kermanpur A.**, *Microstructural and weldability analysis of Inconel617/AISI 310 stainless steel dissimilar welds*, International Journal of Pressure Vessels and Piping, vol. 144, p. 18-24, 2016.

**[2]. Obadele Babatunde Abiodun, Andrews Anthony, Shongwe Mxolisi Brendon, *et al.***, *Tribocorrosion behaviours of AISI 310 and AISI 316 austenitic stainless steels in 3.5% NaCl solution*, Materials Chemistry and Physics, vol. 171, p. 239-246, 2016.

**[3]. Truşculescu Marin, Ieremia Aurel**, *Oţeluri inoxidabile şi refractare*, Editura Facla, Timişoara, 1983.

**[4]. Jun Tian Zhao, Yan Rui Zuo, Wei Ping Zhao**, *A study on mechanical and fatigue properties of a stainless steel*, Advanced Materials Research, vol. 1095, p. 79-82, 2015.

**[5]. Lun You Li, Ya Nan Hu**, *Electrochemical behavior of the initial atmospheric corrosion of 2Cr13 steel in Guiyang city atmosphere*, Advanced Materials Research, vol. 989-994, p. 446-449, 2014.

**[6]. Srikanth S., Saravanan P., Govindarajan P., Sisodia S., Ravi K.**, *Development of lean duplex stainless steels (LDSS) with superior mechanical and corrosion properties on laboratory scale*, Advanced Materials Research, volume 794, p. 714-730, 2013.

**[7]. Yeshwanth B. K., Senthil Kumar S., Hafeez Sharief B., Devendranath Ramkumar K., Narayanan S., Arivazhagan N.**, *Characterisation of microstructure, mechanical properties and corrosion behaviour on GTA welded AISI 310 and Inconel 800*, Advanced Materials Research, vol. 383-390, p. 5863-5868, 2011.

**[8]. Balachandran G., Balasubramanian V.**, *Stainless steel processing to meet advanced applications*, Advanced Materials Research, vol. 794, p. 135-158, 2013.

**[9]. Hosseini H. Shah, Shamanian M., Kermanpur A.**, *Characterization of microstructures and mechanical properties of Inconel 617/310 stainless steel dissimilar welds*, Materials characterization, vol. 62, issue 4, p. 425-431, 2011.

**[10]. Tavares S. S. M., Moura V., da Costa V. C., *et al.***, *Microstructural changes and corrosion resistance of AISI 310S steel exposed to 600-800 degrees C*, Materials characterization, vol. 60, issue 6, p. 573-578, 2009.

**[11]. Rafi H. Khalid, Ram G. D. Janaki, Phanikumar G., *et al.***, *Microstructure and properties of friction surfaced stainless steel and tool steel coatings*, THERMEC 2009, PTS 1-4 Book Series: Materials Science Forum, vol. 638-642, p. 864-869, 2010.

THE ANNALS OF "DUNAREA DE JOS" UNIVERSITY OF GALATI
FASCICLE IX. METALLURGY AND MATERIALS SCIENCE
N°. 3 - 2017, ISSN 1453-083X

# INTRODUCTION TO METALLIC BIOMATERIALS

**Dragoș-Cristian ACHIȚEI[1], Petrică VIZUREANU[1], Mirabela-Georgiana MINCIUNĂ[1], Andrei-Victor SANDU[1], Al Bakri Abdullah MOHD MUSTAFA[2]**
"Gheorghe Asachi" Technical University of Iași, Romania
e-mail: dragos_adc@yahoo.com

## ABSTRACT

*The paper presents a bibliographic study about the metallic biomaterials, synthesizing the aspects related to properties, applicability, obtaining methods. Biomaterials can be used as medical devices, implants and prostheses. The metallic biomaterials are classified, by chemical composition and structure, in: pure technical metals, metallic alloys and composites with metallic matrix. The material quality of an implant must respect the following criteria: biochemical criteria and biomechanical ones. According to the biochemical criterion, the applicability of a material is determined by its biocompatibility, and from the biochemical criteria, it is determined by the fatigue resistance, the most important parameter, but not the only one.*

KEYWORDS: biomaterial, alloys, nickel, chrome, steel, biocompatibility

## 1. Introduction

A biomaterial can be defined in two ways: a synthetic material used to replace a part of the human body or to function straight with a living tissue or an inert biological substance destined for implantation in the living systems [1].

The successful usage of a biomaterial depends on 3 main factors as:

- properties and biocompatibility;
- health state of the patient;
- the efficiency of the surgeon who uses the implant.

According to the chemical composition and physical structure, the metallic biomaterials are classified in:

- pure technical metals;
- metallic alloys;
- composites with metallic matrix.

***Table 1.*** *Biomaterials classification*

| | | | | | |
|---|---|---|---|---|---|
| Medical device | Implant | Prosthesis | Surgical alloy | Artificial organ | Biocomposite |

A. Metals are used in medical field, currently, as surgical implants, as dental materials and in the making of different devices.

There are over 30 metallic elements used in medicine in the shape of:

- implants and orthopedics and dentistry prosthesis: Al, Co, Cr, Fe, Mn, Mo, Nb, Ni, Sn, Ta, etc.;
- precious and semiprecious dental alloys with: Ag, Au, Cu, Ga, In, Ir, Pd, Pt, Rh, Ru, Sn, Ti, Zn, etc.;
- non-precious dental alloys: Al, B, Be, Cd, Co, Cr, Fe, Mn, Mo, Ni, Si, Ti, V, W.

B. Alloys used like surgical implants in orthopedic and dentistry, are divided in:

- austenitic stainless steels;
- cobalt base alloys;
- titanium base alloys.

The most used alloys are the ones based on cobalt – chrome (cca. 70%), followed by titanium alloy; the last one has excellent biocompatibility properties [2, 3]. The dental alloys used for dental rehabilitation:

- crowns and connecting decks;
- glued porcelain on metallic alloys;
- wires for correcting teeth;
- metallic teeth from dental alloys;
- alloys for brazing dental works.

There are over 1000 dental alloys, which are classified in 4 subgroups:

- precious alloys with Au, Pt, Ag content;
- semi-precious alloys with low Au content, but based on Pd;
- non-precious alloys from stainless steel, Co-Cr and Ni-Cr group;
- titanium base alloys.

C. Composite materials with metallic matrix – to which belong:

- dental amalgam with Hg and Ga matrix;
- cermets materials;
- prosthetic components covered with different ceramic layers.

The superficial layers deposited on implants gives them special properties like: corrosion resistance, esthetic aspect, hardness and facilitates the development of the living tissue in the area [4].

## 2. Aspects regarding metallic biomaterials

### *2.1. Titanium and its alloys*

Titanium is an active element chemically wise and should corrode strongly in ambient conditions.

In reality this phenomenon does not manifest due to $TiO_2$ protector layer on its surface.

At air heat, titanium and its alloys strongly interact with the gases from the atmosphere, resulting chemical combinations, which forms the protector layer. When the temperature rises, the oxidation speed intensifies and the possibilities of an explosion happen. Also, the titanium mixes with the nitrogen and hydrogen, forming nitrides and hydrides [5].

Due to small density, associated with good mechanical properties, micro-alloyed titanium and its alloys are superior to the other metallic materials, having a higher resistance (30-40 $daN/mm^2$) reported at density, which is superior to higher alloyed steels (15-35 $daN/mm^2$).

***Table 2.*** *Classification criteria of titanium*

| | |
|---|---|
| *After processing* | Plastic deformable alloys |
| | Cast alloys |
| *After properties* | High plasticity and medium resistance alloys |
| | Enough plastic and high resistance alloys |
| | High corrosion resistance alloys |
| | Super plastic alloys |
| | Amorphous alloys |
| | Shape memory alloys |
| *After the usage field* | For welding constructions |
| | For aviation and space technique |
| | For chemical industry |
| | For prosthetic devices |
| *After structure* | Alloy with Ti$\alpha$ structure |
| | Alloys with $\alpha+\beta$ structure (biphasic) |
| | Alloys with Ti$\beta$ structure |

Titanium alloys which are used in surgical implants manufacture are Ti6Al4V. In specialty references there also appears titanium alloys: TiSnMoAl and Ti13V11Cr3Al.

The TiSnMoAl alloy are known under HILITE 50 commercial name and contain 4 %Al, 2 %Sn and 4 %Mo, difference Ti and are characterized by a high usage resistance.

***Table 3.*** *Chemical composition of Ti6Al4V alloy*

| Al | V | Fe | Other elements | | C | Ti |
|---|---|---|---|---|---|---|
| 5.5-6.5 | 3.5-4.5 | max 0.25 | 0.1 each | 0.4 total | max 0.08 | Difference |

Because of the high melting temperature, and also the sudden increase of chemical activity with the temperature, titanium alloys are elaborated in electrical arc furnace and through induction, only in protective atmosphere with vacuum or inert gases [6].

## *2.2. Cobalt – chrome cast alloys*

These alloys are open to oxidation during melting, and cast alloy is fragile and hard. The alloy has a high melting temperature.

The cooling contraction is 1.9% and makes it difficult to achieve the dimensional accuracy asked by the pattern [7].

Because of that, these alloys are not recommended for precise castings, like teeth crowns or connecting decks, meanwhile their use as a support for melted porcelain is not recommended due to the oxidation suffered by the alloys at work temperature.

Nevertheless, the materials have a good corrosion resistance and are highly tolerated in the mouth cavity.

***Table 4.*** *General composition of a Co-Cr biomaterial*

| Co | Cr | Mo | C | Ni |
|---|---|---|---|---|
| 65% | 25% | 5% | 0.2-0.35 | difference |

The chrome percentage improves the oxidation resistance of the alloys; if the value is over 30%, it will lead to difficulties at casting.

The cobalt increases the elasticity modulus, resistance and hardness higher than nickel.

The safest way to increase the Co-Cr alloys properties is to increase the carbon content. A change of only 0.02 %C modifies the properties in such a way that the alloy cannot be used in stomatology.

In medicine the Co-Cr alloys are used as implantable devices. The Co-Cr alloys are metastable and crystalize in CFC system, and the carbides are present at grains boundary.

The melting temperature is situated between 1250-1450 ºC and is over the melting capacity realized by a natural gas flame; their melting in electromagnetic induction furnace is recommended.

## *2.3. Nickel – chrome cast alloys*

Ni-Cr alloys gained the attention of researchers with the limitations discovered at Co-Cr alloys: low ductility, high contraction at solidification and a rise tendency to oxidation.

In the industry, these alloys are known as NIMONIC and have applications in reaction engine technology.

***Table 5.*** *General composition of a Ni-Cr biomaterial*

| Ni | Cr | Mo | W | Mn | Be | C |
|---|---|---|---|---|---|---|
| 68-80% | 10-25% | 0-13% | 0-7% | 0-6% | 0-2% | 0.1-0.2% |

With these elements we can find small amounts of Al, Ti, Co, B, Si. These alloys are excellent as a support for melted porcelain.

The alloys crystalize in CFC system, and the cast material has a structure with big grains which indicate a dendritic structure.

The solidification contraction is 1.5%, and the alloys melt naturally in induction furnaces and are casting in phosphatic forms.

Because of the low temperature field, the Ni-Cr alloys provide a more precise casting which make the connecting decks and dental crown to have minimal flaws.

## *2.4. Silver-palladium cast alloys*

Silver and palladium present total solubilization.

While Pd has a high affinity for $H_2$ and a high melting temperature (Ttop = 1552 °C), Ag has a lower temperature and is appropriate for base alloys casting.

The cast Ag-Pd alloys are Ag-Pd-Cu ternary system, which can be multi-phasic or mono-phasic.

To theses alloys, we can apply hardened heat treatments through precipitation.

***Table 6.*** *General composition of a Ag-Pd biomaterial*

| Ag | Pd | Cu | Au | Zn |
|---|---|---|---|---|
| 45% | 25% | 15% | 14% | 1% |

These values can vary according the required precision of final element.

The cast precision takes in consideration the attention with which the melting is made, and also its realization in controlled atmosphere.

Materials can be used as a support for melted porcelain, but we have to keep in consideration the porcelain affinity for silver, which leads to obtain a greenish color of them.

The alloys can be hardened through precipitation when the melted porcelain is deposit on them.

## *2.5. Stainless steels*

The first stainless steel used in metallic implants was AISI 302 steel, which is harder than vanadium steel and has good corrosion resistance properties.

The vanadium-alloyed steel cannot be used, because it has an inadequate corrosion resistance.

After, it was introduced AISI 302 steel alloyed with molybdenum to improve the corrosion resistance in salt water. This alloy is AISI 316 steel.

The carbon content was reduced from 0.08% to 0.03%, to obtain a good corrosion resistance in chlorine solution.

The steel becomes AISI 316L steel.

Chrome is a major element in corrosion resistant stainless steels. The minimal concentration is 11%. Chrome is a reactive element, but its alloys can passivate, having an excellent corrosion resistance

***Table 7.*** *Chemical composition of AISI 316 and AISI 316L stainless steels*

| % | C | Cr | Ni | Mo | Mn | Si | P | S | Fe |
|---|---|---|---|---|---|---|---|---|---|
| AISI 316 | 0.006 | 17-20 | 12-14 | 2-4 | 2 | 0.75 | 0.03 | 0.03 | Rest |
| AISI 316 L | 0.002 | 17-20 | 12-14 | 2-4 | 2 | 0.75 | 0.03 | 0.03 | rest |

These stainless steels can be used for metallic implants.

They cannot be hardened through heat treatments but can be hardened through cold processing.

The AISI 316 steel is nonmagnetic and presents a higher corrosion resistance than another stainless steel, also molybdenum alloying increases pitting corrosion resistance in salt water.

Although it is known like a toxic element, nickel is found in chemical composition like alloying element which stabilizes the austenite at ambiance temperature and more, increases the corrosion resistance [8, 9].

The austenite stability at low temperature is also influenced by the chrome content.

The austenitic stainless steels suffer a gardening process in exploitation, that being the reason why it cannot be cold processed without intermediary heat treatments.

The heat treatment cannot determine the appearance of chrome carbides at grains boundary, carbides which can cause the corrosion phenomena formation.

ASM International recommend the AISI 316L steel usage to implants manufacture.

In stomatology, the stainless steels are used to fabricate wires and crowns for partial teeth.

## 3. Conclusions

Biomaterials release ions and metallic particles in the human body, which will concentrate in urine, blood, nails, hair and tissue around implants.

There is danger for allergic reactions or immunological and inflammatory reactions.

The dental alloys based on precious or semi-precious metals are inert and perfectly biocompatible.

Out of biomaterials, titanium and its alloys are the materials which correspond to mechanical, chemical and biological requirements.

Some metals like beryllium, nickel and mercury are already considered prohibited in the human body. Nickel is considered one of the most dangerous metals used like biomaterial.

The metal effects like chemical element are different from its compounds, oxides and organic compounds; these increase the risk of pathological reaction production in human body.

It is recommended the usage of implants or prosthesis superficial covered with various protective films, which are inert to the human body and sometimes can facilitate the development of bone cells.

## References

**[1]. Jiang X. J., Yu G., Feng Z. H., *et al.***, *Abnormal beta-phase stability in TiZrAl alloys*, Journal of Alloys and Compounds, vol. 699, p. 256-261, 2017.

**[2]. Hu Shunbo, Jia Fanhao, Marinescu Cornelia, *et al.***, *Ferroelectric polarization of hydroxyapatite from density functional theory, RSC Advances*, vol. 7, issue 35, p. 21375-21379, 2017.

**[3]. Mareci D., Cimpoesu N., Popa M. I.**, *Electrochemical and SEM characterization of NiTi alloy coated with chitosan by PLD technique*, Materials and Corrosion-Werkstoffe und Korrosion, vol. 63, issue 11, p. 985-991, 2012.

**[4]. Elshalakany Abou Bakr, Ali Shady, Amigo Mata A., *et al.***, *Microstructure and Mechanical Properties of Ti-Mo-Zr-Cr Biomedical Alloys by Powder Metallurgy*, Journal of Materials Engineering and Performance, vol. 26, issue 3, p. 1262-1271, 2017.

**[5]. Li Yong-Hua, Chen Nan, Cui Hai-Tao, *et al.***, *Fabrication and characterization of porous Ti-10Cu alloy for biomedical application*, Journal of Alloys and Compounds, vol. 723, p. 967-973, 2017.

**[6]. Franco Arias L. M., Kleiman A., Vega D., *et al.***, *Enhancement of rutile phase formation in $TiO_2$ films deposited on stainless steel substrates with a vacuum arc*, Thin Solid Films, vol. 638, p. 269-276, 2017.
**[7]. Hu Shunbo, Jia Fanhao, Marinescu Cornelia, *et al.***, *Ferroelectric polarization of hydroxyapatite from density functional theory*, RSC Advances, vol. 7, issue 35, p. 21375-21379, 2017.
**[8]. Izquierdo Javier, Bolat Georgiana, Cimpoesu Nicanor, *et al.***, *Electrochemical characterization of pulsed layer deposited hydroxyapatite-zirconia layers on Ti-21Nb-15Ta-6Zr alloy for biomedical application*, Applied Surface Science, vol. 385, p. 368-378, 2016.
**[9]. Mareci D., Cimpoesu N., Popa M. I.**, *Electrochemical and SEM characterization of NiTi alloy coated with chitosan by PLD technique*, Materials and Corrosion-Werkstoffe und Korrosion, vol. 63, issue 11, p. 985-991, 2012.

THE ANNALS OF "DUNAREA DE JOS" UNIVERSITY OF GALATI
FASCICLE IX. METALLURGY AND MATERIALS SCIENCE
Nº. 3 - 2017, ISSN 1453-083X

# STUDY ABOUT THE PERCEPTION OF PRODUCERS FROM ROMANIA REGARDING THE ECOLABEL

**Antonina TEMEA*, Valentin NEDEFF,**
**Mirela PANAINTE-LEHĂDUŞ, Narcis BÂRSAN, Claudia TOMOZEI**
Department of Environmental Engineering and Mechanical Engineering, „Vasile Alecsandri" University of Bacău, România
e-mail: ninatemea@yahoo.com

## ABSTRACT

*The purpose of this paper is to obtain information about the Romanian producers' perspective on some key elements regarding the environmental aspects of their company, data on the certification SR EN ISO 14001: 2015 and the ecolabel in Romania. A questionnaire of 25 questions was developed and used for data collection, which was sent between February - April 2017 by email to approximately 531 companies representing the five active sectors in Romania. We received 189 responses that will help us to identify the main issues related to the certification SR EN ISO 14001: 2015, the ecolabel and the environmental aspects of different industries. There is a relatively low interest of companies in assessing environmental performance using independent tools. However, the low percentage of participating companies responding to the questions is relatively small, which shows that companies that really wanted to make a comprehensive environmental management assessment have been looking to answer as many as possible of questions.*

KEYWORDS: ecolabel, certification, environmental aspects, producers

## 1. Introduction

Eco labeling is fundamentally different from any other type of certification, primarily because it intends to award environmental performance [1]. Eco-labels are based on determining the life cycle of a product, informing the consumer about the impact a product has on the environment in its various stages of production, distribution, use and disposal [2].

Ecolabels are granted on request by different public and private organizations, being recognized at local, national, regional or international level. Often there are several types of eco-labels that coexist at the same time [3]. Accepting a certain type of eco-labeling is optional, and is usually based on reputation, trust and awareness [4].

An economic operator wishing to obtain a European Ecolabel for one or more of its products must request this from the competent authority. If the product meets the requirements, then it is awarded a European Ecolabel [5].

Environmental management systems are some of the most important strategic tools by which firms can turn environmental protection into an organizational objective, translated into responsible policies and operationalization actions [3]. Worldwide there are two standards that companies, but others, such as public authorities or NGOs, can adopt for the effective design and implementation of an environmental management system: ISO 14001 developed by the International Standard Organization and EMAS (Eco-Management and Audit Scheme - European Eco-Management and Audit Scheme) [6]. The EMAS Regulation, which is more ambitious than ISO 14001, is less well known in Romania, as our country is actually one of the most European EMAS records [7].

## 2. Research methodology

Within the research, a number of 21 organizations that have obtained the Eco-label and 10 EMAS-certified organizations were identified in Romania. As for organizations and firms that have ISO 14001 certification, their number is quite high (at the level of 2009 there were 5,853 companies reaching the level of 2016 at 10581) [8]. According to the Ecolabel scheme, five product groups were selected as follows: textile products, chemical industry, paper industry, tourism services, electrical components, which are of interest in the research [9].

It was first identified in the national database, which is the production sector of each of the SR EN ISO 14001: 2015 certified companies, and the subgroups of certified companies SR EN ISO 14001: 2015 whose production sector is part of those for which EU Ecolabel criteria have been established.

Fig. 1 shows the number of companies identified in Romania that hold ISO 14001 certification as well as the number of non-certified ones.

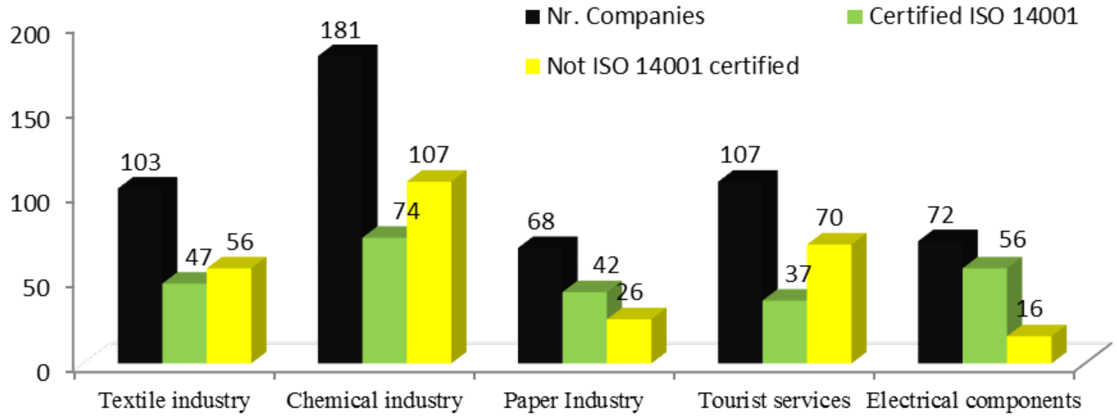


***Fig. 1.*** *Presentation of number of Romanian companies holding / not holding ISO 14001 certification*

Sample size. Questionnaires were sent to all businesses where we could find contact information. We got answers from 189 companies but the response rate is not 50 %.

Managing questionnaires. The questionnaires were applied online. The average duration of a questionnaire is about 20 minutes. In order to increase the response rate and, implicitly, the quality of the sample, respondents who did not respond to the first e-mail were sent another email after a period of up to 2 weeks.

## 3. Results and discussion

Out of a total of 531 companies selected to participate in the survey, 189 companies responded affirmatively (Fig. 2), and 15 companies responded to email and did not want to fill in the questionnaire for various reasons.

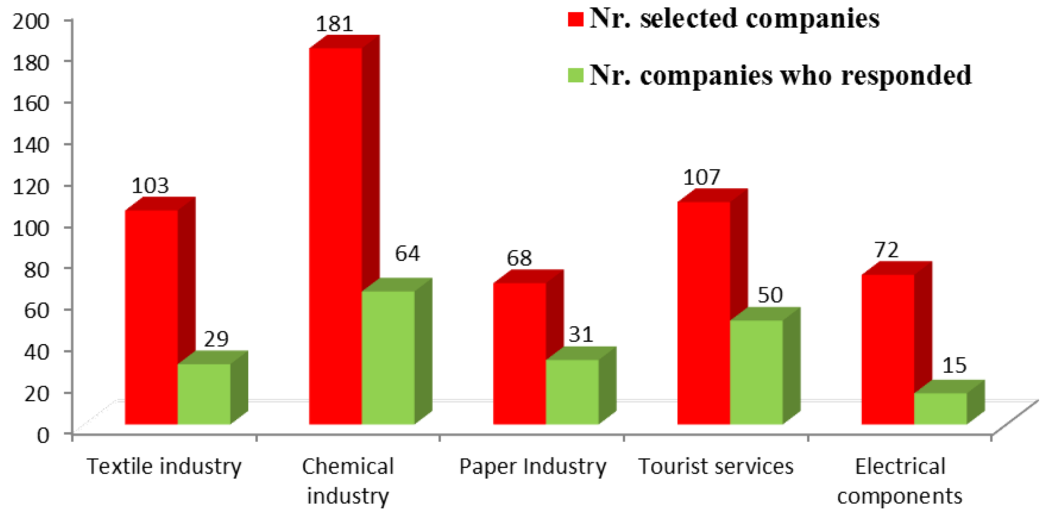


***Fig. 2.*** *Number of companies selected for study*

As regards the number of certified companies according to SR EN ISO 14001: 2015, 118 companies (62.4 %) have certification and 71 companies (37.6 %) not certified ISO 14001: 2015. They completed the questionnaire and 3 companies that have an eco-label.

There is, however, a relatively low interest of companies in assessing environmental performance using independent tools. However, the low percentage of responding companies responding to the questions is relatively small, which shows that those companies that really wanted to make a comprehensive assessment of their environmental management efficiency were looking to answer as many as possible questions.

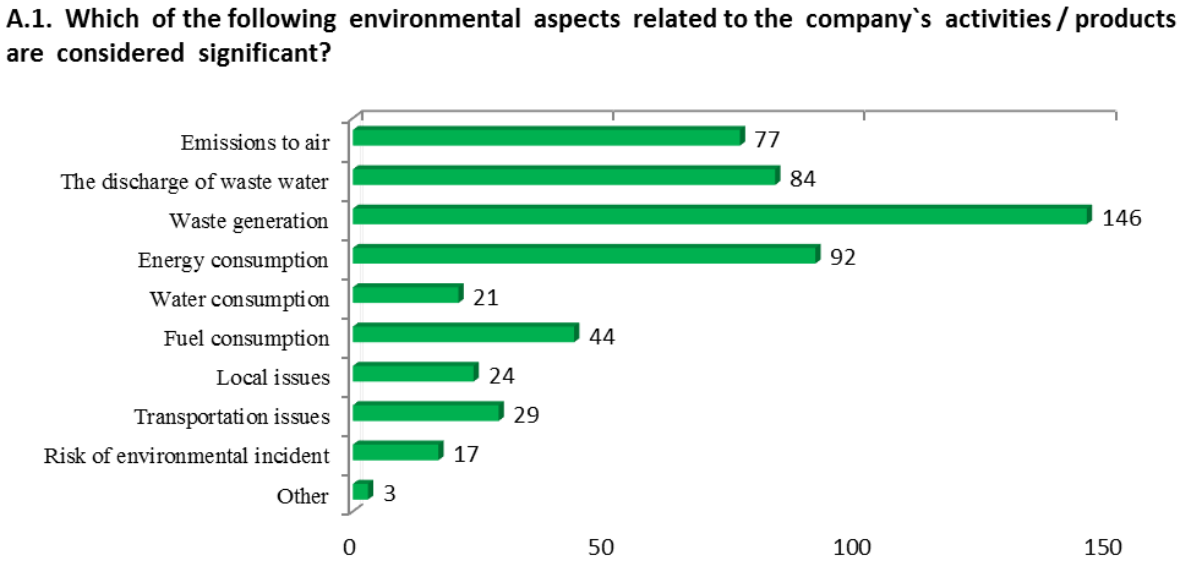


***Fig. 3.*** *List of significant environmental aspects in companies*

Regarding the significant environmental aspects, they can be seen in Fig. 3, with 83.9 % of waste generation being among the most important environmental considerations, after which the energy consumption reaches 52.9 % and waste water discharge 48.3 %. On the opposite side there is the risk of environmental incidents of 9.8 %.

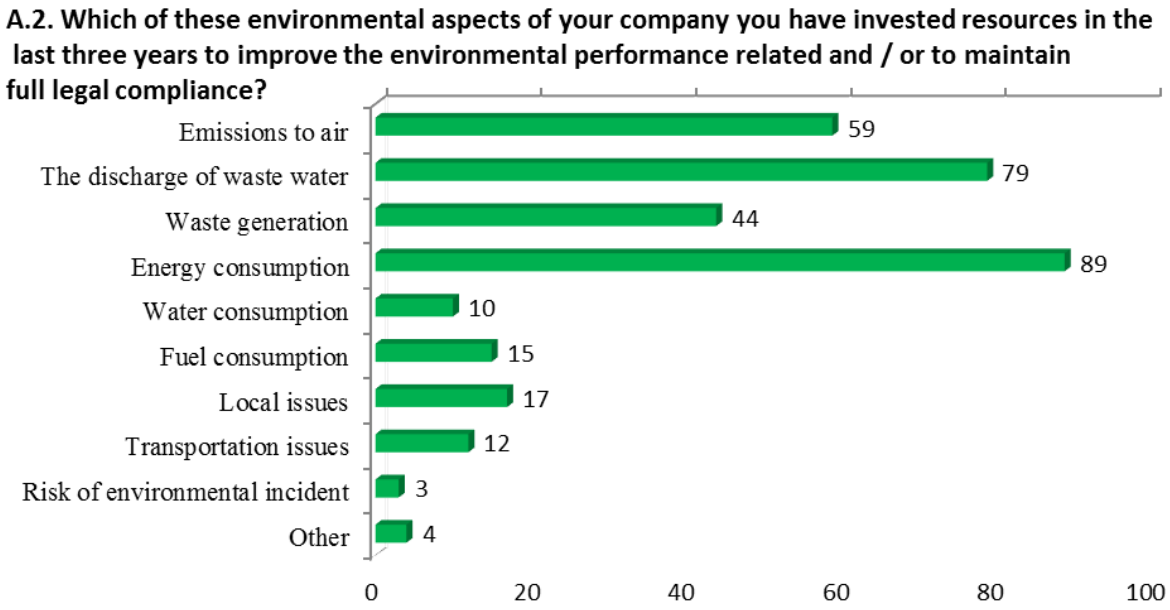


***Fig. 4.*** *List of environmental aspects for which resources have been invested in the past 3 years*

More and more types of organizations are increasingly concerned about achieving and demonstrating clear environmental performance by controlling the impact of their own activities, products or services on the environment and taking into account their environmental policy and objectives. A percentage of 50.6 % showed that the reduction in energy consumption was the most invested in in the last 3 years and at least 1.7 % (Fig. 4) was used to prevent the risk of environmental incidents.

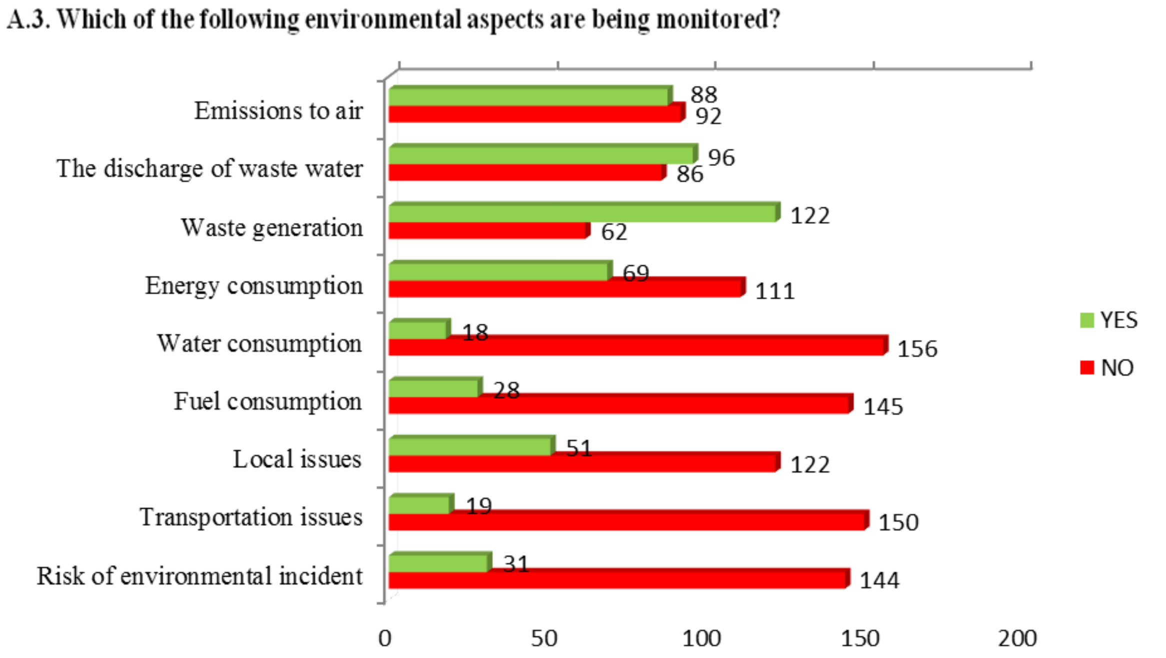


***Fig. 5.*** *Environmental aspects monitored*

Monitoring environmental issues is very important in a company that wants to protect the environment. The most monitored environmental aspect is waste generation (122 companies monitor), followed by waste water discharge (96) and air emissions (88). On the opposite side are energy consumption (156) and transport problems (150).

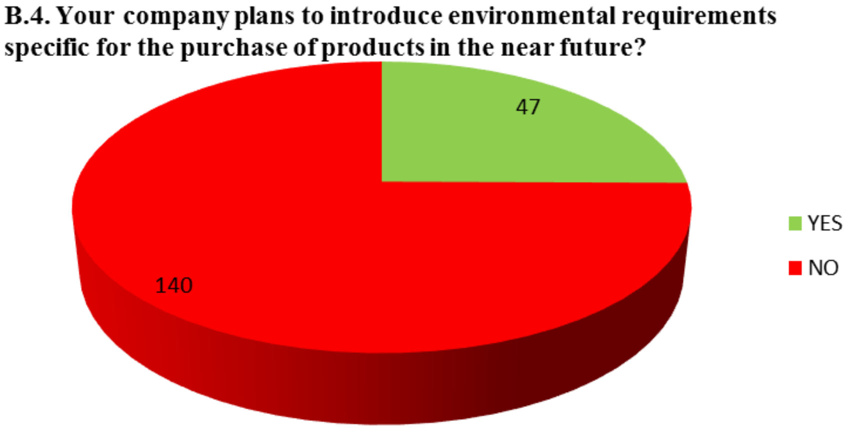


***Fig. 6.*** *Company opinion about the environmental requirements in the future*

Regarding the environmental requirements, there is an increasing interest of companies to introduce them in the future for the purchase of products, 47 companies have said this (Fig. 6).

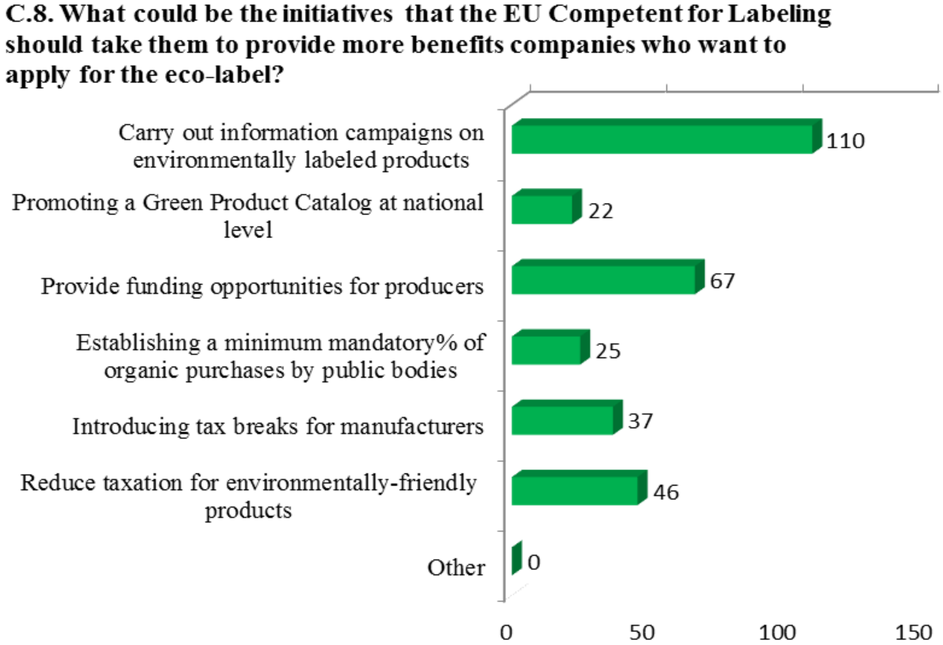


***Fig. 7.*** *Initiatives that the National Organic Labeling Competent Body should take to provide more benefits to companies wishing to apply for the eco-label*

Producers are of the opinion that the EU Organic Competent Organizing Committee should undertake a series of initiatives including: information campaigns on eco-labeled products (78 %), provision of financing opportunities for producers (47.5 %) and the reduction of annual eco-label fees (32.6 %).

In this paper, only a part of the questionnaire results is included and also a small part of the implemented graphics.

## 4. Conclusions

The objective of the questionnaire was to obtain an objective point of view of the producers regarding the SR EN ISO 14001: 2015 certification, the ecological label and the environmental aspects of the company.

In view of the above and the fact that Romania is still making timely progress in enhancing environmental performance, we believe that sustained progress on environmental protection should become a priority for all Romanian organizations. Leaving aside the obligation to comply with EU requirements, which should not be neglected, businesses must perceive the benefits that can be achieved through the implementation of EMS, such as SR EN ISO 14001: 2015, EMAS or the eco-label.

The current market context no longer allows the organization to make decisions without prior investigation into the environment in which it operates, as consumers' requirements are evolving in an accelerated way, competition is becoming more and more fierce, and macroeconomic and legislative elements can have a decisive influence on success or failure of the company on the market. Any decision on the organization's activity should be based on concrete data on the dimensions and components of the marketing environment of the organization in question, so that the products and / or services offered it offers are in line with market requirements.

A general conclusion is that due to the competitive advantages for the producers of goods and service providers and the increasing interest of consumers in these products, it is expected that the number of eco-labeled products will increase significantly in the near future. Since the first eco-labeled product in 2005, the average eco-labeling of products in Romania is one per year, the theory of practice is not very appropriate in this case.

## References

**[1]. Aindrila B., Mousumi R.**, *Green products: an exploratory study on the consumer behaviour in emerging economies of the East*, Department of Management Studies, National Institute of Technology Durgapur, 713209, India, 2007.
**[2]. Biondi V., Frey M., Iraldo F.**, *EMS and SMEs – motivations, opportunities and barriers related to EMAS and ISO 14001 implementation*, Greenleaf Publishing, 2000.
**[3]. Boiral O., Henri J. F.**, *Modelling the impact of ISO 14001 on environmental performance. A comparative approach*, Journal of Environmental Management, vol. 99, 2012.
**[4]. Comoglio C., Botta S.**, *The use of indicators and the role of environmental management systems for environmental performances improvement: a survey on ISO 14001 certified*

*companies in the automotive sector*, Journal of Cleaner Production, 20(1), p. 92-102, 2012.

**[5]. Dainora G., Rodica M.**, *Sustainable incentives in marketing and strategic greening: The cases of Lithuania and Romania*, Kaunas Faculty of Humanities, Vilnius University, Muitines g. 8, Kaunas, LT-44280, Lithuania, Faculty of International Business and Economics, Academy of Economic Studies Bucharest, Str. Mihai Eminescu 13-15, Sector 1, Bucharest, Romania Published online: 21 Oct. 2010.

**[6]. Durif F., Boivin C., Julien C.**, *In search of a green product definition*, Innovative Marketing, 6, p. 25-33, 2010.

**[7]. Lazar G., Nedeff V., Panainte M., Caraman I., Mosnegutu E., Muraru C., Inglezakis V. J., Zorpas A., Venetis C., Coutsikos P.**, *A market research for eco-labeled products in Romania*, Proceedings of the 12th International Conference on Environmental Science & Technology CEST, 131, ISBN 978-960-7475-49-7, 2011.

**[8]. Inglezakis V. J., Zorpas A., Nedeff V., Lazar G., Panainte M.**, *Green products and eco-labelling: an EU-project in Romania, Second International Symposium on Green Chemistry for Environment and Health*, Mykonos, Greece, September 26-29, 2010.

**[9]. Mirela P. Vasilis I., Iuliana C., Mihai C. Nicolescu, Emilian M., Florin N.**, *The evolution of eco-labeled products in Romania*, "Vasile Alecsandri" University of Bacau, Romania, 600115, Bacau, Roumania; Nazarbayev University, School of Engineering, Chemical Engineering Department, 53 Kabanbay Batyr Ave., 010000, Astana, Kazakhstan, SC European Focus Consulting SRL, Banatului 16, Bacau, Romania.

THE ANNALS OF "DUNAREA DE JOS" UNIVERSITY OF GALATI
FASCICLE IX. METALLURGY AND MATERIALS SCIENCE
Nº. 3 - 2017, ISSN 1453-083X

# THE IMPORTANCE OF USING MEMBRANES IN SEAWATER DESALINATION AS A RESULT OF EXCESSIVE EXPLOITATION OF WATER SOURCES

**Laurențiu TĂTARU, Valentin NEDEFF, Narcis BÂRSAN, Mirela-Panainte LEHĂDUȘ, Dana-Alexandra CHIȚIMUȘ**
Department of Environmental Engineering and Mechanical Engineering, "Vasile Alecsandri" University of Bacău, street Mărășești 157-Bacău, România
e-mail: tataru_lauri@yahoo.com

## ABSTRACT

*This paper is a detailed study of the need to find and implement new solutions for water filtration and the promotion of modern techniques that are more effective than traditional methods. As a result of extension waste water pollution as well as low efficiency through classical filtration means, more and more research is being discussed and researched worldwide, focusing on the use of hybrid membranes for seawater desalination. Hybrid membrane filtration processes present a number of advantages including superior water quality but also reduced energy consumption that was needed in previous purification processes. This review describes the water desalination process in detail by looking at the relationship between membrane module operating parameters and energy efficiency. The methodology and the experimental installation of the desalination process will be presented in part. The results of the study clearly showed that the combined use of membrane processes is efficient due to the flexibility of exploitation, the low acquisition costs and the high degree of water filtration through low energy consumption. A major advantage in the use of membranes is that the energy required to conduct filtering processes can be obtained from solar, wind energy, which means significant environmental benefits by promoting "green energy". The worldwide implementation of the use of membrane water desalination methods also involves increasing the percentage of fresh water, so this is a solution to be considered in present and future research.*

KEYWORDS: desalination, reverse osmosis, hybrid membranes, salt wastewater

## 1. Introduction

The relationship between water and energy is the one that will always gravitate around human existence [1, 2]. Freshwater resources are limited and the oceans are the only ones that can provide water for all human needs [3]. However, ocean water is salty, which implies finding methods and techniques for removing salt. In this context, there is a need for energy consumption that involves both costs and emissions of pollutants into the environment [3-5].

A very effective solution to solving the water crisis but also to cushioning environmental pollution as a result of noxious emissions is desalination of water through membranes that can use both renewable energy and solar energy [6, 7].

Desalination is the process by which the salt contained in seawater is removed by means of a membrane under a certain pressure and at the same time the ratio of water without salt and feed salt water [8].

At 25 °C, filtering a cubic meter of salt water containing around 34,500 ppm requires an energy consumption of approximately 0.6 kW/h [8].

The combination of desalination technologies with solar energy capture systems, especially in arid regions, is a promising option for sustainable development, as drinking water needs can also be met, as well as reducing the negative impact on environmental factors due to harmful emissions [9].

This approach requires intensive research because it is essential that desalination technology is compatible with solar recovery, but it is still a solution that offers an alternative to the conservation of natural resources and also brings benefits to the environment and human health [10].

The membranes used in the desalination of water can be organic or inorganic of ceramic material, which involves high temperature thermal filtration processes [10], without the membrane being deteriorated and thus the supply water, irrespective of contamination with chemical agents, does not ease damaging the membranes used in filtering processes [11].

One of the most analyzed inorganic filtration membranes in the field of recent research is the mesoporous membrane of ɣ-alumina that serves in nano-filtration processes and the pore size is 3-5 nm and the molecular weight of the particles corresponding to this membrane is around 3,000-10,000 Da [12].

Some researchers tested a membrane of this kind but with a pore size of 1 nm and the permeate obtained was above the industrial expectations, being approximately of 5 L/m$^2$/h using a pressure of 1 bar, and other investigations tested a membrane of the same type but having a pore size of 1.61 nm, solvent-resistant, and the permeability was about 17 L/h/m$^2$ at a pressure of 1 bar [13].

Modern membrane desalination methods using renewable energies have advantages that increase future implementation confidence: desalinated water can be achieved on a large scale, operating temperatures are not very high, in some ways, the supply water does not require pre-treatment, maintenance and operating costs are reduced but, at the same time, with the operation of the installations specific to these modern methods, the staff does not require any higher qualification [14].

## 2. Methods of water desalination based on the use of solar energy

### *2.1. Desalination through ceramic membranes in several steps*

Through this method, the solar energy is captured through a concentration system that has the power and capacity to make an entire desalination plant especially installed for this type of energy [15].

The desalination membranes allow only the passage of water vapor therethrough, since the distillation process produces pure water. Finally, salt is removed.

First, the solar thermal energy is collected and stored through the solar field, and then with the hot water coming into contact with cold salt water, the vaporization phenomenon occurs.

Parameters that follow this desalination method are: the concentration of energy obtained by the solar field because it influences the pressure, thus the entire process, the flow of the supply water according to the pressure, the quality of the filtered water as a result of the salinization concentration retained by the membrane module.

Current research predicts that in the near future, the cost of green energy technologies will decrease as they become more and more used [16].

Figure 1 shows the schematic diagram of the solar-based desalination plant:

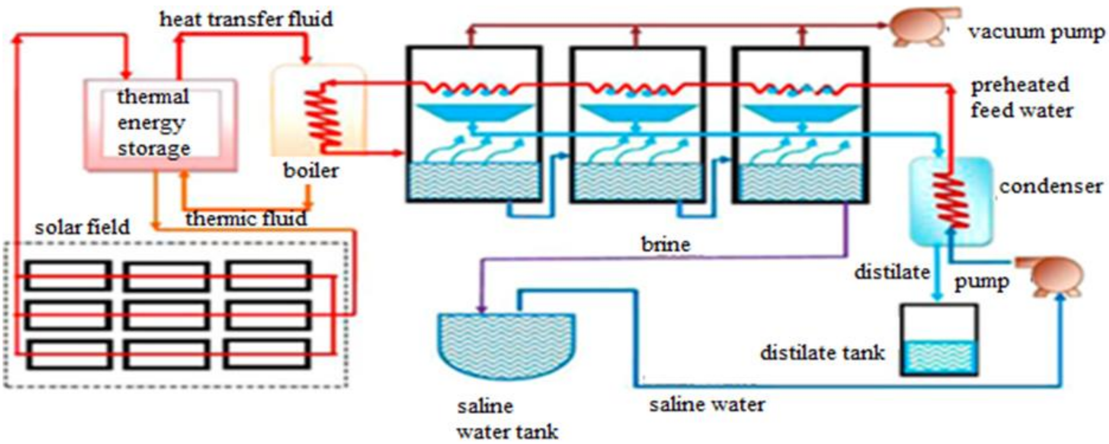


***Fig. 1.*** *Experimental installation of desalination using solar energy* [14]

### *2.2. Multi-effect distillation*

This desalination method raises its market share for being the most compatible with this solar energy system; studies have shown that over a year, such an installation with a working area of approximately 30,000-40,000 m$^2$ can produce around 1,000,000 m$^3$ of distilled water [14].

Some researchers compared the economy difference between the solar-based desalination technique and the water desalination method using fossil fuels, and found that for distilled water, the cost of desalination with solar energy is lower compared to a classic system works on diesel when the price reaches about $ 10/GJ [17].

In order for the desalination process to proceed in good conditions, the solar energy capture installation must be compatible with the desalination plant. The parameters to be monitored at such an installation refer to the captured solar power, the pump pressure, the steam generator pressure required by the desalination plant, the flow rate according to the feed temperature.

The performance of the desalination plant combined with a TC (thermal compression) solar energy capture unit is proven by doubling the salting water filtration efficiency, since the operation of this desalination plant can be done at a steam pressure of only 1 atm. [18].

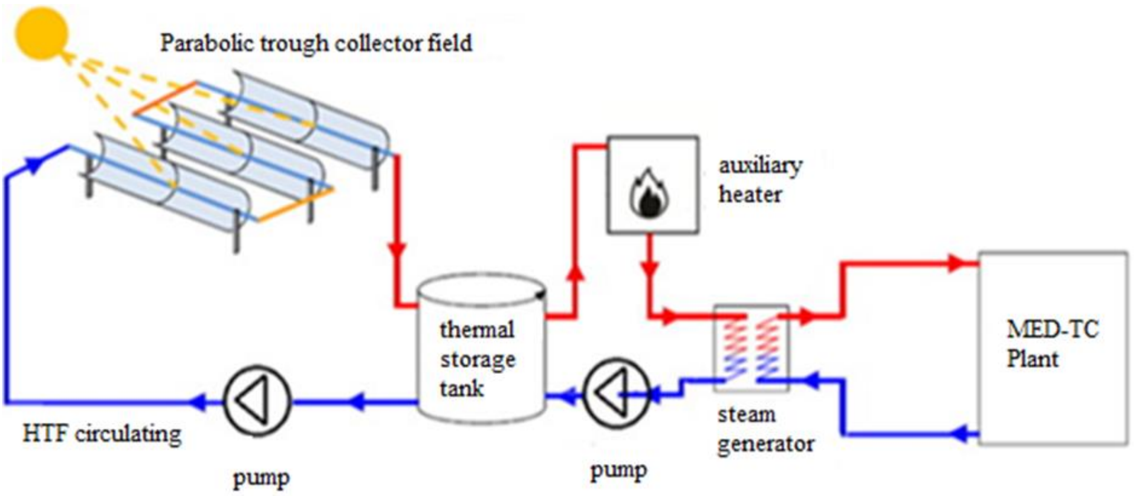


***Fig. 2.*** *The energy capture plant compatible with desalination plant* [19]

The solar thermal capture installation (Fig. 2) is the part which ensures the operation of the desalination plant (Fig. 3). Steam with high pressure feeds a steam jet ejector at a pressure of 1 atm. [20].

The water vapor from the last effect of the desalination unit is sucked by the high-pressure vapor and thus avoids loss of energy in the condenser. The two pressures equalize and the steam becomes overheated.

The first effect dehydrates the steam mixture, producing saturated steam used as heat even for the desalination unit of the first effect.

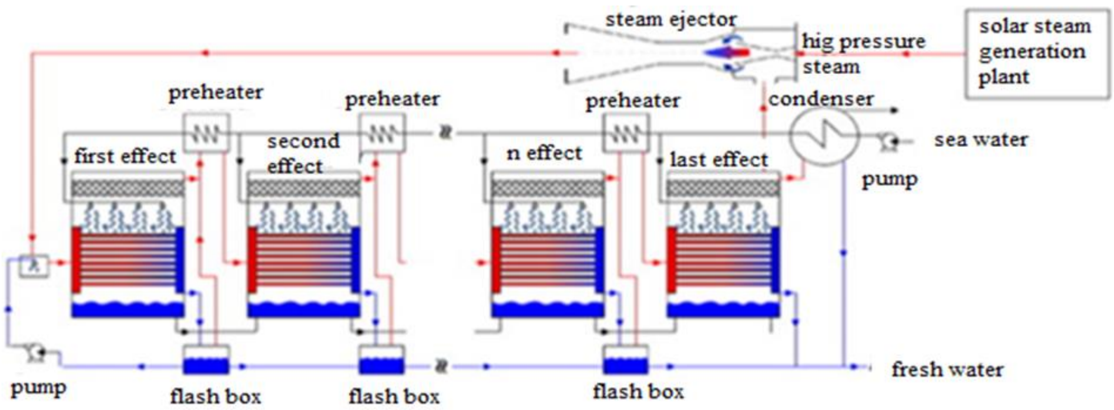


***Fig. 3.*** *The energy capture plant compatible with desalination plant* [20]

The low compression ratio reduces the amount of steam in the desalination unit, which increases the filtration capacity [21]. The flow temperature does not adversely affect the distillation process, since the temperature difference between the effects and the temperature of the last effect are the ones that are observed during the process [22].

Studies on the feasibility of a desalination plant, such as Figure 2, show that the tap water temperature and the pressure in the ignition chamber influence the production of water, meaning lowering the evaporation pressure results in a higher amount of distilled water [23].

### *2.3. Reverse osmosis using solar thermal energy*

With the help of a solar power concentrating plant, the heat can be generated which can then be used to obtain the electrical energy necessary for the operation of the desalination plant pumps by reverse osmosis (Fig. 4) [14].

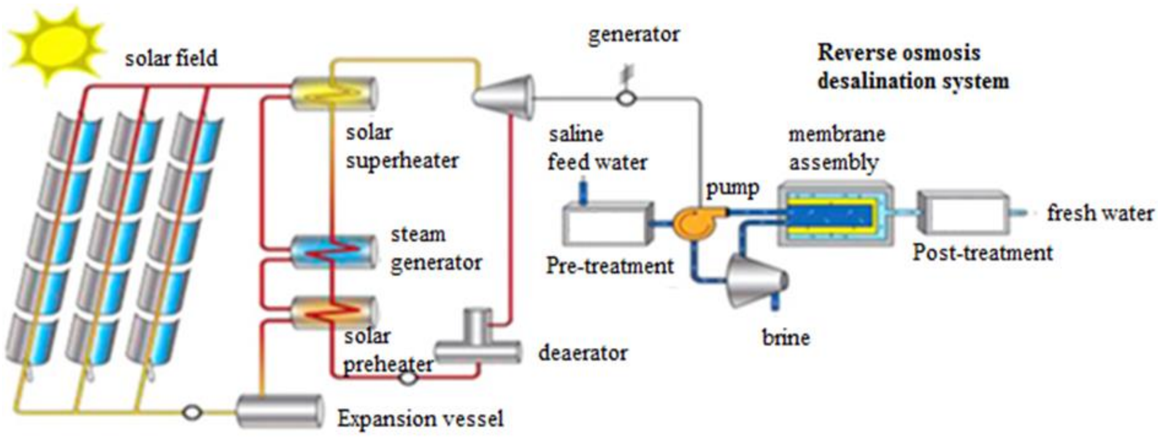


***Fig. 4.*** *The energy capture plant compatible with desalination plant* [20]

The high-pressure pump is powered by the generator that converts the solar energy produced by the solar field into electricity.

Prior to the osmosis process, a pretreatment of salted water is required to retain coarse particles as much as possible. Then the pump feeds the membrane module and before fresh water is collected, another treatment is required.

During the process of osmosis through the membrane, the following are observed: the variation of the pump pressure depending on the turbine steam fluctuations due to the solar energy capture, membrane lifecycle during the process, water flow at the membrane inlet, membrane efficiency of the membrane filtering due to the quality of distilled water in the unit of time.

### *2.4. Reverse Osmosis based on energy obtained by photovoltaic panels*

This modern seawater treatment technique is increasingly being promoted where water scarcity is increased and requirements are high. In other words, the areas concerned are arid and the predominant water sources are those with salt water.

Desalination of water through osmosis (Fig. 5) now exceeds 50% of the modern methods used in world-wide processes [24].

Always before the osmosis process, pre-purifying water is required. In this case, various chemical agents that do not endanger the type of membrane are introduced into the feed water, then by means of pre-treatment filters, larger particles or those that have increased their size due to applied chemical substances during the process remain on the filter surface.

Then the high-pressure pump feeds the membrane module to obtain the distilled water. The solar energy produced by the photovoltaic panels (Fig. 5) is the main source that puts the pumps into action [25].

Researches show that pre-filtering can successfully use nano-filtration to reduce turbidity, bacteria and reduce total dissolved solids [26].

During the salt water osmosis process, the parameters related to the energy produced for the operation of the filtration plant as well as the parameters of the desalination plant were followed, namely: the feed rate, the pressure applied to the module by the pump, the volume of the permeate in a time already established, the degree of purification of the distilled water.

Depending on these parameters, the efficiency of the use of the distillation membranes is determined by using the different pressures of the desalination plant.

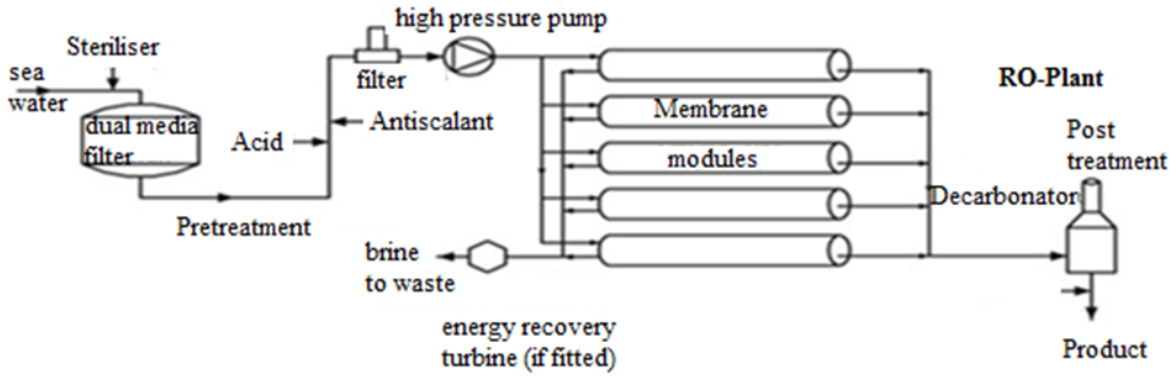


***Fig. 5.*** *The energy capture plant compatible with desalination plant* [22]

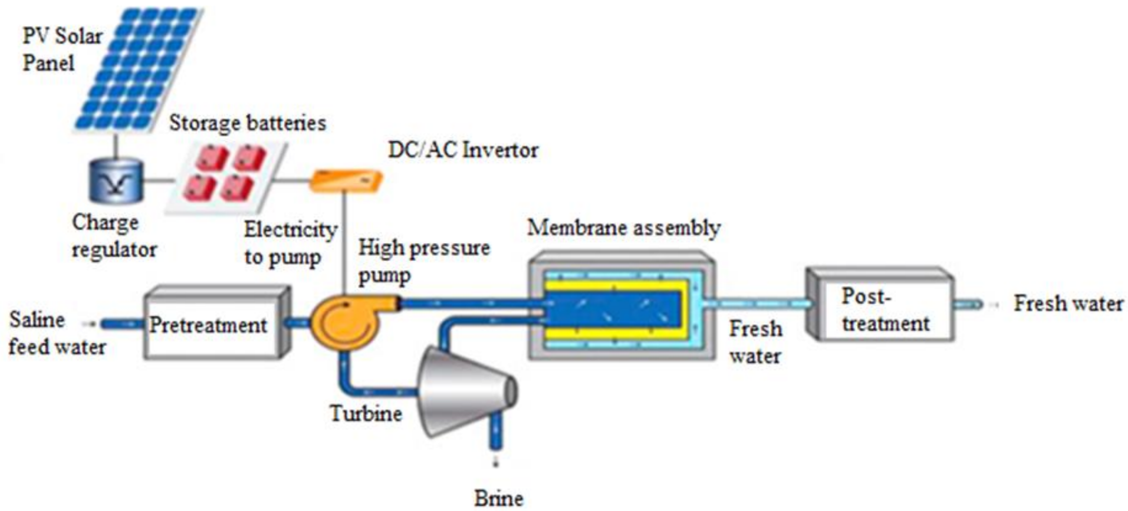


***Fig. 6.*** *The energy capture plant compatible with desalination plant* [28]

The results of the research have shown that, per $m^2$ of membrane, the production of distilled water / day is up to 500-1500 L but this largely depends on the degree of loading of the membrane due to the salt concentration in the salt water (Fig. 6).

## 3. Results and discussions

### *3.1. Discussions on the tracked parameters*

The purpose of this review was to test desalination membranes on the principle of exclusive use of renewable energies. Careful attention was paid to certain parameters, namely the feed flow, the pressure exerted by the feed pumps, the permeate concentration due to the salt rejection, the polarization of the concentration in a given unit of time. The focus was on membrane parameters, namely: water permeability, section area, hydraulic diameter, thickness of membrane feed space, density, salt diffusion coefficient, salinity and feed rate, permeate quality, etc.

Membrane testing has tracked the dependence of these parameters as a result of the solar power system being supplied by photovoltaic panels [19, 20].

Hydraulic resistance is the parameter that affects the membrane as a result of increasing pressure applied to it. In this case, flux sensitivity, permeate concentration, polarization of concentration and salt rejection [19] were analyzed.

The experimental data obtained from the experiments were compared with those of a ROSA (DOW) industrial software warehouse for the type of membrane tested, and the flow factor was 0.75.

This flow factor expresses the degree of performance of a system as a result of membrane weathering in relation to temperature and pressure applied over time during filtration processes [21].

### 3.1.1. Supply water pressure

As is known, feed pressure is one of the most important parameters in an installation that uses the membrane module in the case of osmosis. Therefore, it depends exclusively on the power supply of the pump, so of the energy captured by the photovoltaic panels.

The performance of the membrane is affected by these fluctuations as the authors say in their research. The pressure fluctuations of the supply water are shown in Fig. 7 as a result of the solar energy variation in time, i.e. from about 32 bars to 47 bars [19].

### 3.1.2. Feed flow

It is totally dependent on the pressure exerted by the pump. In other words, the varying of the pressure, change the flow of water. In correlation with Fig. 7, Fig. 8 shows the flow rate dependent on pressure fluctuations [19].

The same thing is observed in 810 minutes, although the pressure decreases, however, it is the same as that of the 905 minutes. Purple lines are the ones that show this and this fluctuation is due to the sudden increase in pressure, respectively from 32 to 47 bars [22].

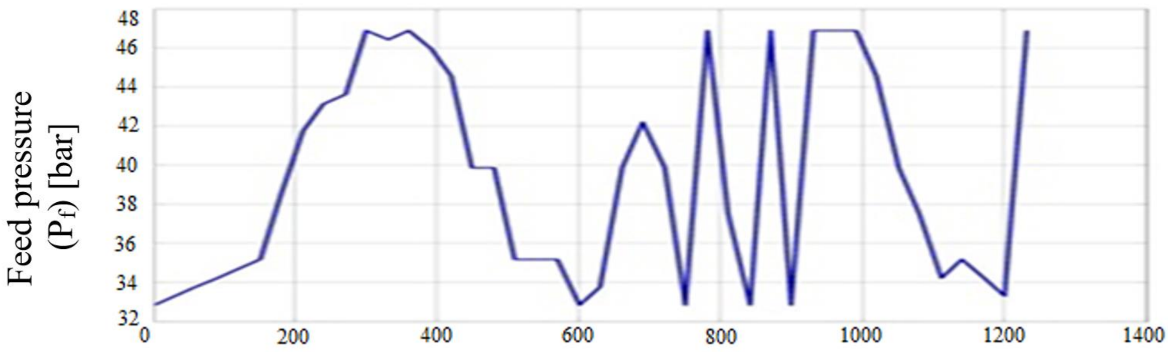


***Fig. 7.*** *Time pressure fluctuations within the desalination plant* [19]

Fig. 8 shows the flow variation according to the pump supply pressure; in minutes 300 and 900 the flow is the same, so the same pressure if we take into account the hydraulic resistance of the membrane.

The membrane compaction phenomenon also causes the permeate flow to fall. Figure 8 shows that the results of the ROSA software are smaller than those of the theoretical model without taking into account the hydraulic resistance, which means that the 0.75 flow factor describes an old membrane that leads to the decrease of the flow of permeate by approximately 19 %, due to membrane compaction due to unstable operation [22].

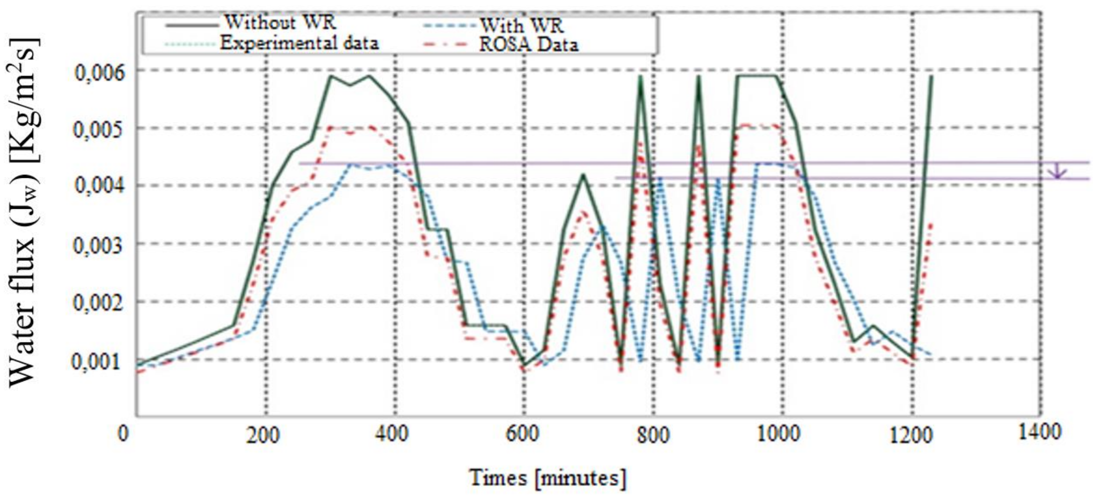


***Fig. 8.*** *Variations of supply water flow over time, depending on pump pressure* [22]

### *3.2. Discussions on the efficiency of renewable energies used in desalination processes*

Solar energy captured by photovoltaic panels is especially effective in arid areas. The only problem here is the cost of the panels. Instead, all desalination methods are compatible with solar energy capture methods.

The inorganic desalination membranes and ceramic ones that have been tested in the above experiments have shown increased filtration efficiency indifferently of the chemical agents used or the temperature. This is a major advantage.

Multi-effect desalination methods are being used more and more often and current research is increasingly focusing on this topic. The use of this method tends to be from the medium level to large and the cost of such an installation, per $m^3$, can be between 950-1900 euro compared to the solar panels at which the cost per one $m^3$ of the plant is between 1500-2500 euro [27].

For this reason, photovoltaic desalination technology occupies a lower place in the ranking of the use of solar desalination technologies and its use is low.

The use of osmosis through desalination technologies is increasingly successful, the scale of use being small to large and the cost per $m^3$ of plant is between 900-2500 euro but the membranes can be replaced at 4 or 5 years which means high lifetime efficiency of membranes used [27].

In conclusion, the desalination of water relative to the cost of acquisition and maintenance is most efficient by using the multi-effect desalination method, then osmosis through solar panels.

Modern desalination methods using renewable energies are reliable, operating costs are acceptable and the energy required for plant operation is reduced [28].

Osmosis begins to be in the top of current research due to the quality of the filtered water but a disadvantage is the need for high operating pressures and the fact that before water enters the membrane requires pre-treatment. Another disadvantage is the warping of the membrane, the greater the operating pressure means the higher the loading on the surface of the membrane [29].

## 4. Conclusions

Organic and inorganic desalination membranes are a key element for current research due in particular to efficiency in the quality of filtered water.

Osmosis is the process behind the desalination of water, and the pressure plays the essential role because the higher the permeate volume of the same quality in a lesser time.

Current research is increasingly focusing on the use of membranes used in desalination but also combines filtering processes with renewable energy installations.

Renewable energies can be successfully combined with desalination plants and bring benefits both in terms of environmental protection through emissions and reduced maintenance costs.

The experiments carried out in the research have also emphasized the safety of the installations due to the need for high pressures but the cases of danger were little confirmed by the tests carried out over a long period of time.

Although in the case of saltwater filtration, certain parts of the installations may be affected by corrosion, the present research focuses on finding the best substitutes for certain parts of the system where there is contact with salty water.

In modern saltwater filtration methods, the most efficient desalination solution remains osmosis, regardless of whether high pressure is required or that the volume of permeate is low.

The supply water concentration related to the type of load as well as the pressure of the feed pumps are essential parameters in the salting water desalination processes;

Research experiments have shown increased system reliability; in terms of electricity consumption, it is mainly used for the commissioning of pumps.

Modern desalination methods have particularly focused on compatibility with the capture of solar energies as renewable energy.

This review article emphasized the dependence between the parameters of the desalination plant and those of solar energy capture equipment as the main source of energy.

The results of the research have highlighted both the advantages and drawbacks of using sea water filtration membranes as a key element in increasing the percentage of fresh water to meet different consumption requirements.

## References

**[1]. Kalogirou S.**, *Survey of solar desalination systems and system selection soteris*, Energy, 22(1), p. 69-81, 1997.

**[2]. Barsan N., Nedeff V., Temea A., Mosnegutu E., Chitimus A. D., Tomozei C.**, *A perspective for poor wastewater infrastructure regions: a small-scale Sequencing Batch Reactor treatment system*, Chemistry Journal of Moldova, vol. 12, no. 1, p. 61-66, 2017.

**[3]. Kalogirou S.**, *Seawater desalination using renewable energy sources*, Prog. Energy Combust Sci, 31(3), p. 242-81, 2005.

**[4]. Grubert E., Stillwell A., Webber M.**, *Where does solar-aided seawater desalination make sense? A method for identifying sustainable sites*, Desalination, 339, p. 10-7, 2014.

**[5]. Garcia-Rodriguez L.**, *Seawater desalination driven by renewable energies: a review*, Desalination, 143, p. 103-113, 2002.

**[6]. Barsan N., Nedeff V., Mosnegutu E., Panainte M.**, *Heat balance components of a small Sequencing Batch Reactor applied for municipal wastewater treatment*, Environmental Engineering & Management Journal, vol. 11, no. 12, p. 2133-2140, 2012.

**[7]. Tirtoaca Irimia O., Tomozei C., Panainte M., Mosnegutu E. F., Barsan N.**, *Efficiency of filters with different filtering materials: comparative study in water treatment*, Environmental Engineering & Management Journal, vol. 11, no. 12, p 2133-2140, 2012.

**[8]. *****, *Encyclopedia of Desalination and Water Resources (DESWARE), Energy requirements of desalination processes*, www.desware.net/desa4.aspx.

**[9]. Al-Karaghouli A, Kazmerski L. L.**, *Energy consumption and water production cost of conventional and renewable-energy-powered desalination processes*, Renew Sustain Energy Rev, 24, p. 343-56, 2013.

**[10]. Dong H., Zhao L., Zhang L., Chen H., Gao C., Winston Ho W. S.**, *High-flux reverse osmosis membranes incorporated with NaY zeolite nanoparticles for brackish water desalination*, J. Membr. Sci., 476, p. 373-383, 2015.

**[11]. Lorente-Ayza M. M., Perez Fernandez O., Alcala R., Sanchez E., Mestre S., Coronas J., *et al.***, *Comparison of porosity assessment techniques for low-cost ceramic membranes*, Bol. Soc. Esp. Ceram. Vidrio, p. 1-10, 2016.

**[12]. Chen X., Zhang W., Lin Y., Cai Y., Qiu M., Fan Y.**, *Preparation of high-flux γ-alumina nanofiltration membranes by using a modified sol–gel method*, Microporous Mesoporous Mater., 214, p. 195-203, 2015.

**[13]. Wang Z., Wei Y., Xu Z., Cao Y., Dong Z., Shi X.**, *Preparation, characterization and solvent resistance of γ-$Al_2O_3$/α-$Al_2O_3$ inorganic hollow fiber nanofiltration membrane*, J. Membr. Sci., 503, p. 69-80, 2016.

**[14]. Sharon H., Reddy K. S.**, *A review of solar energy driven desalination technologies*, Renew Sustain Energy Rev, 41, p. 1080-1118, 2015.

**[15]. Mezher T., Fath H., Abbas Z., Khaled A.**, *Techno-economic assessment and environmental impacts of desalination technologies Desalination*, 266 (1), p. 263-273, 2011.

**[16]. Ghaffour N., Missimer T. M., Amy G. L.**, *Technical review and evaluation of the economics of water desalination: current and future challenges for better water supply sustainability*, Desalination, 309, p. 197-207, 2013.

**[17]. Saffarini R. B., Summers E. K., Arafat H. A.**, *Technical evaluation of stand-alone solar powered membrane distillation systems*, Desalination, 286, p. 332-341, 2012.

**[18]. Ali El-Nashar**, *The economic feasibility of small solar MED seawater desalination plants for remote arid areas*, Desalination, 134, p. 173-186, 2001.

**[19]. Pankratz T., Tonner J.**, *Desalination.com: An environmental primer*.

**[20]. Dimitriou E., Karavas C., Mohamed E. Sh., Kyriakarakos G., Piromalis D., Dounis A., Arvanitis K., Papadakis G.**, *A test bench for the optimization of autonomous renewable energy driven reverse osmosis desalination units Euromed*, Desalination for Clean Water and Energy, 2015.

**[21]. Diego C. Alarcón-Padilla, Lourdes García-Rodríguezb, Julián Blanco-Gálveza**, *Design recommendations for a multi-effect distillation plant connected to a ouble-effect absorption heat pump: A solar desalination case study*, Desalination, 262 (1-3), p. 11-14, November 15 2010.

**[22]. Ibrahim Al-Mutaz, Irfan Wazeer**, *Current status and future directions of MED–TVC desalination technology*, Desalin. Water Treat., 2014.

**[23]. Zhao D., Xue J., Li S., Sun H., Zhang Qing-Dong**, *Theoretical analyses of thermal and economical aspects of multi-effect distillation desalination dealing with high-salinity waste water*, Desalination, p. 273-292, 2011.

**[24]. Juyuan Jiang, Tian He, Mingxian Cui, Lijian Liu**, *Proof-of-concept study of an integrated solar desalination system*, Renew. Energy, 34 (12), p. 2798-2802, December 2009.

**[25]. Dimitriou E., Mohamed E. Sh., Kyriakarakos G., Papadakis G.**, *Experimental investigation of the performance of a reverse osmosis desalination unit under full- and part-load operation*, Desalin. Water Treat., 53 (12), p. 3170-3178, 2014.

**[26]. Widiasa N., Paramita V., Kusumayanti H.**, *BWRO desalination for potable water supply enhancement in coastal regions*, J Coast Dev, 12 (2), p. 81-88, 2009.

**[27]. Luft W.**, *Five solar energy desalination systems*, Int J Solar Energy, 1, p. 21, 1982.

**[28]. Adam S., Cheng R. C., Vuong D. X., Wattier K. L.**, *Long Beach's dual-stage NF beats single-stage SWRO*, Desalination Water Reuse, 13 (3), p. 18-21, 2003.

**[29]. Tzen E., Morris R.**, *Renewable energy sources for desalination*, Solar Energy, 75(5), p. 375-379, 2003.

THE ANNALS OF "DUNAREA DE JOS" UNIVERSITY OF GALATI
FASCICLE IX. METALLURGY AND MATERIALS SCIENCE
N°. 3 - 2017, ISSN 1453-083X

# RECYCLING OF HEMATITE FINE WASTE BY PELLETISATION

**Anișoara CIOCAN, Beatrice TUDOR**
"Dunarea de Jos" University of Galati
e-mail: aciocan@ugal.ro

## ABSTRACT

*A large volume of by-products and residues is generated during iron and steel production. Much of these represents valuable materials and can be recovered and recycled inside the flow of integrated steel plants. The fine-grained residues, which are rich in iron, are usually recycled through sinter plants. This study aims at investigating the potential of palletization of two types of hematite fine waste resulted from process of chemical pickling of steel strip. The pelletizing tests were performed in an experimental disc pelletizer. The hematite was mixed with different fluxing and binding agents. The green pellets were then dried, sintered and cooled. The effect of materials mixtures on the physical and chemical characteristics of pellets was determined and analyzed in relation with nature of pelletized components.*

KEYWORDS: hematite, recycling, pelletizing

## 1. Introduction

The rolling is an essential industrial process for steel sheet production. During the deformations of steel, oxygen from the air reacts with the iron and forms iron oxides or scale as a fine layer on the surface of the steel strip. The constituents of mill scale are wustite (FeO), magnetite ($Fe_3O_4$) and hematite ($Fe_2O_3$) phases. FeO is usually closest to the metal surface while $Fe_2O_3$ forms the outer layer (Figure 1).

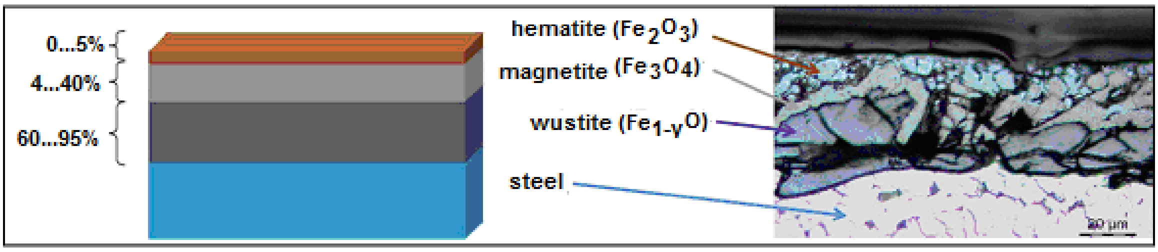


***Fig. 1.*** *Cross section of the three-layers steel oxide scale formed during the hot rolling stage on surface of the steel strip* [1]

The oxides layer must be removed before as other processing to be applied to steel band. The scale or oxide film can be removed from surface of steel strip by immersing in acid solution, usually in hydrochloric acid bath. This is named ″batch pickling process″. When steel is pickled, iron oxides and metallic iron react with the hydrochloric acid. From chemical reactions involved in this process result ferrous chloride, water and hydrogen gas [2].

$$FeO_{(s)} + 2HCl_{(aq)} \rightarrow FeCl_{2(aq)} + H_2O_{(l)} \tag{1}$$

$$Fe_3O_{4(s)} + Fe_{(s)} + 8HCl_{(aq)} \rightarrow 4FeCl_{2(aq)} + 4H_2O_{(l)} \tag{2}$$

$$Fe_2O_{3(s)} + Fe_{(s)} + 6HCl_{(aq)} \rightarrow 3FeCl_{2(aq)} + 3H_2O_{(l)} \quad (3)$$

$$Fe_{(s)} + 2HCl_{(aq)} \rightarrow FeCl_{2(aq)} + H_{2(g)} \quad (4)$$

During the pickling process, a large amount of waste pickle liquor or spent acid is produced. In the exhausted pickling solutions, a metal content of up to 150-250 g/L is accumulated [3]. The recovery of the pickling acid waste from environmental and economical cleaning process is an important issue, from points of view. By treatment the acid is regenerated and can be reused. During the treatment the metallic oxide appears (Figure 2). Thus, the regeneration reduces the cost of fresh acid supply and eliminates the cost of disposal of spent acid. There are more methods that allow efficient reuse of the pickling liquor [4, 5].

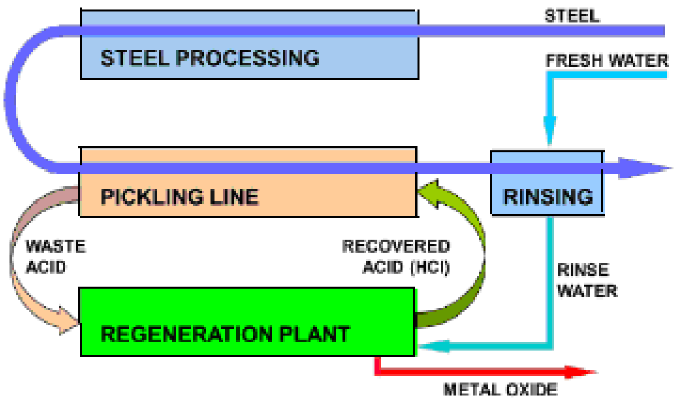


***Fig. 2.*** *Succession of operations at ferric oxide generation* [5]

Hydrochloric acid is vaporized and heated to high temperatures without decomposing in other compounds. The technology of regeneration of pickling acid waste includes heating in two stages of the galvanic waste sludge. Firstly, to evaporate water and to recycle acid, the treatment is carried in range of 200-500 °C. A secondary treatment involves the calcination at high temperatures (850 °C). The recovery reaction, on which all HCl recovery processes depend, is the oxidation with hydrolysis of ferrous chloride. The iron chloride ($FeCl_2$) is converted into hydrochloric acid by reaction with oxygen and water vapor (hydrolytic decomposition).

$$2FeCl_2 + 2H_2O + 1/2O_2 = Fe_2O_3 + 4HCl \quad (5)$$

Thus, during regeneration of used pickling acid, additionally is obtained the ferric oxide ($Fe_2O_3$) as a dry powder. Very fine oxide particles are a high quality secondary material. It must be recycled due to its high iron content, low impurities and stable chemical composition. According to its properties, the iron oxide from regeneration can be used for different purposes: hard and soft ferrites production, for foundry applications, as binder for refractories, as fine aggregate in mixtures for the production of clay bricks, as coloring pigments [3, 6, 7]. A simple recycling solution is the direct using in the integrated steel production flow. Because of its physical, chemical and mineralogical properties, the iron oxide powder can be used as a raw material in metallurgical processes as feed for blast furnace, after sintering, palletization or briquetting. Thus, the recycling brings economic benefits, the iron oxide powder used as raw materials reduces the iron ore consumption. On the other hand, this solves the environmental problems of integrated steel plant, generated by own waste. In this work is studied the recovery through pelletizing. The possibility to convert the fines into valuable product, suitable for blast furnace was analyzed.

## 2. Experimental

The ferric oxide powder sample was supplied from a metallurgical company. The hematite used in experiments had very high content of $Fe_2O_3$. The fine material is composed of small particles (Figure 3).

***Fig. 3.*** *Ferric oxide powder sample*

In order to obtain pellets with suitable mechanical and chemical properties, the iron oxide micro fines must be agglomerated as larger pieces. In literature it was studied the use of various types of binders for making pellets. Some of these were applied in the industry [8]. In this work the hematite powder was mixed with solutions of sodium silicate ($Na_2OxnSiO_2$, n = 2.4-3.5) or calcium chloride (as solution 30 %) and lime. They are alternative binders to bentonite used for iron ore pelletizing. They ensure the resistance of pellets in handling operation and in metallurgical process. In addition, were used the lime for increasing of CaO content and also foundry graphite for the carbon. The coarse dust lime had the following composition: 57.50-58.74 % CaO, 1.00-3.85 % MgO, 0.74-0.88 % $Fe_2O_3$, 0.20-0.25 % $Al_2O_3$, 0.70-1.00 % $SiO_2$.

The pellets were prepared in laboratory using a disc pelletizer (Figure 4).

***Fig. 4.*** *Laboratory installation for palletization*

The produced green pellets were dried in air for three days to ensure the evaporation of water used for palletization process. In accordance with mixture composition and water added were obtained pellets with different dimensions (Figure 5). The average compressive strength of oven dried pellets was controlled.

***Fig. 5.*** *Mixture of dried pellets obtained with different binders*

## 3. Results and discussion

The size analysis of the $Fe_2O_3$ powder sample was carried. Samples were dried previously at 105 ºC. The granulometric distribution of the hematite is given in Table 1.

***Table 1.*** *Particle size analysis of $Fe_2O_3$ powder*

| Sieve diameter, [mm] | $Fe_2O_3$ powder, [wt. %] |
|---|---|
| +0.5 | 0.0 |
| -0.5, +0.1 | 57.20 |
| -0.1, +0.05 | 39.4 |
| -0.05, +0,04 | 3.40 |
| -0.04 | 0.05 |

All particles of dry powder are below 500 microns. 96.60% of the sample had sizes between 50 and 500 microns, showing the fine nature of the studied material. Also 3.45% of the particles are less than 50 μm. This is important for transporting fine material either for reuse or disposal in landfills. The fine particles have the possibility to disperse and air pollution. The particles with sizes larger than 1 μm have different forms, from spherical to irregular.

The chemical analysis of hematite powder highlighted the high content of iron oxide (Table 2).

***Table 2.*** *Characteristics of hematite powder*

| Characteristics | Value |
|---|---|
| $Fe_2O_3$, [%] | 99.33% |
| Fatty substances, [%] | 2.08% |
| $SiO_2$, [%] | - |
| Soluble substances in water, [%] | 0.23% |
| Soluble substances in HCl, [%] | 0.24% |
| Moisture, [%] | - |
| pH (aqueous suspension) | 6.0 |
| Bulk density in compressed state, [g/dm$^3$] | 0.704 kg/dm$^3$ |
| Chemical reactivity, [%] | 1.39% |

The powder used in the palletization did not have a neutral nature. The value of pH when hematite particles have been suspended in water was 6. The knowledge of pH value allows to infer its possible influence on soil when this by-product is stored. The value determined exceeds the limit required for waste disposal in landfills or for temporary storage inside of metallurgical plant (Table 2). Consequently, the concrete platforms or preliminary treatments are required. For using in the metallurgical process, the literature recommends pellets with pH ranged of 5 and 8.

The hematite micro fines were bonded with sodium silicate or calcium chloride and lime. The composition of the experimented samples is presented in Table 3.

The chemical composition of pellets was determined by X-ray fluorescence analysis (Table 4).

***Table 3.*** *Materials participation in the mixtures for palletization*

| Sample | Material, [%] | | | | |
|---|---|---|---|---|---|
| | Hematite | Lime | Sodium silicate | Foundry graphite | Calcium chloride |
| $R_A$ | 80 | 4 | 8 | 8 | - |
| $R_B$ | 80 | 4 | - | - | 8 |

***Table 4.*** *Chemical composition of the pellets*

| Pellets | $Fe_2O_3$ | MnO | $SiO_2$ | CaO | MgO | $Al_2O_3$ | PC |
|---|---|---|---|---|---|---|---|
| $R_A$ | 67.29 | 0.61 | 10.11 | 2.45 | 0.00 | 1.58 | 13.80 |
| $R_B$ | 81.10 | 0.77 | 0.18 | 5.46 | 0.00 | 1.68 | 9.61 |

The pellets obtained can be considered composite materials. Their binder matrix is formed by addition of the sodium silicate or the calcium chloride and the lime. Taking this approach into account, the hematite is considered the complementary phase, homogenous dispersed in the matrix of pellets. The shape of microparticles and the binder have a positive influence on mechanical properties of pellets. Quality of the pellets is influenced by the nature of the ferrous waste, type and amount of fluxes added. These factors in turn result in the variation of physicochemical properties of the coexisting phases and their distribution during the hardening of pellets. Hence properties of the pellets are largely governed by the form and degree of bonding achieved between the particles and the stability of these bonding phases during reduction of iron oxides in the blast furnace. The formation of phases and micro-structure during heating depend on the type and amount of fluxes added. This effect of fluxing agents on quality of pellets is analyzed in terms of $CaO/SiO_2$ ratio and CaO content. As example, at lime addition, CaO in contact with water forms the calcium hydroxide. On palletization, this calcium hydroxide provides primary bonding amongst the particles and imparts strength to the green pellets [9].

The values of compressive strength of dried pellets confirm these appreciations (Table 5). The pellets strength was measured by a compression test. These were individually compressed to failure and the maximum load was recorded. Tests were performed on 5 uniformed sized pellets, and the average compressive strength values were calculated.

***Table 5.*** *Compression strength of pellets*

| Sample | Average pellet diameter, [cm] | Applied force*, [N] | Pressure, [bar] | Compressive strength, [daN/cm$^2$] |
|---|---|---|---|---|
| $R_A$ | 1.5 | 1015.594 | 2.3 | 57.5 |
| $R_B$ | 1.2 | 1015.594 | 2.3 | 89.8 |

*piston diameter = 7.5 cm

Analyzed like composites, the aggregation of materials in pellets is the result of bonding forces. The adhesion and cohesion forces manifested at the contact surface of different components. In the experimented pellets, the additions of binders ensure the surface connection of hematite microparticles with other components, and in consequence the strength of pellets. The compressive strength obtained is within the standards required for iron ores or ores sintered introduced in the blast furnace. The values are above the acceptable limit of crushing strength: 200 kg/pellets, for conventional type, fired between 1300-1350 °C or 400 kg/cm$^2$ for lump ore-oven dried [10, 11].

## 4. Conclusions

The hematite pellets can be used as a substitute for ores and sinter in the blast furnace due to the properties. The hematite powder from pickling process has a high content of iron oxide and it has no other impurities. Since it results from a chemical process, it is formed of fine and uniform particles: 96.60% of samples is formed of particles sized between 50 and 500 microns.

By adding sodium silicate or calcium chloride and lime as binders were obtained pellets with suitable compression strength. Lime and calcium chloride proved to be more beneficial additives for hematite micro fines. When water glass was used, the $SiO_2$ content increased in the pellets. For lime and calcium chloride we obtained the so-called ″lower silica″ pellets. This is an advantage because the utilization of pellets with high values of $CaO/SiO_2$ ratio reduces the slag volume in the blast furnace and the pellets reducibility is higher. As a result, blast furnace productivity is increased and the coke rate requirement is decreased.

## References

**[1]. Graf M., Kawalla R.**, *Scrap development on steel hot strip rolling*, La Metallurgia Italiana, 2, p. 43-49, 2014.

**[2]. Jatuphaksamphan Y., Phinichka N., Prapakorn K., Supradist M.**, *Pickling kinetics of tertiary oxide scale formed on hot-rolled steel strip*, Journal of Metals, Materials and Minerals, vol. 20, no. 1, p. 33-39, 2010.

**[3]. Quaranta N., Caligaris M., López H., Unsen M., Pelozo G., Pasquini J., Cristóbal A.**, *Reuse of red powder of steel plants as fine addition in ceramic bricks manufacture*, WIT Transactions on Ecology and The Environment, vol. 155, 2012.

**[4]. Regel-Rosocka M.**, *A review on methods of regeneration of spent pickling solutions from steel processing*, Journal of Hazardous Materials, vol. 177, p. 57-69, 2010.

**[5]. Baerhold F., Mitterecke S.**, *Acid recovery in the steel and metallurgical industry - process characteristics and fuel saving options*, IMPC 2016: XXVIII International Mineral Processing Congress Proceedings.

**[6]. Zaspalis V., Kolenbrander M.**, *Design principles for spray-roasted iron oxides for the manufacturing of ferrites*, Powder Technology, vol. 161, p. 169-174, 2006.

**[7]. Woon H. S., Lim K.P., Puteri N., Rozaimah R., Tan C. Y.**, *Synthesis and characterization of hot-roll and cold-roll byproduct-derived strontium hard ferrites*, American J. of Engineering and Applied Sciences, 2 (4), p. 580-583, 2009.

**[8]. Eisele T. C., Kawatra S. K.**, *A review of binders in iron ore pelletization*, Miner. Process. Extr. Metall. Rev, 24, p. 1-90, 2003.

**[9]. Pal J.**, *Utilization of Microfines in Iron and Steel Making*, Steel World, p. 86-90, June 2016.

**[10]. Halt J. A., Komar Kawatra S.**, *Review of Organic Binders for Iron Ore Agglomeration*, 2013.

**[11]. Socalici A., Heput T., Ardelean E., Ardelean M.**, *Ferrous waste processing by pelletizing, briquetting and mechanically mixed*, International Journal of Energy and Environment, issue 4, vol. 5, p. 532-540, 2011.

# EXAMINING THE EVOLUTION OF MICROSTRUCTURE AND ITS EFFECT ON THE MECHANICAL AND TRIBOLOGICAL PROPERTIES

**Stela CONSTANTINESCU**
"Dunarea de Jos" University of Galati
e-mail: constantinescu_stela@yahoo.com

## ABSTRACT

*This paper investigates the superior frictional performance of Ti-DLC films, by examining the evolution of microstructure and its effect on the mechanical and tribological properties. The superior frictional performance of Ti-DLC films can be attributed to the special microstructure related to the development of embedded fullerene-like microstructures as a result of incorporation of $TiO_2$ clusters. The factors contributing to the ultralow friction include high hardness and cohesion, excellent toughness, and high load bearing capacity (brought by the increased crosslinking and elastic energy storage ability), the friction-induced structural transformation rendering an ultralow shear resistance and the excellent resistance to oxidation-induced mechanical property degradation (due to the doped $TiO_2$).*

*The Raman, high resolution transmission electron microscopy, atomic force microscope and micro-indentation measurements consistently reveal or indicate the formation of curved graphene sheets or fullerene-like microstructures with increasing $CH_4$/Ar ratio.*

KEYWORDS: microstructure, mechanical, tribological, frictional, wear

## 1. Introduction

In this work, a series of Ti-DLC films were prepared by adjusting the gas composition (i.e., $CH_4$/Ar ratio) and the effect of $CH_4$/Ar ratio on the structural, mechanical, and tribological properties of these films is examined and discussed.

Diamondlike carbon (DLC) films prepared from hydrogen-rich $CH_4$ source gas have been reported to exhibit a super low friction coefficient of 0.001-0.003 and wear rate of $10^{-6}$-$10^{-7}$ $mm^3/N{\cdot}m$ in dry nitrogen environment. However, such a super low friction behavior obtained from hydrogenated DLC coated surfaces cannot be sustained under ambient conditions due to the potential destruction by oxygen when exposed to air [1].

Various methods have been taken to address this issue and one commonly employed method is to incorporate metal or nonmetal elements into the carbon matrix [2-5]. But the choice of dopant plays a significant role in tailoring specific properties of DLC films for desired applications [6]. Of those doped elements, titanium has been selected because of its good adhesion to most substrate materials and easy reaction with carbon [7]. The TiC-rich surface is able to greatly improve the oxidation resistance of DLC films by forming a diffusion barrier to hinder the diffusion of into the sublayer, which is much helpful to prevent the incursion and destruction of to the cross-linked carbon network.

Extensive studies on the microstructural, mechanical, and tribological properties of Ti-doped carbon films have been reported [8-10]. Tribologically, the investigation of Ti-DLC films has been carried out in a wide range of normal load, ranging from micro-Newton and milli-Newton, aiming at possible application to micro electromechanical systems and micromechanical assemblies, to about 100 N, in order to meet the needs of the service requirement of high precision ball bearing and automotive parts that are often subjected to high applied load.

Usually, a higher TiC concentration (e.g., >25 %) in TiC/a-C:H films would give friction coefficients 0.1-0.3 when sliding against steel balls at room temperature [11, 12].

However, it was reported an ultralow friction of <0.025 in dry air for TiC/a-C:H films with a TiC fraction higher than 25%. A glassy microstructure with fine TiC microparticles (e.g., 2 μm) embedded in hydrocarbon matrix was reported to show excellent toughness and wear resistance due to suppressed microcrack propagation [13, 14]. To the best of our knowledge, however, few studies have been reported on Ti-DLC films showing an ultralow friction performance (COF < 0.015). Based on previous work in synthesizing ultralow friction pure carbon films, we synthesized a new kind of Ti-doped DLC films [15].

The Ti-DLC films showed an ultralow and steady friction behavior (0.008-0.015) in ambient air and nearly independent of counterpart materials. A combined effect of the inherent mechanical properties, the friction-induced structural transformation, and the presence of a transfer film was proposed to explain the lubrication performance. However, it remains unclear to what degree the microstructure and/or the mechanical properties will affect the friction and wear of Ti-DLC films and how they affect it. More efforts are needed to clarify the mechanism and, if possible, to intentionally design the structure to make the ultralow and steady friction behavior controllable.

## 2. Experiment

### *2.1. Film deposition and characterization*

Ti-DLC films were deposited on polished substrates and n-type Si (100) wafers by a hybrid radio frequency enhanced chemical vapor deposition (CVD) [15]. A mixture of $CH_4$ (99.99%) and Ar (99.99%) was used as the source gas of CVD to synthesize carbon film into which titanium was doped the titanium (99.99%) targets. The mass flow rate ratio of $CH_4$ to Ar ($CH_4$/Ar) was adjusted from 27% to 50% in gas mixture under a constant working pressure. Detailed deposition parameters are listed in Table 1. An adhesive interlayer of Si, 5-10 μm thick, was deposited silicon targets (99.999%). The overall film thickness was 10 ± 0.1 μm. A non-doped DLC film was also prepared for comparison.

***Table 1.*** *Deposition parameters for Ti-DLC films*

| Parameter | Value | | | |
|---|---|---|---|---|
| Working pressure (Pa) | | | 0.6 | |
| Ti target current (A) | | | 4.0 | |
| Bias frequency (kHz) | | | 30 | |
| Duration (min) | | | 120 | |
| Mass flow rate of $CH_4$ (sccm) | 34 | 45 | 54 | 60 |
| Mass flow rate of Ar (sccm) | 68 | 60 | 54 | 48 |
| $CH_4$/Ar ratio | 27% (Film 1) | 35% (Film 2) | 43% (Film 3) | 50% (Film 4) |

The microhardness and elastic modulus of the films were determined using a Micro-Hardness Tester (MTS Indenter XP). Five indentations were made for each sample, and the hardness was calculated by averaging five measurements from loading–unloading curve. The elastic recovery was calculated using the formula (dmax_dmin)/dmax, where dmax and dmin are the maximum and minimum displacement during unloading, respectively.

Frictional properties of the Ti-DLC films were evaluated on a reciprocating-type ball-on-flat tribometer (CSM), which was equipped with a chamber where the relative humidity and gaseous environment could be controlled. Sliding tests were performed in ambient air environment at an average sliding velocity of 90 mm/s under room temperature.

$Si_3N_4$ ball (~ 6 mm in diameter) was used as the counter face. Worn surfaces of films and mated balls were observed on an Olympus STM6 Measuring Microscope and a MicroXAM surface mapping microscope.

High resolution transmission electron microscopy (HRTEM) images were obtained on a JEOL 2010 TEM operated at 200 kV. The film sample for HRTEM observation was first deposited on NaCl substrates followed by dissolution of the

NaCl substrate with deionized water was used. The surface morphology of the films was observed using a Digital Instruments Nanoscope III Multimode atomic force microscope (AFM). The cross-section micrographs were obtained on a field emission scanning electron microscope (FESEM, JEOL JSM-6701F).

## 3. Results and discussion

Fig. 1, the microhardness, elastic modulus, and elastic recovery of films consistently increase with increasing $CH_4$/Ar ratio. The hardness grows monotonically from 8 MPa at $CH_4$/Ar¼27 % to 14 MPa at 50 %. Correspondingly, the elastic recovery increases from ~65 % to ~70 %.

To better understand the microstructural evolution as a function of $CH_4$/Ar ratio and its correlation to the Raman spectra, the Ti-DLC films were characterized by HRTEM and FESEM.

Figure 2 shows the HRTEM plan-view images of four Ti-DLC films. As shown, planar graphene sheets greater than 5 µm could be seen at 27 %. However, once the $CH_4$/Ar ratio was raised to 35 %, a considerable amount of short-length curved sheets starts to show up. A further development of curved sheets into closed-cage fullerene-like structures could be seen at $CH_4$/Ar¼43 %.

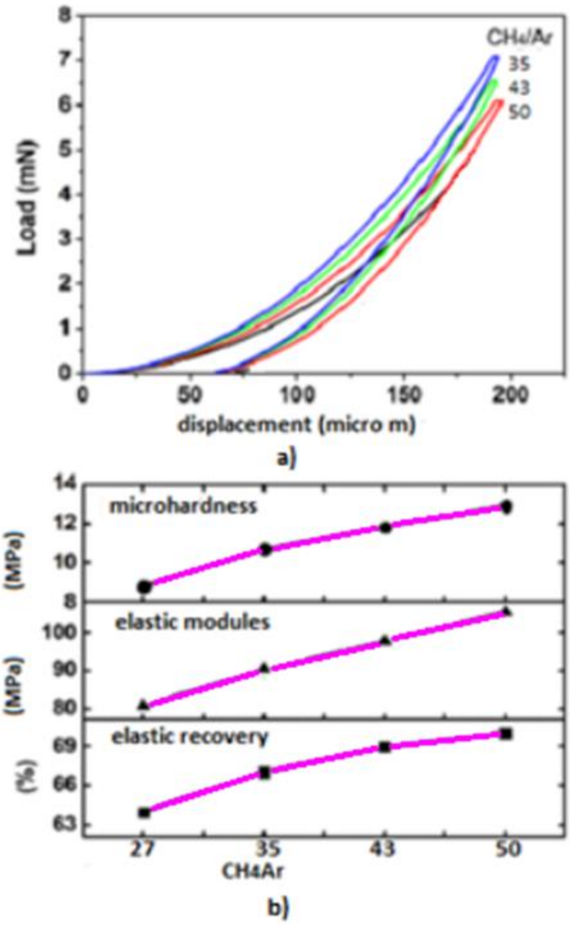


***Fig. 1.*** *(a) Micro-indentation load–displacement curves for Ti-DLC films. (b) Calculated hardness, elastic modulus, and elastic recovery*

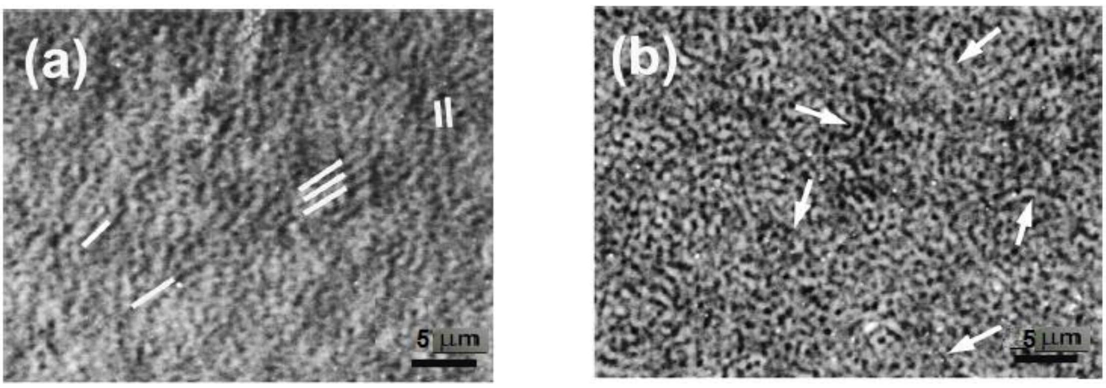

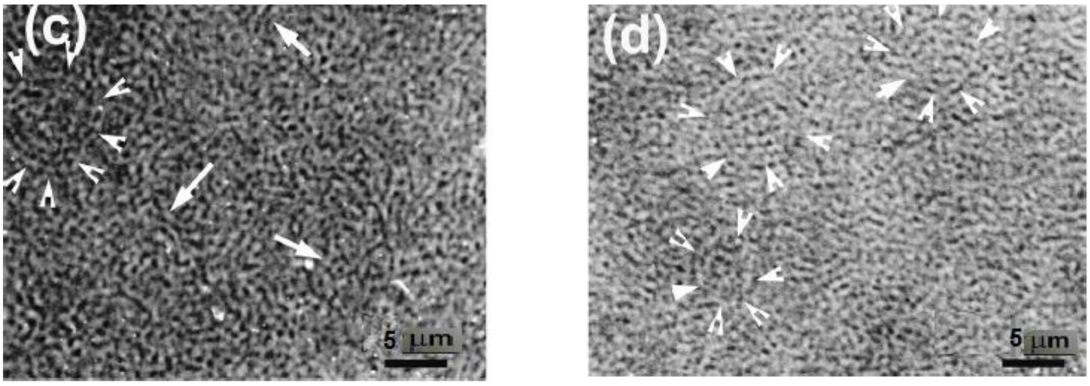


***Fig. 2.*** *HRTEM plan-view images for the films. The arrows show the curved sheets or closed cage structure*

Then, with a further increase in $CH_4$ to 50 %, a greater amount of multi-shell fullerenes (carbon inions) tend to form. Since the hardness has been proposed to correspond to the density of enthalpy of many hard-homogeneous bulk materials, that is, the number of bonds per unit volume multiplying the binding energy of each bond, or, in other words, the cohesion energy of the material, the enhanced elastic recovery should be due to the increased amount of resilient structures such as curved graphene sheets, close-caged fullerene, and multi-shell carbon inions.

The cross-sectional FESEM micrographs of two typical films (27 % and 50 %) are shown in Fig. 3.

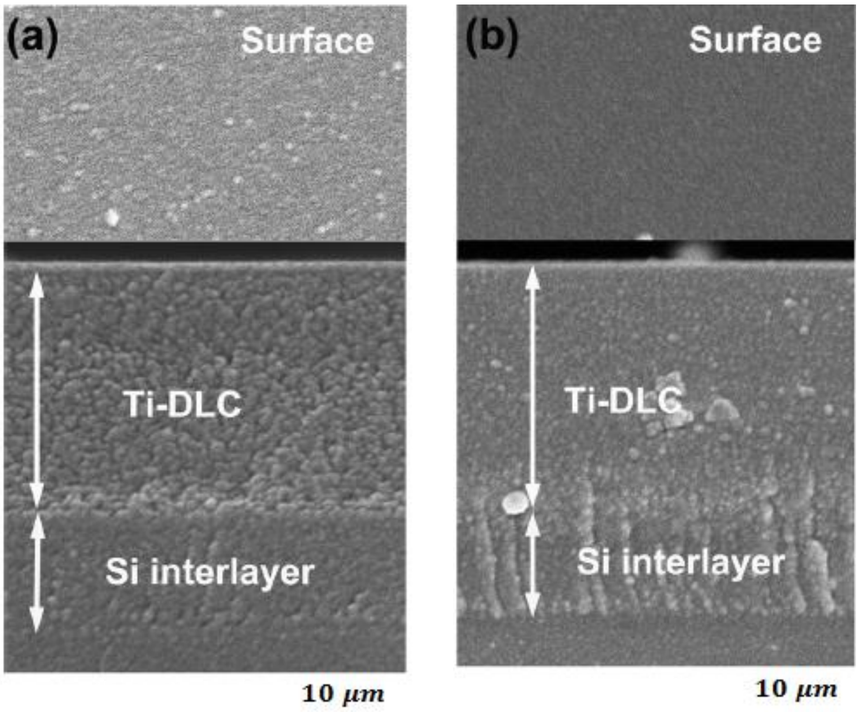


***Fig. 3.*** *Cross-sectional and surface FESEM micrographs of two typical films: (a) $CH_4$/Ar ¼ 27 % and (b) $CH_4$/Ar ¼ 50 %*

The surface images are also given for comparison. As seen, larger-size particles are generated at 27 %, thus leading to a more porous structure and rougher surface. By comparison, the fine particles at 50 % give a denser structure without clearly visible pores and the surface is much smoother. To further examine the surface topography of Ti-DLC films, AFM characterization was conducted and the images are shown in Fig. 4. A smoothened surface could be clearly seen with increasing $CH_4$/Ar ratio. The average energy per carbon atom would be higher at $CH_4$/Ar¼27 % than at $CH_4$/Ar¼50 %. This would lead to a larger thermal spike volume and higher mobility and thus promote the formation of more graphitic clusters at $CH_4$/Ar¼27 %. In addition, the higher energy of carbon species may increase the possibility of C-Ti bonding and also the surface growth of graphitic carbon film, as described in the sub plantation model. The combined effect of surface growth and TiC microparticles may account for the higher surface roughness at $CH_4$/Ar¼27 %. As the $CH_4$/Ar increases to 35 %, the average energy per carbon atom drops to a lower level, which would increase the fraction of sub-planted carbon atoms due to reduced mobility. The formation of fullerene-like structures in carbon films is conditional, depending on the ion impact energy, substrate temperature, duty cycle of bias, and incorporation of proper foreign atoms like nitrogen and their concentration.

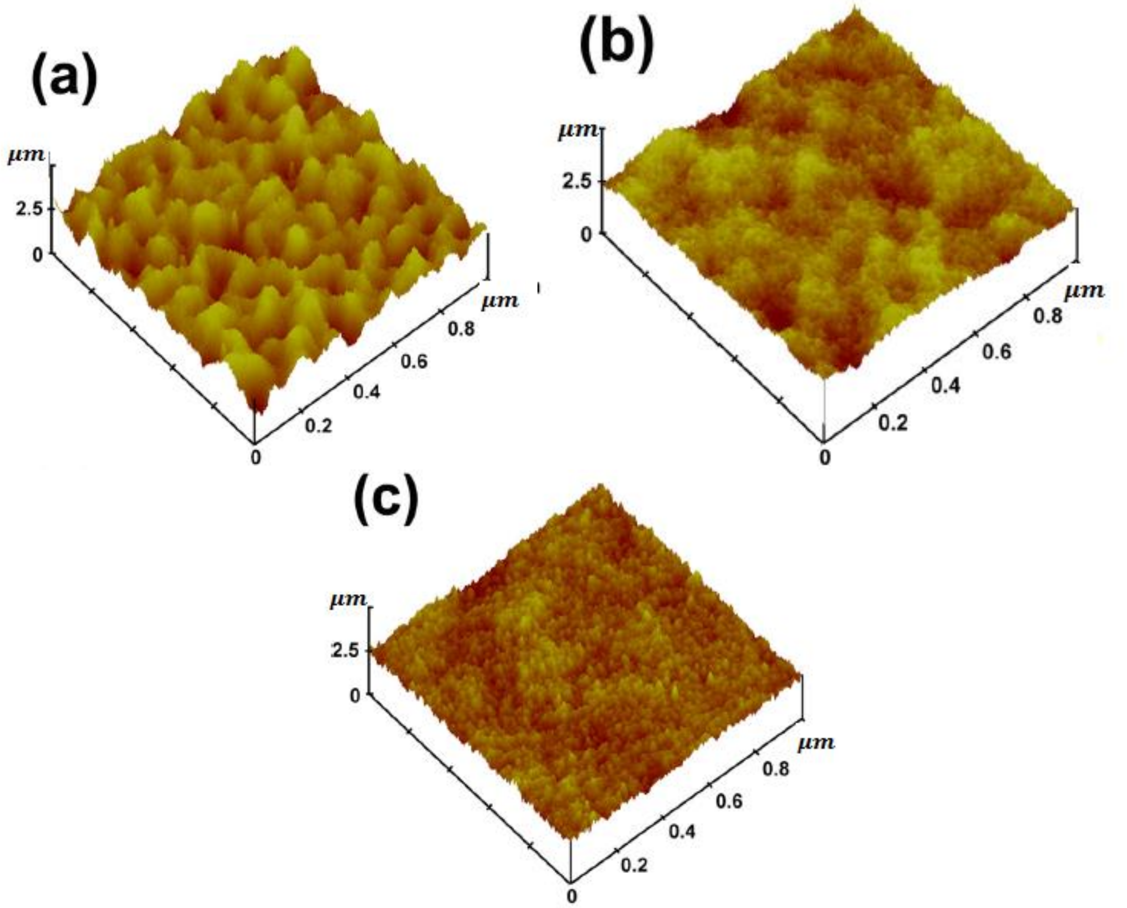


***Fig. 4.*** *AFM images of Ti-DLC films prepared at different $CH_4$/Ar ratios: (a) 35 %, (b) 43 %, and (c) 50 %*

For present Ti-DLCs, the evolution of curved graphene sheets or fullerene-like onions is considered to be due to the catalysis effect of doped $TiO_2$ because major curved structures were observed at the edge of $TiO_2$ clusters, which will be discussed in detail elsewhere. In addition, the effect of proper ion incident energy per carbon atom and the size of embedded $TiO_2$ clusters size should also be taken in to account because a more graphitic microstructure has been found even at a higher concentration of $TiO_2$.

The evolution of microstructure as a function of $CH_4$/Ar ratio leads to totally different mechanical and tribological properties of Ti-DLC films. Apart from the difference in hardness and elastic recovery, the cohesion and toughness of films also differ from each other. As shown in Fig. 5, when the films delaminate from stainless Steel surface without Si interlayer as a result of accumulated internal stress, the film 1 at 27 % tends to break into small pieces, indicating the brittle nature of it. For film 2, however, it would wrinkle to release stress, with only minor cracks. Further improvement of toughness could be seen for film 3 and film 4, which do not show any visible cracks.

Figure 3 shows the optical micrographs of Ti-DLC films peeled off from interlayer free substrates as a result of internal stress.

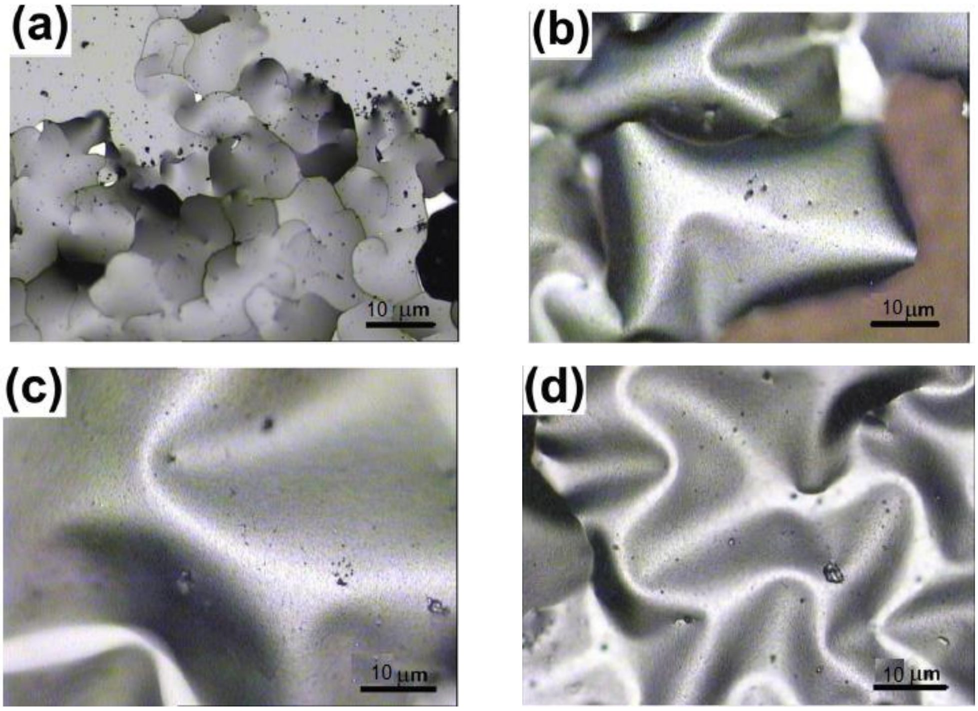


***Fig. 5.*** *Optical micrographs of Ti-DLC films peeled off from interlayer substrates as a result of internal stress*

Figure 6 shows the friction behavior of Ti-DLC films sliding against $Si_3N_4$ balls under a normal load of 10 N in ambient air environment. The corresponding wear rate of each film is given in Fig. 7. Generally, the increased $CH_4$/Ar ratio leads to gradually reduced friction coefficient and wear rate. As seen, the friction behavior of film-1 is much different from that of the other three films, which could be expected from the above characterizations of microstructure and mechanical properties.

For film 1, the friction coefficient is unstable and increases rapidly with sliding distance, reaching ~0.10 at the end of the test. The corresponding wear rate is ~2.8x10$^{-6}$ mm$^3$/N·m. While the other three films all show very smooth friction curves, and the steady state friction coefficient drops from ~0.012 for film 2 to ~0.008 for film 4. Correspondingly, the specific wear rate decreases from ~3.1x10$^{-7}$ mm$^3$/N·m for film 2 to ~1.2x10$^{-7}$ mm$^3$/N·m for film 4, 1 order of magnitude lower than that of film 1.

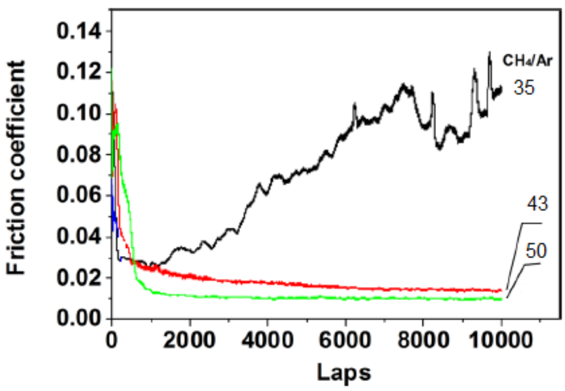


***Fig. 6.*** *Friction curves of Ti-DLC films sliding against $Si_3N_4$ balls (d ¼ 6 mm) in ambient air. Normal load: 10 N; mean velocity: 90 mm/s*

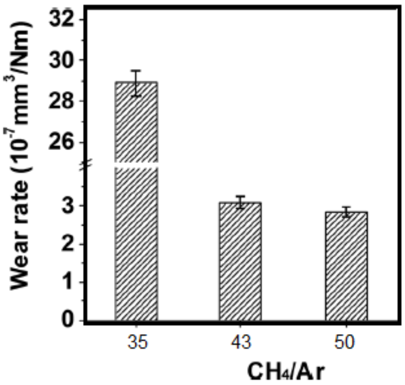


***Fig. 7.*** *Specific wear rate of Ti-DLC films*

Figure 8 shows the optical micrographs of wear tracks of films and wear scars on mating balls after friction tests. The 3D micrographs of wear tracks and the corresponding cross-sectional profiles are given in Fig. 9. As seen, the wear track of film 1 [Fig. 8(a)] is clearly different from the others [Figs. 8(b)–8(c)]. A large number of black debris can be seen both inside and outside the wear track. And the wear track shows a width of ~5 µm and a depth of ~3 µm. The wear depth is much higher than the film thickness, indicating that the film has been worn out by the end of the test (due to the low hardness and brittleness). Hence, for film 1, the friction test was actually conducted between $Si_3N_4$ ball and steel substrate rather than the Ti-DLC film. As a result, it does not only make the friction coefficient increase with great fluctuation, but also leads to severe wear of the mated ball which shows deep scratches on the worn surface [Figs. 8(b1) - 8(c1)]. In contrast, the wear for film 2 to film 3 is much milder. The width of all the three wear tracks is below 2 µm, and the depth only 8-10 µm (the wear scar becomes gradually shallower with increased $CH_4$/Ar ratio). For the mated balls, no scratched grooves due to abrasive wear could be seen, with only a layer of transferred film on the worn surface.

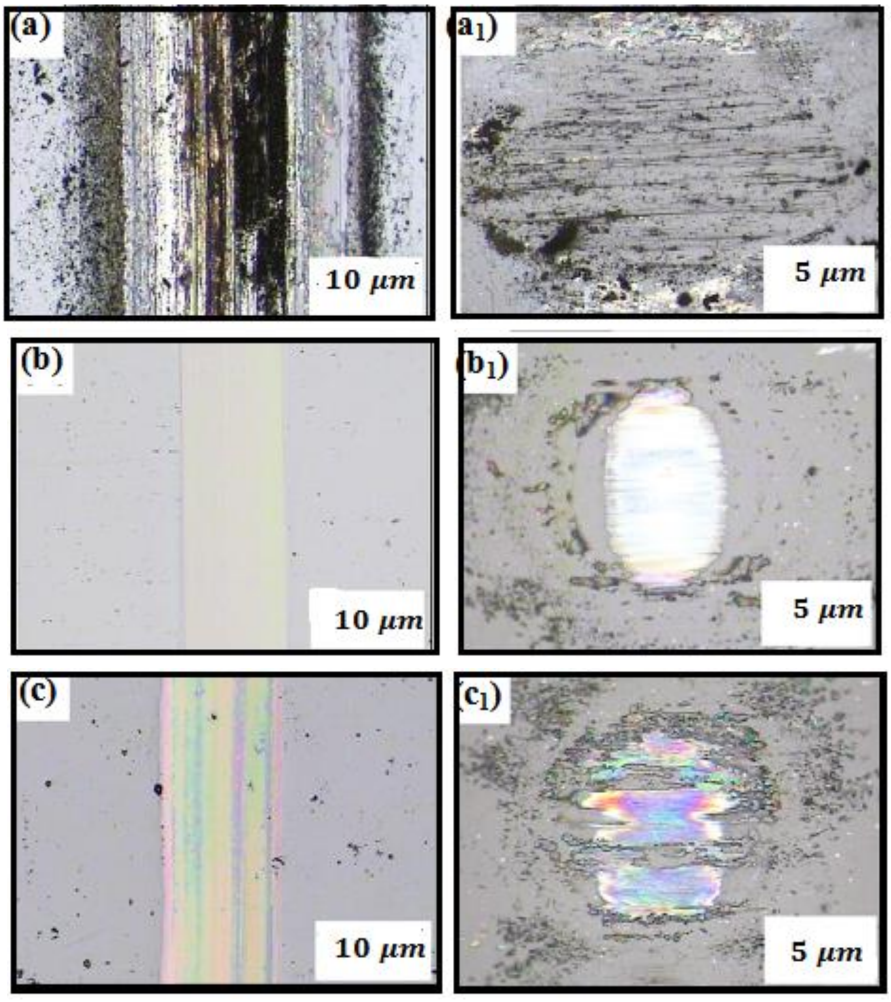


***Fig. 8.*** *Optical micrographs of wear tracks on films and wear scars on balls after friction tests. (a) and (a1): $CH_4$/Ar ¼ 35 %; (b), (b1): $CH_4$/Ar¼ 43 %; (c) and (c1): $CH_4$/Ar ¼ 50 %*

The friction and wear result once again confirm the better toughness and cohesion strength of films 2, 3, and then film 1, which leads to less possibility of brittle fracture and abrasive wear induced by hard particles. Therefore, the friction coefficient remains stable in the whole course of test. Moreover, the wear of films in this case should be dominated by adhesion, which transfers film to the mated ball surface during repeated rubbing process. The wear mode transition from abrasive wear to adhesive wear with reduced amount of incorporated metal is consistent with the previous study [16]. Usually, a higher cohesion strength and hardness would lead to less severity of adhesion wear. Moreover, the wear rate drops from film 2 to film 3 with gradually shallower wear track. It keeps decreasing from film 2 to film 3, Fig. 6, even with a deteriorated continuity of the transfer film [Fig. 8(b1)]. The ultralow and steady friction behavior of Ti-DLC films has been discussed previously by the authors from the perspectives of inherent film property, the friction induced structural transformation, and the transferred layer on mated ball 42.

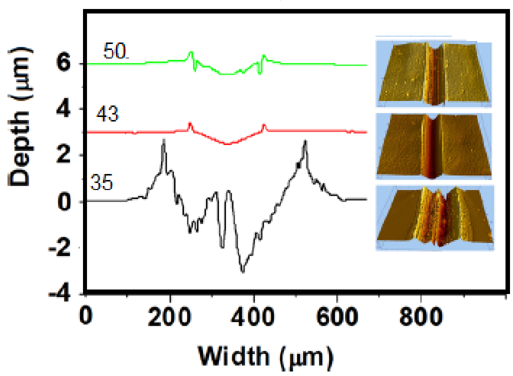


***Fig. 9.*** *D micrographs of wear tracks and the corresponding cross-sectional profiles*

This paper further investigates the superior frictional performance of Ti-DLC films, by examining the evolution of microstructure and its effect on the mechanical and tribological properties. The superior frictional performance of Ti-DLC films can be attributed to the special microstructure related to the development of embedded fullerene-like microstructures as a result of incorporation of $TiO_2$ clusters and proper ion impact. This special structure with increased crosslinking and elastic energy storage ability leads to enhanced hardness and cohesion, improved toughness, and load-bearing capacity (resilient to withstand severe deformation) together with the surface structure transformation to render ultralow interfacial resistance and the excellent resistance.

## 4. Conclusions

An ultralow and steady friction behavior (0.008-0.01) in ambient air was shown by previously prepared Ti-doped DLC films. The initial examination revealed a combined effect of several factors that might contribute to the ultralow friction behavior, including inherent mechanical properties, the friction-induced structural transformation, and the presence of a polymerlike thin transfer film. To clarify the effect of microstructure and composition on the mechanical and tribological properties of the low friction Ti-DLC films, and thus to make the ultralow friction behavior controllable by intentional structural design, we synthesized a series of Ti-DLC films with varied microstructure and Ti content by adjusting feed gas composition (i.e., $CH_4$/Ar ratio). The characterization results reveal that the low $CH_4$/Ar ratio of 27 % would lead to a higher Ti-doping content (~6.5 at.%) and promote the formation of Ti-C clusters. However, the higher average energy per carbon atom in this case would also lead to the formation of graphitic clusters (planar sheets in HRTEM images) both inside the carbon matrix and on the growing surface, thus resulting in a rough surface and low hardness even in the presence of a considerable amount of TiC clusters. The increased $CH_4$/Ar ratio to 35 % would reduce the impact energy of incident carbon atoms and increase the fraction of sub planted carbon atoms due to reduced mobility

The increased local stress could force curvature in graphitic clusters and result in the evolution of odd-membered carbon rings. The increased cross-linking drastically improves the mechanical properties of Ti-DLC films, including greatly enhanced toughness, elastic recovery, and hardness. Further increase in $CH_4$/Ar ratio to 43 % promotes the formation of more curved graphene sheets and some close caged structures start to show up. As the $CH_4$/Ar ratio was raised to 50 %, multi shell carbon onion structures embedded in the carbon matrix could be seen and higher hardness, higher cohesion, higher elastic recovery, and lowest friction coefficient (<0.01) were shown. The formation of fullerene-like microstructures in present Ti- DLC films seem to be through the latter path, because major curved structures were observed at the edge of $TiO_2$ clusters. Further efforts to analyze the catalysis effect of doped $TiO_2$ are needed.

To sum up, this paper investigates the superior frictional performance of Ti-DLC films, by examining the evolution of microstructure and its effect on the mechanical and tribological properties. The superior frictional performance of Ti- DLC films can be attributed to the special microstructure related to the development of embedded fullerene-like microstructures as a result of incorporation of $TiO_2$

clusters. The factors contributing to the ultralow friction include high hardness and cohesion, excellent toughness, and high loadbearing capacity (brought by the increased crosslinking and elastic energy storage ability), the friction-induced structural transformation rendering an ultralow shear resistance and the excellent resistance to oxidation-induced mechanical property degradation (due to the doped $TiO_2$).

## References

**[1]. Erdemir O. L. Eryilmaz, Fenske G.**, J. Vac. Sci. Technol., A 18, 1987, 2000.

**[2]. Galvan Y. T. Pei, De Hosson J. T. M.**, Surf. Coat. Technol. 201, 590, 2006.

**[3]. Dimigen, Kiages C.-P.**, Surf. Coat. Technol., 49, 543, 1991.

**[4]. Gilmore, Hauert R.**, Thin Solid Films, 398-399, 199, 2001.

**[5]. Erdemir, Donnet C.**, J. Phys. D., Appl. Phys., 39, 311, 2006.

**[6]. Gayathri, Kumar N., Krishnan R., Ravindran T. R., Amirthapandian S., Dash S., Tyagi A. K., Sridharan M.**, Ceram. Int. 41, 1797, 2015.

**[7]. Kulikovsky Y., Fendrych F., Jastrabik L., Chvostova D.**, Surf. Coat., Technol., 91, 122, 1997.

**[8]. Bharathy V., Nataraj D., Chu P. K., Wang H., Yang Q., Kiran M. S. R. N., Silvestre-Albero J., Mangalaraj D.**, Appl. Surf. Sci. 257, 143, 2010.

**[9]. Pauleau, Thie`ry F.**, Surf. Coat. Technol., 180-181, 313, 2004.

**[10]. Tsai C., Hwang Y.-F., Chiang J.-Y., Chen W.-J.**, Surf. Coat. Technol., 202, 5350, 2008.

**[11]. Zehnder, Patscheider J. O.**, Surf. Coat. Technol., 133-134, 138, 2000.

**[12]. Zhang X. L. Bui, Jiang J., Li X.**, Surf. Coat. Technol., 198, 206, 2005.

**[13]. Pei T., Huizenga P., Galvan D., Hosson J. T. M. D.**, J. Appl. Phys., 100, 114309, 2006.

**[14]. Pei T., Galvan D., De Hosson J. T. M.**, Acta Mater., 53, 4505, 2005.

**[15]. Zhao H. Li, Ji L., Wang Y., Zhou H., Chen J.**, Diamond Relat. Mater., 19, 342, 2010.

**[16]. Han F. Yan, Zhang A., Yan P., Wang B., Liu W., Mu Z.**, Mater. Sci. Eng., A 348, 319, 2003.

THE ANNALS OF “DUNAREA DE JOS” UNIVERSITY OF GALATI
FASCICLE IX. METALLURGY AND MATERIALS SCIENCE
Nº. 3 - 2017, ISSN 1453-083X

# STUDY ON THE SOIL CHEMICAL POLLUTION IN THE AREA OF THE RESIDUAL BAUXITE LAKE "MINERI" – TULCEA

**Beatrice TUDOR, Anișoara CIOCAN**
“Dunarea de Jos” University of Galati
e-mail: beatrice.tudor@yahoo.com

## ABSTRACT

*The paper presents a study on the impact of chemical pollution of the soil, from residual bauxite lake, from "Mineri", in the areal of Tulcea. Soil samples were taken from the lake, and from the immediate area of the lake, where there are agricultural crops. We analyzed the samples in order to determine the chemical elements and pH of the soil, and the bioremediation methods that could be applied to diminish the effects of chemical soil pollution.*

KEYWORDS: bauxite, chemical soil, pollution

## 1. Introduction

At present, pollution is an international issue of humanity because pollutants have reached high values and disturbances are strong and cross-border.

The causes for the occurrence of pollution can be summarized as follows:

- chaotic use of natural reserves;
- accumulation of unusable substances in the environment;
- emergence of new substances where the rate of consumption and recycling by organisms is much lower than the rhythm of occurrence;
- rapid demographic growth, especially in the last two centuries;
- intensive development of industry, transport and agriculture;
- emergence of overcrowded urban areas.

Industry pollutes absolutely all environments (air, water, soil), causing damage to the health of people and creatures, to agriculture, transport, construction and culture [1, 3].

A large number of studies are being carried out on pollutants emitted by industrial branches, on immediate and long-term effects of pollution, on the effects of measures to reduce pollutant emissions. The industry pollutes through harmful materials on soil, underground, by biological and radioactive contamination, by risks both in exploitation and in the possibility of accidents (explosions).

Around industrial plants, toxic elements for plants and animals can be found in the air, water and soil.

Soil contamination consists in: physical degradation (compaction, structural degradation); chemical degradation (increased content of heavy metals, pesticides, pH modification); biological degradation (with pathogenic germs) [6, 7].

As soil is a much more complex system than air and water, pollution affects its properties, therefore fertility. In addition, pollutants can pass from soil to plants, water or air, and depollution is a difficult and sometimes even impossible to achieve.

Soil resistance to heavy metal pollution differs depending on the nature of the soil. Thus, clay soils retain more pollutants, neutral and carbonate soils retain strongly, and sandy soils retain the least (leaching is strong, except Mo and Se). Also, the finer the soil texture, the more the pollutants retained in the soil, which further pass to plants [2, 4].

Soil pollution with heavy metals causes: imbalance of physical, chemical and biological processes in the soil; decrease in biological activity; - inhibition of nitrification processes; toxic action for plants.

Particularly toxic to plants and animals are Hg, Cd, B, As. It has been forbidden to produce mercury-containing fungicides, usable for seed treatment, because it has resulted in deaths of both animals and humans. Cadmium causes decalcification of organisms. Arsenic in the human body causes vascular diseases, which may even lead to limb amputations [5].

## 2. Experimental Results

As part of this research, a study was carried on the impact of chemical soil pollution in the area of the residual bauxite lake Mineri in Tulcea county.

We used soil samples taken from the area of the residual bauxite lake Mineri in Tulcea, as well as adjacent soil samples from the agricultural area to determine the pH and the chemical composition.

***Fig. 1.*** *Residual bauxite lake "Miners"- Tulcea*

From this area, soil samples from 3 distinct points were collected from a depth of 50 cm using a sampling probe.

### *2.1. Determination of pH in soil samples*

In the laboratory of the faculty, the pH was determined for the soil samples taken from the lake and the agricultural area in the lake using a HQ40d type multi-parameter (Fig. 2)


***Fig. 2.*** *Multi-parameter HQ40d*

The amount of sample soil (samples a and b) is mixed with distilled water (pH distilled water = 5) by a steering rod for 4 minutes (Fig. 3).

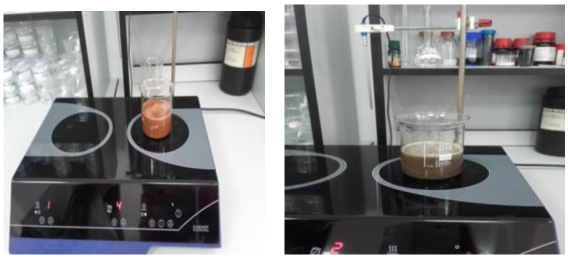

a) b)

***Fig. 3.*** *Soil taken from residual bauxite lake (a), and soil taken from the agricultural area (b)*

With a filter paper, the solution required to measure the pH is obtained. The pH was determined using a HQ40d device, obtaining the values shown in the graph of Fig. 4.

After pH determination in the samples of soil and lake and the agriculture area, a higher pH was noticed in the soil sample from the lake, respectively 9.8, the soil being strongly alkaline, while in the agricultural area soil samples the pH was 8.1, implying a slightly alkaline soil.

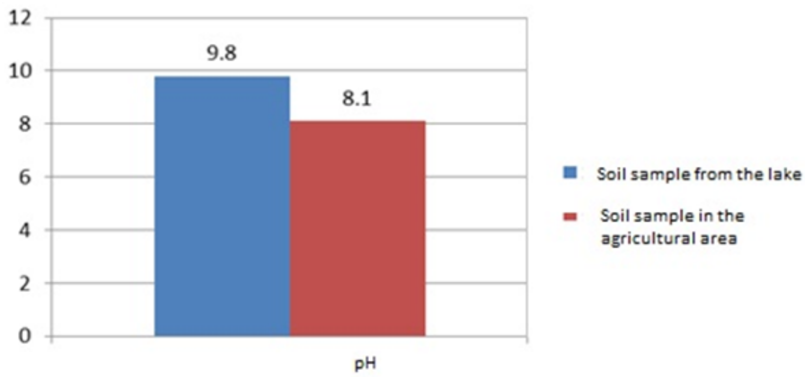


***Fig. 4.*** *PH values of soil samples, from the lake and the agricultural area*

### *2.2. Determination of soil chemical composition*

Determination of the chemical composition of the soil was carried out as follows: the soil samples were crushed in a crucible and then inserted into the X-ray Spectrometer (Fig. 5).

***Fig. 5.*** *X-ray Spectrophotometer The chemical elements detected in the soil samples are shown in Table 1*

The soil sample taken from the residual bauxite lake according to Order 756/97 shows exceedances of the admissible limits for lead (SR ISO 11047-99), barium (SR EN 11885-09), zinc (SR ISO 11047-99), cobalt (SR EN 11885-09).

At the soil sample taken from the agricultural area, the detected elements fall within the permissible limits, but there are no essential elements for plant development, such as chromium and iron.

Therefore, it is necessary to apply soil bioremediation methods, such as the use of bacteria for soil decontamination, so that they can be used as agricultural land.

***Table 1.*** *Chemicals elements detected in soil samples*

| Chemical elements detected in soil samples | Soil sample from the lake [ppm] | Soil sample from the agricultural area [ppm] |
|---|---|---|
| Lead | 77 | 19.33 |
| Strontium | 56.33 | 126.33 |
| Rubidium | 14.33 | 65.33 |
| Zirconium | 511 | 307.67 |
| Titanium | 68.677 | 4.365 |
| Barium | 209 | 5.340 |
| Chromium | 3.049 | - |
| Iron | 21400 | - |
| Zinc | 567 | 49 |
| Cobalt | 16.4 | 2.573 |
| Manganese | - | 440 |

## 3. Conclusions

In plants, lead accumulates in parts containing chlorophyll, thus blocking the photosynthesis process, and in the most severe forms changes the mechanism of the reproduction process. The lead present in the human body causes anemia, affects the nervous system, and, in cases of severe intoxication, it causes lead poisoning.

Zinc has a role in chlorophyll synthesis, plant growth, increased resistance to drought and frost, fertilization, nitrogen fixation in the case of legumes. Zinc lack causes: whitening of corn leaves; "small leaves” disease in tobacco, live, barley, sunflower.

Manganese has a stimulating role in plant growth, flower formation, vitamin and carbohydrate synthesis. Lack of manganese causes large losses in oats, spinach, wheat, beans, potatoes, peas. Yellow spots appear on the beet leaves.

After the determination of pH in soil samples taken from the lake and the agricultural area, a higher pH resulted in the soil sample in the lake. This was 9.8, which means the soil is highly alkaline. At the sample in the agricultural area the pH was 8.1, that is a weak alkaline soil. Most grown plants prefer weak acid and neutral soils.

Analysis on the quality of determinations carried out soil samples investigated, highlights that an alert threshold has been exceeded at Zn, Pb, and Fe, requiring for bioremediation activities of these soils.

## Acknowledgement

The authors wish to thank the student Gabriela Nastase, who helped us in this study.

## References

**[1]. Barnea M., Papadopol C.**, *Poluarea şi protecţia mediului*, Ed. Ştiiţifică şi Enciclopedică, Bucureşti, 1975.
**[2]. Butnariu I., Constantin N.**, *Protecţia mediului înconjurător şi microclimat*, lito Inst Politehnic, Bucureşti, 1994.
**[3]. Ciplea L. I., Ciplea Al.**, *Protecţia mediului înconjurător*, Ed. Tehnică, Bucureşti, 1994.
**[4]. Negulescu M., Vaicum L., Ianculescu S., Bonciu G., Pătru C., Pătru O.**, *Protecţia mediului înconjurător*, Ed. Tehnică, Bucureşti, 1995.
**[5]. Gore Al.**, *Earth in the Balance, Ecology and the human spirit*, Penquin Books USA Inc., 1993.
**[6]. Dăduianu Vasilescu I.**, *Protecţia mediului înconjurător – componentă majoră a politicii macro şi microeconomice*, INID, Bucureşti, 1994.
**[7]. Negulescu M., Vaicum L., Ianculescu S., Bonciu G., Pătru C., Pătru O.**, *Protecţia mediului înconjurător*, Ed. Tehnică, Bucureşti, 1995.

MANUSCRISELE, CĂRŢILE ŞI REVISTELE PENTRU SCHIMB, PRECUM ŞI ORICE CORESPONDENŢE SE VOR TRIMITE PE ADRESA:

MANUSCRIPTS, REVIEWS AND BOOKS FOR EXCHANGE COOPERATION, AS WELL AS ANY CORRESPONDANCE WILL BE MAILED TO:

LES MANUSCRIPTS, LES REVUES ET LES LIVRES POUR L'ECHANGE, TOUT AUSSI QUE LA CORRESPONDANCE SERONT ENVOYES A L'ADRESSE:

MANUSCKRIPTEN, ZIETSCHRITFTEN UND BUCHER FUR AUSTAUCH SOWIE DIE KORRESPONDENZ SID AN FOLGENDE ANSCHRIFT ZU SEDEN:

After the latest evaluation of the journals by the National Center for Science Policy and Scientometrics (**CENAPOSS**), in recognition of its quality and impact at national level, the journal will be included in the $B^+$ category, 215 code (http://cncsis.gov.ro/userfiles/file/CENAPOSS/Bplus_2011.pdf).

The journal is already indexed in:

SCIPIO-RO: http://www.scipio.ro/web/182206

EBSCO: http://www.ebscohost.com/titleLists/a9h-journals.pdf

Google Academic: https://scholar.google.ro

The papers published in this journal can be viewed on the website of "Dunarea de Jos" University of Galati, the Faculty of Engineering, pages: http://www.sim.ugal.ro, http://www.imsi.ugal.ro/Annals.html.

**Name and Address of Publisher:**
Contact person: Elena MEREUȚĂ
Galati University Press - GUP
47 Domneasca St., 800008 - Galati, Romania
Phone: +40 336 130139
Fax: +40 236 461353
Email: gup@ugal.ro

**Name and Address of Editor:**
Prof. Dr. Eng. Marian BORDEI
Dunarea de Jos University of Galati, Faculty of Engineering
111 Domneasca St., 800201 - Galati, Romania
Phone: +40 336 130208
Phone/Fax: +40 336 130283
Email: mbordei@ugal.ro

**AFFILIATED WITH:**

**- THE ROMANIAN SOCIETY FOR METALLURGY**
**- THE ROMANIAN SOCIETY FOR CHEMISTRY**
**- THE ROMANIAN SOCIETY FOR BIOMATERIALS**
**- THE ROMANIAN TECHNICAL FOUNDRY SOCIETY**
**- THE MATERIALS INFORMATION SOCIETY**
**(ASM INTERNATIONAL)**

## Edited under the care of
## the FACULTY OF ENGINEERING

**Annual subscription (4 issues per year)**

Editing date: 15.09.2017
Number of issues: 200
Printed by Galati University Press (accredited by CNCSIS)
47 Domneasca Street, 800008, Galati, Romania